1-1-2015

Cep290 and the Primary Cilium- Understanding the Protein's Role in Ciliary Health and Disease

Adam Paul Wojno
University of Pennsylvania, wojno@mail.med.upenn.edu

Cep290 and the Primary Cilium- Understanding the Protein's Role in Ciliary Health and Disease

Abstract
Mutations in CEP290 are associated with phenotypes ranging from early onset retinal degeneration to embryonic lethal, multisystem disease. The association of CEP290 with disease in multiple tissues is believed to be due to its role in stabilizing the primary cilium, an organelle found on almost every cell in the body whose involvement in human health and disease has only recently been identified. Like many ciliary proteins, CEP290's exact function in this structure and how mutations affecting the protein lead to disease remains relatively unclear. Here, a proposed mechanism of CEP290-associated disease pathogenesis is explored, finding severity of CEP290-associated disease correlates with the amount of functional CEP290 protein predicted to result from a given patient's genotype. In addition, a potential interaction between CEP290 and TTBK2, a kinase recently discovered to traffic to the base or the primary cilium before the onset of ciliogenesis, was observed, providing insight into a role of CEP290 in the early stages of cilium formation.

Degree Type
Dissertation

Degree Name
Doctor of Philosophy (PhD)

Graduate Group
Cell & Molecular Biology

First Advisor
Jean Bennett

Keywords
CEP290, Ciliogenesis, Ciliopathies, Primary cilium

Subject Categories
Molecular Biology

CEP290 AND THE PRIMARY CILIUM- UNDERSTANDING THE PROTEIN'S ROLE IN CILIARY HEALTH AND DISEASE

Adam P. Wojno

A DISSERTATION

in

Cell and Molecular Biology

Presented to the Faculties of the University of Pennsylvania

in

Partial Fulfillment of the Requirements for the

Degree of Doctor of Philosophy

2015

Supervisor of Dissertation

_____

Jean Bennett M.D., Ph.D., F.M. Kirby Professor of Ophthalmology

Graduate Group Chairperson

_____

Dan Kessler Ph.D., Chair, Cell and Molecular Biology Graduate Group

Dissertation Committee

Phil Johnson M.D.
Professor of Pediatrics

Katherine High, M.D.
Professor of Pediatrics

Joshua Lipschutz M.D.
Professor of Nephrology

Valder Arruda M.D., Ph.D.
Associate Professor of Pediatrics

Ben Black, Ph.D.
Associate Professor of Biochemistry and Biophysics

For Elia

ACKNOWLEDGEMENT

My first acknowledgement is to Dr. Jean Bennett for allowing me the opportunity to carry out my graduate studies in her laboratory. Jean's brilliance as a scientist is only matched by her humbleness, and despite a schedule that could surely use several more hours in the day, she is never without time for her students. I have always admired this.

Next, I would like to thank my parents. I don't know life any other way than always having two people in my corner. They offer only support for the decisions I make and a willingness to laugh with me in hindsight at the ones that don't turn out so well. I understand very few people have this, and it is something I will always be grateful for.

Finally, to my wife, Elia. I tell you everyday that I love you, but this might be the only opportunity I get to put it in writing and have it published. I love you. Thank you for choosing to stand next to me as we go through life. I really could not have asked for a better friend.

ABSTRACT

CEP290 AND THE PRIMARY CILIUM- UNDERSTANDING THE PROTEIN'S ROLE IN CILIARY HEALTH AND DISEASE

Adam P. Wojno

Jean Bennett M.D., Ph.D.

Mutations in *CEP290* are associated with phenotypes ranging from early onset retinal degeneration to embryonic lethal, multisystem disease. The association of CEP290 with disease in multiple tissues is believed to be due to its role in stabilizing the primary cilium, an organelle found on almost every cell in the body whose involvement in human health and disease has only recently been identified. Like many ciliary proteins, CEP290's exact function in this structure and how mutations affecting the protein lead to disease remains relatively unclear. Here, a proposed mechanism of *CEP290*-associated disease pathogenesis is explored, finding severity of CEP290-associated disease correlates with the amount of functional CEP290 protein predicted to result from a given patient's genotype. In addition, a potential interaction between CEP290 and TTBK2, a kinase recently discovered to traffic to the base or the primary cilium before the onset of ciliogenesis, was observed, providing insight into a role of CEP290 in the early stages of cilium formation.

TABLE OF CONTENTS

LIST OF FIGURES

PREFACE

I first became interested in Centrosomal Protein 290 kDa (CEP290) through its association with Leber Congenital Amaurosis (LCA), an inherited, retinal degenerative disease that results in abnormal vision first manifesting in infancy. Whatever (poor) vision is present then disappears over time as the retinal photoreceptors degenerate. The initial focus of the Bennett lab was on a form of LCA that is relatively rare – caused by mutations in the RPE65 gene. Mutations in the Centrosomal Protein 290 kDa (*CEP290*)-encoding gene are more common than those in the RPE65 gene, and are associated with over 20% of all cases of LCA. In addition to retinal degeneration, mutations in CEP290 are also associated with a spectrum of more severe disease states, including Senior-Loken syndrome, Joubert Syndrome, and Meckel Gruber syndrome. This spectrum of diseases, including LCA, is responsible for phenotypes ranging from early onset retinal degeneration to embryonic lethal, systemic disease and is attributed to the role that CEP290 plays in stabilizing the primary cilium in multiple different cell types, including photoreceptors.

Primary cilia are found on nearly every mammalian cell where they function as sensory organelles, taking part in the first stages of signaling cascades such as those involving Hedgehog and Wnt. In addition, the organelle that connects the cellular body of a photoreceptor with the light sensing outer segment is known to be a modified primary cilium.

While the Bennett laboratory has had success using adeno-associated virus (AAV) vectors in a gene augmentation approach for LCA due to mutations in the gene encoding RPE65, the *CEP290* cDNA is roughly twice the size of the AAV cargo capacity. Thus, those afflicted with *CEP290*-associated disease are currently not candidates for an analogous gene augmentation therapy intervention. In addition, outside of its association with multiple disease states, relatively little is known about CEP290's function in cilia and photoreceptors. The goal of this work has been to address this void with an emphasis on the relationship of *CEP290* mutations and disease as well as the protein's role in the development and maintenance of the primary cilium and/or photoreceptor.

In Chapter 1 of this discussion, I will briefly cover the history of the primary cilium with a focus on key findings that have brought the organelle to the attention of scientists from multiple fields. Chapter 2 will incorporate some of what we know about the role of cilia in the body with our understanding of CEP290 in an attempt to generate a model for *CEP290*-asociated disease pathogenesis. In Chapter 3, I will take a step back to look more closely at the role of CEP290 in ciliary health and maintenance. Specifically, I will begin to investigate the potential role that CEP290 might play in the initiation of ciliogenesis and, in addition, comment on our current understanding of this process as well as contemplate the potential role of other proteins in cilium formation. Finally, in Chapter 4, I will discuss some remaining questions related to the work presented here and the potential future directions to address these.

CHAPTER 1: The primary cilium- from vestigial to valuable

The primary cilium, an organelle found on the surface of almost every cell type in the body (Singla and Reiter, 2006), has attracted an impressive surge of scientific interest since the beginning of the century. This non-motile structure, argued to be vestigial since it was first observed on human cells over a hundred years ago (Romero et al., 2011), is now known to be linked to multiple signaling pathways and diverse cellular functions. Mutations in genes newly discovered to be expressing ciliary protein products are continually being linked to previously unexplained diseases. How the primary cilium has emerged as a key cellular player after so many years can be explained in part by technological advances, but also, and perhaps more readily, by the continued pursuit of a small community of scientists that maintained interest in an overlooked organelle. A commentary on this pursuit, highlighting crucial observations and the scientists involved will be discussed below.

Cilia, flagella, and primary cilium

To begin a discussion on the primary cilium, a few clarifying points should be made. Cilia, flagella, and primary cilia are all composed of three regions, the basal body, the transition zone, and the axoneme (Avasthi and Marshall, 2012; Seeley and Nachury, 2010). A pair of centrioles docked at the cellular membrane is the foundation of the basal body. From the basal body, a microtubule shaft is extended from the end of the mother centriole, producing the axoneme of the structure. The area at the base of the microtubule axoneme, most proximal to the

mother centriole is defined as the transition zone (Kobayashi and Dynlacht, 2011). (Fig. 1, Top Panel) With a few exceptions, the axoneme of motile cilia and flagella, responsible for cellular locomotion or fluid movement in the case of a stationary cell, are composed of a 9+2 arrangement of microtubules while the non-motile primary cilia are composed of a 9+0 arrangement (Fig. 1, Lower Panel) (Bloodgood, 2009). Outside of this difference, the main structural and mechanical characteristics of these ciliary organelles are very similar and, as such, related observations made in motile cilia or flagella, which tend to be much larger, are often conveyed to the smaller non-motile type. While the following discussion will

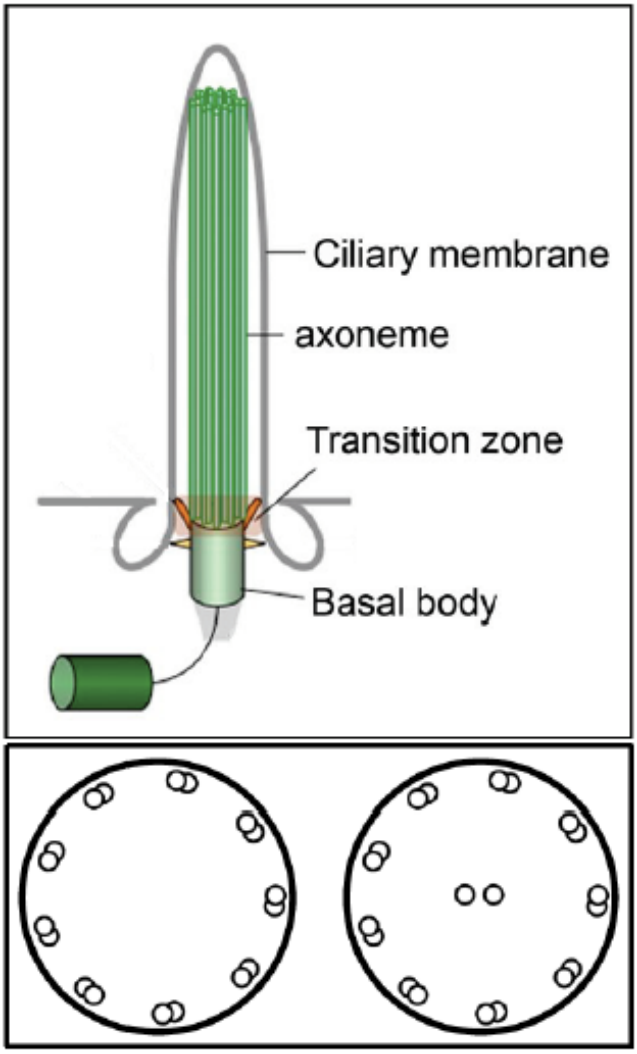

Figure 1: The primary cilium. Top Panel- Cilia, flagella, and primary cilia are all composed of a basal body, transition zone, and axoneme. The ciliary membrane separates the axoneme from the extracellular space. Bottom Panel- A 9+0 arrangement of microtubules is depicted on the left and a 9+2 arrangement is depicted on the right. *Figure 1, Top Panel adapted from Kobayashi and Dynlacht, 2011

mainly center on the emergence of the non-motile cilia as an organelle of utmost importance, the history of cilia in general starts with motile cilia and flagella, described by many as the first observed cellular organelle (Bloodgood, 2009).

Antony van Leeuwenhoek- "Little feet"

Born in Delft, Holland in 1632, Antony van Leeuwenhoek came from an unlikely start to become the first person to identify and describe protozoa and bacteria just years after Robert Hooke described the first example of a microorganism, the microfungus Mucor (Gest, 2004; Dobell, 1932). The son of a basket maker and a brewer's daughter, Antony moved to Amsterdam at the age of 16 to work in a Linen-draper's shop. After around seven years, working the previous few years as the shop's bookkeeper, he returned to Delft, married, and opened a draper's shop of his own.

With no formal scientific training but armed with what he described as, "a craving after knowledge," (Waggoner, 1996) Antony began making microscopes in his free time, observing up close a variety of subjects, from mold to bees. Resisting to publish anything himself, in part due to the fact that he only spoke and wrote in Dutch (Dobell, 1932), all of Leeuwenhoek's work is described in letters that he sent to others. Many of these letters were addressed to Henry Oldenburg who held the post of the first Secretary of the Royal Society of London, a society based on the "promotion of natural knowledge" (Dobell, 1932). Oldenburg then translated and sent out Leeuwenhoek's work to interested parties. In a letter to Oldenburg in 1674, Antony describes his findings made in a

sample of water taken from a pond that he noticed became a cloudy green color in the summer after being clear all winter. In this sample, Antony described several “earthy particles, and some green streaks, spirally wound serpent-wise.” (Dobell, 1932) In addition he mentioned the quick motion with which these particles moved and that they were no thicker than a strand of hair.

A year later, in his 18th and probably most famous letter to the Royal Society, Leeuwenhoek further describes these particles. It is in this letter in which flagella and cilia are mentioned for the first time, describing the flagella in terms of the “motion, of stretching out and pulling together the tail,” and cilia as, “incredibly thin little feet, or little legs” (Dobell, 1932). Leeuwenhoek goes on to describe finding these creatures in various types of water under an assortment of conditions, helping to enlighten the world of a new, fascinating universe inhabited by microorganisms.

The central flagellum

Around 200 years after Leeuwenhoek’s discovery, improved microscopes and the development of a new stain, iron-hematoxylin, finally led to the discovery of primary cilia, at the time termed the “central flagella.” (Bloodgood, 2009) The first to describe and illustrate (Fig. 2) these structures on mammalian cells in 1898 was Karl Wilhelm Zimmerman. In all, Zimmerman described the “central flagellum” on various cell types, including those from kidney tubules, pancreatic ducts, thyroid glands, uterine follicles, and seminal vesicles (Bloodgood, 2009). While never being able to determine if the structure was motile or not,

Zimmerman did make several key findings regarding the “central flagellum.” Of these, Zimmerman noted that nearly every cell had a “central flagellum,” he

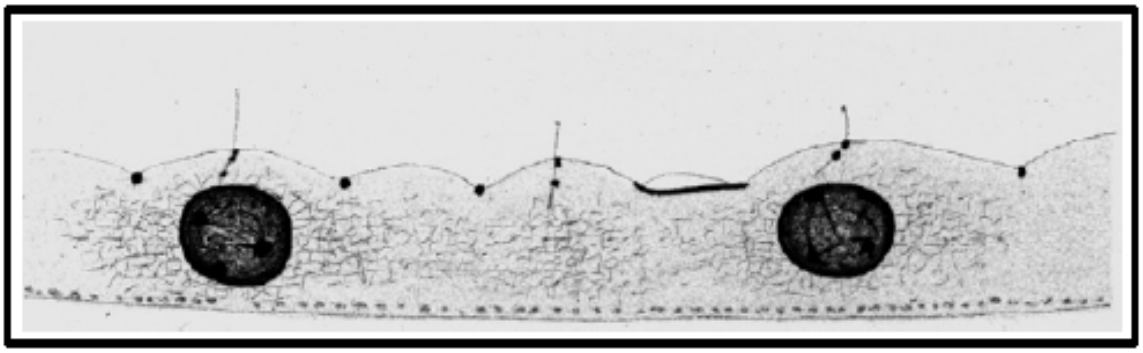

Figure 2: The central flagellum. Drawing of one side of rabbit kidney tubule made by Karl Zimmerman in 1898. The “central flagella” or primary cilia are depicted as thin lines emanating from two black dots at the top of the cells. *Figure adapted from Bloodgood, 2009

observed that the structure was always associated with the distal centriole of an associated centrosome and that the “central flagellum” was a separate class of cilia or flagella from the already described motile cilia and flagella (Bloodgood, 2009).

Aside from the discovery and description of the “central flagellum” on mammalian cells, however, Zimmerman is most regarded for his correct hypothesis, made a century before being shown experimentally, that the structure he was observing was likely linked to cellular signaling in some way, postulating while studying “central flagella” of kidney tubules that, “changes in the configuration of the secretions flowing inside the glandular lumen might have a stimulating effect upon the flagellum, whereby the secretory function might be qualitatively or quantitatively affected” (Bloodgood 2009, Romero et al., 2001).

Connecting cilium

Over the course of the following century, the cellular importance of the primary cilium continued to be debated with some groups in the camp of Zimmerman, suggesting a sensory role for the organelle, and many groups believing that the organelle was merely a by-product of evolution (Barnes, 1961; Munger, 1958; Sorokin, 1962). An important side step in this discussion and one very important to retinal biology was the use of Electron Microscopy (EM) to demonstrate that the structure connecting the inner and outer segments of photoreceptor cells was actually a modified primary cilium. This was demonstrated in a series of papers from Fritiof S. Sjostrand and Eduardo de Robertis. Both experts in EM, Sjostrand first published images of retinal rods inner segments in 1953. In analyzing these images (Fig. 3) Sjostrand commented extensively on the structure connecting the inner and outer segment, noting it contained “16-18 straight fibrils” which he

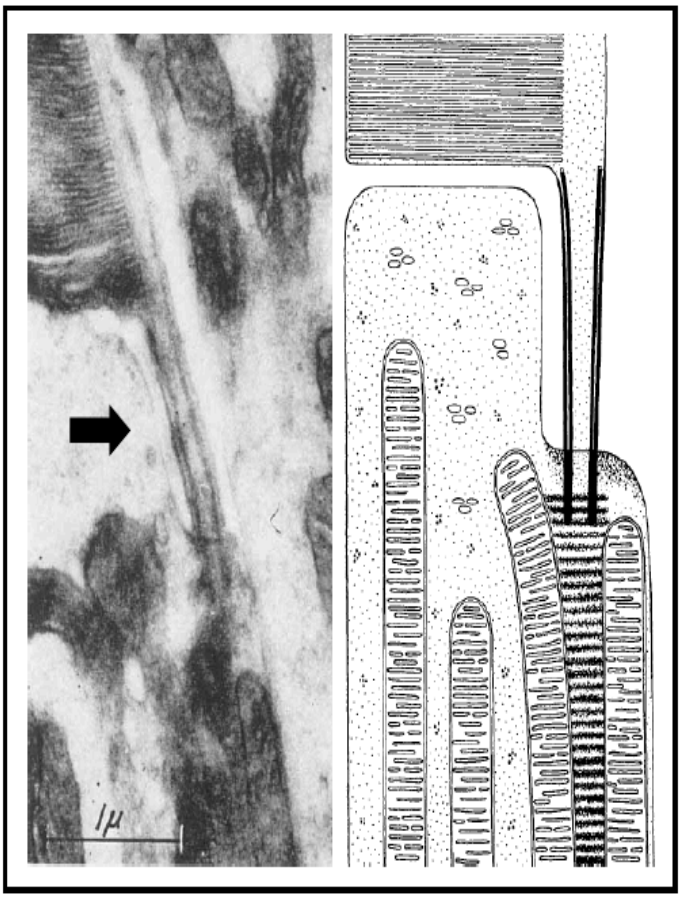

Figure 3: The connecting cilium. Left panel- EM image taken of a rod photoreceptor by Sjostrand in 1953 with a black arrow added to point out the connecting cilium. Right panel- Sjostrand illustration of the structure depicting inner and outer segments of the photoreceptor connected by the cilium. *Figure adapted from Sjostrand, 1953

termed “the connecting fibrils” and that the fibrils entered the inner segment where they terminated shortly thereafter (Sjostrand, 1953). In addition, Sjostrand observed that besides the structure containing the connecting fibrils, the inner and outer segments of the photoreceptor were, “completely separated,” suggesting the architecture of the cell prevented the mixture of each segment’s components. In terms of function, Sjostrand hypothesized that the structure containing the connecting fibrils was used by the photoreceptor to pass an “excitatory state” from the outer segment to the inner segment of the cell after sensing light. Three years later, Eduardo de Robertis expanded upon Sjostrand’s structural observations when he correctly observed the structure containing the connecting fibrils was very similar to a cilium, containing nine pairs of filaments anchored at a basal body in the inner segment of the cell. As such, de Robertis termed the structure the “connecting cilium” (de Robertis, 1956).

Intraflagellar transport

At the end of the 20th century, close to 100 years after Zimmerman first predicted a sensory function for the primary cilium, Joel Rosenbaum’s laboratory at Yale University invigorated the field with the discovery of Intraflagellar Transport (IFT) in eukaryotic cilia (Kozminski et al., 1993). IFT, described as the bi-directional movement of particles along the flagellar axoneme, was discovered while observing flagella of *Chlamydomonas reinhardtii* by means of differential interference contrast (DIC) microscopy and EM. Chlamydomonas, a species of single celled green algae, has proven to be an invaluable tool in flagellar and

ciliary biology due to the presence of very large flagella, the ability to easily make mutant specimens, and the close homology of many of its proteins to mouse and human ciliary proteins (Johnson et al., 1993; Pazour et al., 2000). Using DIC microscopy (which allows for enhanced contrast of live samples) to study flagella, Rosenbaum's group was able to not only show the movement of particles up and down the flagellar axoneme but that the movement actually took place between the microtubule axoneme and the flagellar membrane. Further examination of the particles by EM verified their location and gave insight into their approximate size (Fig. 4). In addition, the group was able to track the movement of these particles, showing that they moved at a constant pace. Further, the rate of movement during flagellar assembly and disassembly was similar to that during movement

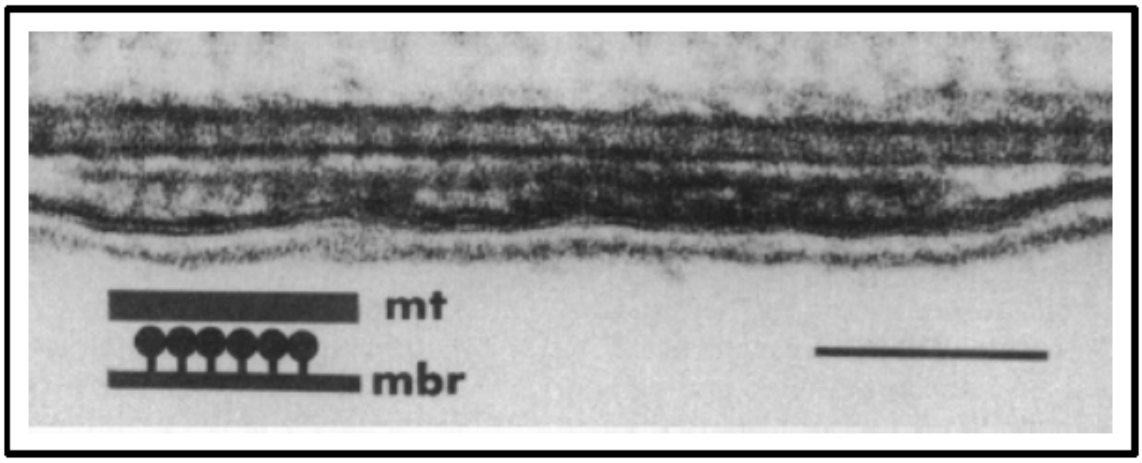

Figure 4: Intraflagellar transport. DIC image showing particles sandwiched between the microtubule axoneme of a *Chlamydomonas* flagellum with an illustration depicting this in the bottom left. *Figure adapted from Kozminski, et al. 1993

in full-length, stable, flagella, suggesting a maintenance role for the system in addition to roles in assembly and disassembly (Kozminski et al., 1993). Further work investigating these IFT particles showed they are made up of at least 15

proteins, divided into two complexes, A and B. Included in these complexes are kinesin-II motors and dynein 1b/2 protein (Pazour and Rosenbaum, 2002).

Using a previously described temperature sensitive mutant strain of *C. Rheinhardtii*, Rosenbaum and colleagues were able to show that inhibition of the kinesin-II motor protein of the IFT complex led to flagellar reabsorption and a failure to assemble new flagella (Cole et al., 1998). Work in George Witman's laboratory demonstrated that chlamydomonas containing deletion alleles of the dynein 1b/2 protein resulted in short, immotile flagella (Pazour et al., 1998). Interestingly, in addition to this phenotype, the flagella were also found to contain large amounts of raft-like particles previously described to be associated with the IFT complexes (Kozminski et al., 1993; Pazour et al., 1998). Taken together, these findings provided evidence that IFT forward, or anterograde, transport was likely dependent on kinesin motors while dynein motors were probably responsible for reverse, or retrograde, transport. In addition, it was noted that when homologues of these proteins in *Caenorhabditis elegans* (*C. elegans*) were mutated, the cilia of the sensory neurons were observed to be defective, both in structure and function (Cole et al., 1998).

While the discovery of IFT was indeed exceptional, the molecular analyses carried out by the Rosenbaum laboratory and others on the individual protein complexes of the flagella and cilia have been crucial in delineating the protein identity of these structures. It is with these studies that other groups have

been able to relate known disease genes with unknown functions to ciliary maintenance and health.

The cilia and polycystic kidney disease- Zimmerman's prediction verified

Shortly after the Rosenbaum laboratory's first paper on IFT was published, Richard Woychik's group of the Oak Ridge National Laboratory described the creation of a transgenic mouse line that demonstrated a phenotype very similar to human autosomal polycystic kidney disease. The line was created after insertional mutagenesis led to a disruption of a gene named *Tg737* (Moyer et al., 1994). The mouse, named Oak Ridge Polycystic Kidney (*orpk*), demonstrated cyst development in the collecting ducts of the kidneys, and an inability to concentrate urine (Yoder et al., 1996, Yoder et al., 1997). While the group extensively characterized the phenotype of the mice and further mutations in *Tg737* in subsequent manuscripts, no function for the protein associated with *Tg737* was found.

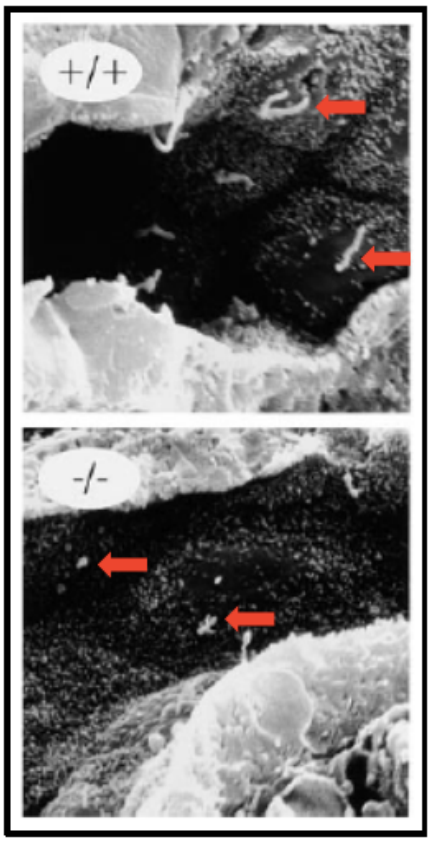

Figure 5: *orpk* mice cilia. SEM images of primary cilia on the kidney tubules of wild-type mice (Top panel) or Tg737 mutant mice (Bottom panel). Examples of cilia indicated by red arrows. *Figure adapted from Pazour, et al., 2000

A few years following the development of the *orpk* mice, however, Douglas Cole's

laboratory in collaboration with Joel Rosenbaum, George Witman and others cloned a Chlamydomonas IFT subunit, IFT88, in order to elucidate its function as an IFT particle. Amino acid sequence analysis of IFT88 carried out by the group showed that the protein was very likely to be a homologue of both mouse Tg737 and human Tg737 (Pazour et al., 2000). As IFT88 null chlamydomonas failed to form flagella and IFT88 and Tg737, a polycystic kidney-like disease gene, appeared to be homologues, the researchers looked at the primary cilia on the kidney tubules of both WT and *orpk* mice. Scanning electron microscopy (SEM) analysis of *orpk* kidney tubules taken from 4 day old mice revealed substantially shorter cilia than those of WT mice, measured at around 1um and 3um, respectively (Fig. 5)(Pazour et al. 2000). Of note, the *orpk* mouse is believed to carry a hypomorphic mutation in the *Tg737* allele, resulting in low but observable levels of *Tg737*-associated protein (Murcia, et al., 2000). Further studies, published by Richard Woychik's group at about the same time as the IFT88/ *Tg737* manuscript, of the *Tg737* gene show that null mutations result in a much more severe phenotype with a failure to develop past mid-gestation due to multiple defects, including those in neural tubes and left-right symmetry, and, of particular importance, a failure to express the central cilium on ventral node cells (Murcia et al., 2000). Taken together, the work done by these labs demonstrated for the first time that defects in ciliary health, in this case due to disruption in IFT, may lead to human disease.

An insight into how ciliary health affects kidney health, and the finding that validated Zimmerman's hypothesis, came from Praetorius and Spring a year later

when they demonstrated that the primary cilium of cultured kidney cells has the ability to serve as a mechanoreceptor, potentially sensing flow in kidney tubules. Praetorius and Spring observed that when the cilium is bent through being pushed by flow or pulled by suction, the cell connected to the cilium responds by increasing cellular calcium levels (Praetorius and Spring, 2001). This calcium increase was also shown to spread to neighboring cells, likely through gap junctions, suggesting that the primary cilia of cells lining the kidney tubules have the ability to affect the physiology of not only the cells they are attached to but also potentially the tissue as a whole.

The primary cilium's first link to development

Shortly after the connection was made between ciliary health, specifically IFT mutations, and kidney disease, Kathryn Anderson's laboratory of the Sloan-Kettering Institute made the observation that mutations in IFT led to defects in Hedgehog (Hh) signaling of developing mice (Huangfu et al., 2003).

The Hedgehog signaling pathway, first described in 1980, is known to be crucial for the correct patterning of the neural tube and limb buds during embryogenesis as well as development of multiple organ systems (McMahon et al., 2003; Wong and Reiter, 2008). Three Hh genes have been identified in mammals to date- Sonic Hedgehog, Indian Hedgehog, and Desert Hedgehog. While a role for Desert hedgehog has been identified in spermatogenesis and Indian hedgehog appears to function in bone development (Wong and Reiter, 2008), Sonic hedgehog (Shh) appears most crucial for development as well as

continued homeostasis (Chiang et al., 1996; Echelard et al., 1993). Not surprisingly, mutations contributing to irregular Shh signaling have been implicated in multiple birth defects, including cyclopia, and several cancers (Hooper and Scott 2005).

The Anderson laboratory, while looking for mutations affecting embryonic patterning in mice, observed two different mouse mutants, termed *wimple* (*wim)* and *flexo* (*fxo*). The embryonic mice were found to arrest at mid-gestation, lacking populations of ventral neural cell types. In addition, the developing heads of *wim* embryos failed to close the neural tube, and *fxo* mutants demonstrated preaxial polydactyly. As these phenotypes are hallmarks of Shh signaling defects (Wong and Reiter, 2008) with proper development dependent on concentration and time of exposure to Shh ligand, the group began mapping the mutations responsible to determine which step of the Hh pathway might be affected. Surprisingly, both mutations were mapped to genes associated with IFT. *Wim* was identified as a new mouse homologue of Chlamydomonas IFT172 and *fxo* was determined to be another hypomorphic mouse allele homologous to Chlamydomonas IFT88 (Huangfu et al., 2003). Further experiments involving these two alleles allowed the group to generate two hypotheses of the role of IFT in Hh signaling. The first explanation they developed gives the primary cilium a role in the signaling pathway. Recognizing that IFT particles are necessary for the development of primary cilia, the authors suggested that a signal originating from the cilia might be necessary for proper Hh signaling and without healthy IFT particles, the cilia would not be capable of signaling. The other hypothesis they

put forward is that cilia actually have no role in the Hh signaling pathway but that IFT particles have more than one function- one in developing and maintaining cilia and the other in cellular protein trafficking outside of the cilium. The later hypothesis suggests IFT particles may be responsible for trafficking Hh proteins to the correct cellular location for signaling to occur.

Shortly after the publication of the Anderson lab's findings, Jeremy Reiter's group at the University of California, San Francisco provided evidence that the first hypothesis was likely correct (Corbit et al., 2005). In doing so, the Reiter lab showed a key activator of the Hh pathway, Smoothened (Smo) locates to the primary cilium and that ciliary localization of Smo is necessary for activation of the Hedgehog pathway (Corbit et al., 2005).

While linking kidney dysfunction to mutations in ciliary proteins created a tremendous boost to the field of ciliary biology, the impact of discovering a crucial signaling pathway in human development that was connected to the organelle led to heightened interest in studies of this once overlooked structure. Since its association with Hh signaling was suggested by the Anderson lab and confirmed by the Reiter lab, the primary cilium has been associated with multiple other signaling cascades, including wnt signaling and platelet derived growth factor (PDGF) signaling, in addition to the previously described mechanosensation in the kidney tubules (Lancaster et al., 2011; Schneider, et al., 2005; Praetorius and Spring, 2001).

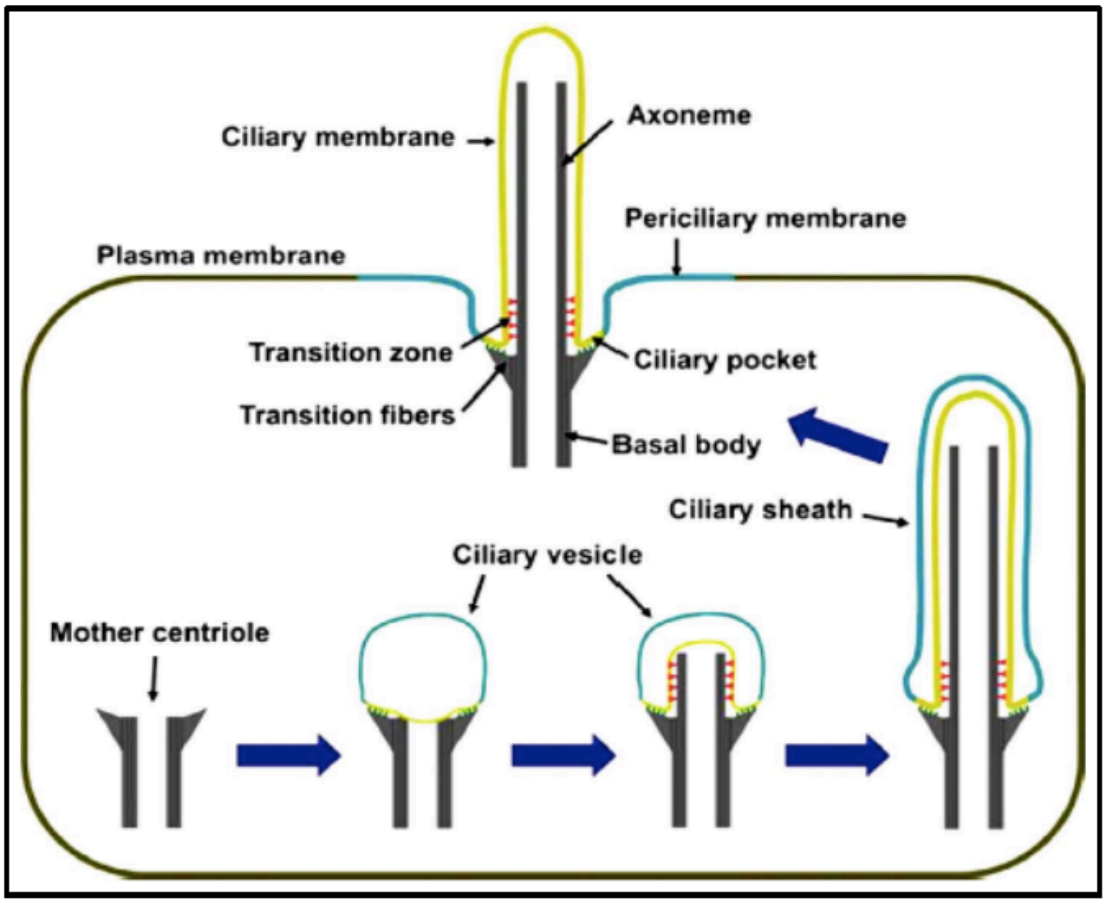

Figure 6: Initiation of ciliogenesis. The mother centriole captures a ciliary vesicle after an unknown cellular signal. The vesicle elongates before fusing with the cellular membrane. *Figure adapted from Garcia-Gonzalo and Reiter, 2012

A closer look at ciliary formation and structure

With a few exceptions, primary cilia are found on the surface of almost every quiescent or terminally differentiated cell in the body (Wheatly et al., 1996). During cellular replication, however, the pair of centrioles that make up the basal body are found away from the membrane and more closely associated with the nucleus at the center of the centrosome (Dawe et al., 2007). During cellular replication, the centrosome is composed of a mother and daughter centriole surround by pericentriolar matrix. The centrioles themselves are barrel-shaped

and composed of triplet microtubules, which are arranged in a 9-fold symmetrical manner (Prosser et al., 2015). The mother centriole, which is passed on from the mother cell to the daughter cell during division, is distinguishable from the daughter centriole in that it has distal and sub-distal appendages protruding from its sides (Kobayashi and Dynlacht, 2011) with the sub-distal appendages appearing to help anchor microtubules to the centriole (De Brababder et al., 1982; Piel et al., 2000).

The conversion of the centriole pair from functioning at the centrosome to developing into the basal body of the cilium occurs after an unknown signal (Kobayashi and Dynlacht, 2011). The first step, however, involves the anchoring of the mother centriole to a cellular vesicle (Sorokin, 1962). The mother centriole then begins to nucleate the microtubule shaft, composed of nine, doublet microtubules, that eventually becomes the ciliary axoneme and, in doing so, invaginates the side of the newly attached vesicle. As the microtubule shaft continues to grow, the whole complex begins migrating to the cellular membrane where eventually the vesicle surrounding the microtubule shaft fuses with the cellular membrane (Fig. 6)(Sorokin, 1962). At the membrane, the distal appendages of the mother centriole appear to anchor the newly formed basal body in place while striated rootlets from the bottom of the basal body can be observed extending into the cytoplasm generating further support for the base of the cilium (Tachi et al. 1974). Immediately proximal to the basal body, where the triplet microtubule formation of the mother centriole changes to a doublet formation, the transition zone of the cilia begins. Visible Y-link structures can be

seen in the transition zone, which appear to connect the microtubule axoneme to the ciliary membrane (Fig. 7). These links are likely providing further support for the structure and potentially acting as a diffusion barrier to help maintain the proteomic identity of the primary cilium (Kobayashi and Dynlacht, 2011; Craige et al. 2010). Past the transition zone, the axoneme continues, maturing into the cilia dictated by the cell type.

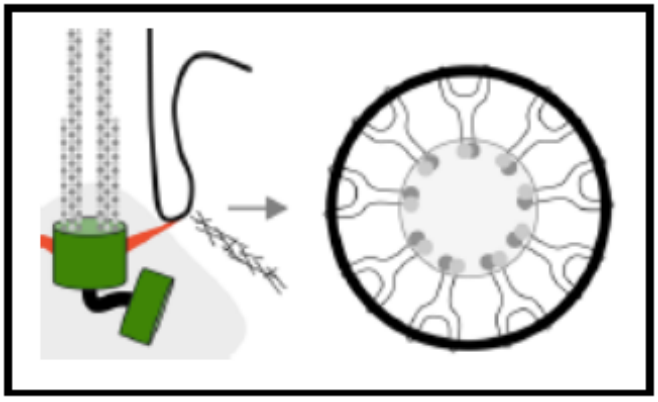

Figure 7: Y-links. Cross-section illustration of the Y-links at the transition zone, immediately proximal to the top of the mother centriole/ basal body. *Figure adapted from Basten and Giles, 2013

Understanding the ciliary proteome- Centrosomal protein 290 kDa (CEP290)

While initial studies on the IFT complexes have helped to identify new ciliary proteins, link the organelle to multiple signaling pathways, and connect mutations in ciliary genes to human disease, our understanding of the proteomic identity of the cilia is only just beginning to take shape. Of the three ciliary regions, the transition zone remains the least understood, both structurally and functionally. One transition zone protein, and the topic of this discussion, that the Bennett laboratory has focused on in recent years is Centrosomal protein 290 kDa (CEP290). First identified from a human brain cDNA library in 1997 (Nagase et al., 1997), CEP290 has been shown to localize to multiple cellular locations

depending on cell type and cell cycle phase. These locations include the centrosome, specifically the distal ends of each centriole (Tsang et al., 2008), during interphase (Valente et al., 2006), the basal body during G_0 (Gordon et al., 2008), the pericentriolar matrix particles (Kim et al., 2008), and the transition zone of chlamydomonas flagella and mammalian connecting cilia (Craige et al., 2010, Cideciyan et al., 2007). Of utmost importance, Brian Dynlacht's group at New York University's school of medicine demonstrated that siRNA knockdown of *CEP290* mRNA in cells suppressed the formation of primary cilia.

Localization of CEP290 to the transition zone of mammalian photoreceptors is specifically important to the Bennett laboratory, due to our interest in Leber Congenital Amaurosis (LCA). LCA is an early onset, retinal degenerative disease, typically causing severely impaired vision first recognized in infants and young children. What little vision the patients have early in life, is lost due to the degenerative nature of the disease. Of all known LCA cases, mutations in *CEP290* are believed to be account for over 20% of cases of LCA. In addition to retinal disease and very characteristic of ciliary genes, mutations in *CEP290* are also associated with a spectrum of other diseases, including Senior Loken Syndrome, Joubert Syndrome and Joubert Syndrome Related Disorders, as well as Meckel-like and Meckel Gruber Syndrome (den Hollander et al., 2006; Genetics Home Reference, 2015; Brancati et al., 2007; Genuardi et al., 1993; Ahdab-Barmada and Claassen, 1990). These disease states are all classified as ciliopathies due to the observation that inflicted patients have defects in ciliary health.

Structure

Human CEP290 is a relatively large protein, composed of 54 exons with an open reading frame of approximately 7.9 kb and molecular weight of 290 kDa (Tsang et al., 2008; Guo et al., 2004). The amino acid sequence is known to encode 13 coiled-coil domains, making up over 60% of the protein (Guo et al., 2004; Sayer et al., 2006) In addition, the protein contains a region of sequence similarity to Structural Maintenance of Chromosomes (SMC) chromosome segregation ATPases, three tropomyosin homology domains, six KID motifs, an ATP/GTP binding site motif A (P-loop), and a nuclear localization signal (Sayer et al., 2006).

Function

Most of our knowledge related to CEP290's potential function in the cell is speculative through observing its interaction with other cellular and ciliary proteins. In 2010, however, George Witman's laboratory published a study using chlamydomonas to identify a potential ciliary role of CEP290 for the first time. Like many ciliary proteins, CEP290 is highly conserved across species, including between humans and chlamydomonas (Craige et al., 2010). Using EM, Witman's group was able to show that CEP290 localized to the transition zone of the flagellum (Craige et al., 2010). Cross-sections of the structure allowed the localization to be determined at higher resolution with antibodies specific to CEP290. These studies showed the protein's position on or adjacent to the Y-link, a position where it could help secure the relationship of the ciliary axoneme

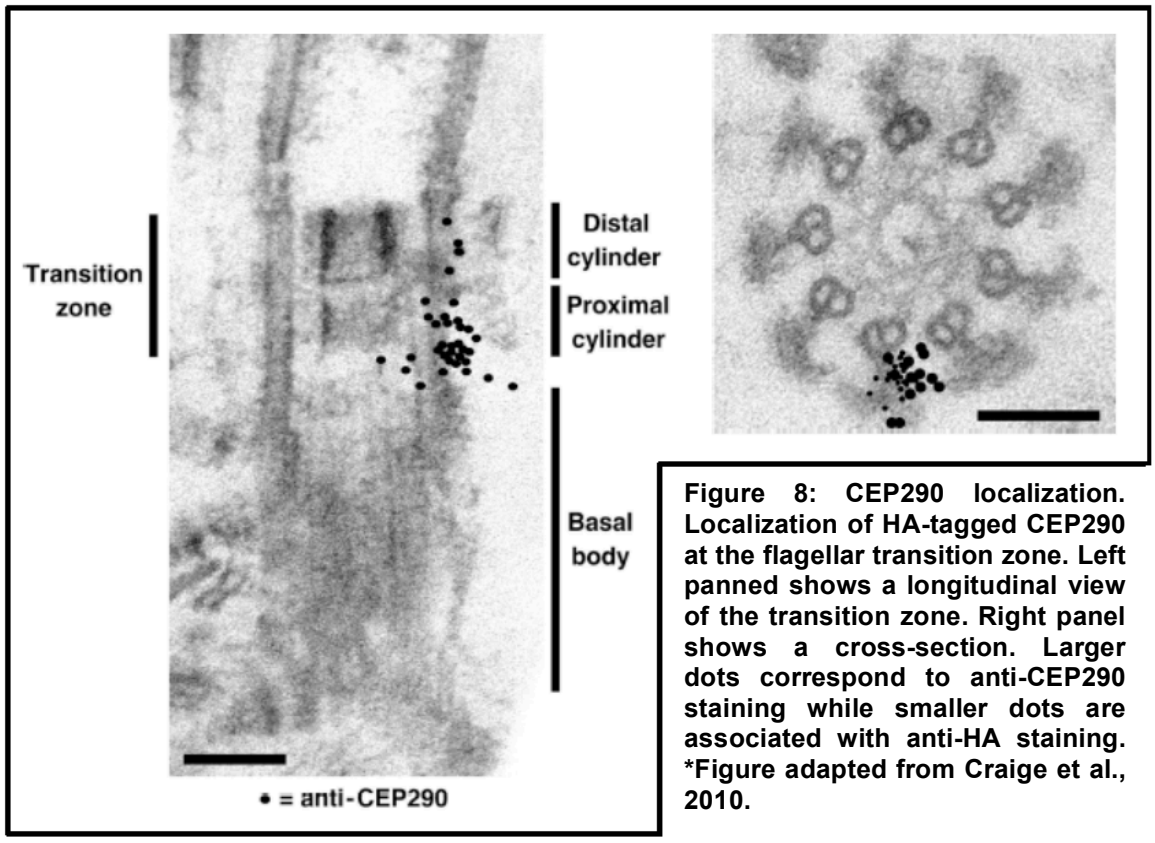

Figure 8: CEP290 localization. Localization of HA-tagged CEP290 at the flagellar transition zone. Left panned shows a longitudinal view of the transition zone. Right panel shows a cross-section. Larger dots correspond to anti-CEP290 staining while smaller dots are associated with anti-HA staining. *Figure adapted from Craige et al., 2010.

and membrane (Craige et al., 2010)(Fig. 8). Interestingly, further analysis of *Cep290* mutant flagella by EM showed that the transition zone Y-links were almost completely absent (Fig. 9), suggesting CEP290 may contribute to these Y-links and thus, flagellar and ciliary stability.

The flagella of *cep290* mutants were characterized to be very short with some observed to elongate with time. Examining these short flagella by EM, the group noticed points where the membrane seemed to bulge around areas of high electron density, a phenotype observed in chlamydomonas lacking proteins associated with retrograde IFT. Analyzing these flagella by western showed mutant flagella to contain uncharacteristically high levels of IFT complex B proteins and low levels of IFT complex A proteins. However, through monitoring

the IFT activity by DIC, both anterograde and retrograde trafficking was normal. As one hypothesized role of CEP290 is that it forms a diffusion barrier at the base of the cilium, the group also analyzed the flagellar levels of other known ciliary proteins, finding mutant cilia to be enriched in some proteins and completely lacking others. These findings suggested CEP290 might in fact serve as a diffusion barrier, a function distinct from its IFT function.

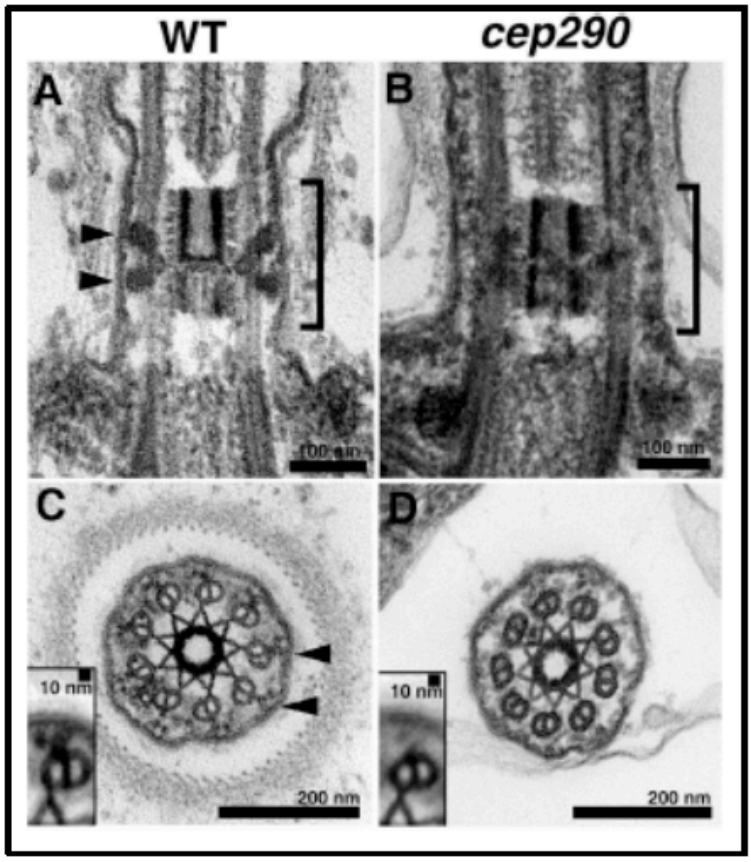

Figure 9: Comparison of Y-links. Y-links visible in WT flagella appear compromised or absent in mutant *cep290* flagella. Inset images in C and D show magnified examples of the areas typically composed of the Y-links. *Image adapted from Craige et al., 2010

Recently, the Bennett laboratory has extended these findings to human CEP290, identifying both a microtubule binding region of the protein as well as a membrane binding region through a series of immunofluorescence and biochemical experiments (Drivas et al., 2013). These regions are likely critical for CEP290's roles in the cell.

While a cellular role for CEP290 is beginning to be defined, our understanding of the variable pathogenesis resulting from *CEP290* mutations remains limited. Guided by many of the previously reported findings described above and a relatively defined patient population, I sought to determine a mechanism by which *CEP290*-associated disease could be explained.

CHAPTER 2- Model of *CEP290*-associated disease pathogenesis

As mentioned previously, mutations in *CEP290* are associated with a spectrum of disease states including Leber congenital amaurosis (LCA), Senior-Loken syndrome (SLS), Joubert syndrome (JS), Joubert syndrome-related disorders (JSRD), Meckel-like syndrome (ML), and Meckel Gruber syndrome (MKS). All of these diseases are classified as ciliopathies due to deficits in ciliary structure and/or function that patients with these diseases suffer. While mutations in *CEP290* can lead to any one of these diseases, why one mutation leads to LCA and another mutation is associated with MKS has previously been unexplained. In trying to understand this, I began to wonder if perhaps the location of the mutation in the open reading frame that encodes each protein was also playing a role in the pathogenesis of associated disease. Using a combination of published *CEP290* genotypes and phenotypes as well as cell lines generated from a population of *CEP290* patients, I, together with Theodore Drivas explored this thought, eventually proposing a model of disease pathogenesis whereby disease severity was associated with level of functional CEP290 protein. Specifically, I hypothesized that mutations predicted to result in low levels of protein would lead to more severe disease phenotypes than mutations predicted to result in higher relative levels of protein.

Leber congenital amaurosis, first described by Theodor Leber in 1869, is an autosomal recessive form of retinal degeneration, which typically leads to severe visual deficits early in life (Perrault et al., 2010). Considered the most

severe of inherited retinal dystrophies because of its early onset, mutations in at least 18 different genes can lead to LCA. Included in this set is Retinal Pigment Epithelium-Specific Protein 65 kDa (RPE65) in which the disease is classified as LCA2, nicotinamide monocucleotide adenylyltransferase 1 (NMNAT1) in which the disease is classified as LCA9 (Koenekoop et al., 2012), and CEP290 in which the disease in classified as LCA10 (den Hollander et al., 2006). The common symptom in all LCA patients is retinal disease.

Patients afflicted with Senior-Loken syndrome suffer from both retinal involvement as well as severe kidney disease. SLS is also an autosomal recessive disease, with roughly one in 1,000,000 people affected worldwide. Kidney disease in SLS patients takes the form of cyst development early in life, which typically leads to renal failure by adolescence (Genetics Home Reference, 2015). In addition to *CEP290*, there are currently five other known SLS disease genes.

Mutations associated with Joubert Syndrome lead to hypotonia, ataxia, oculomotor apraxia, and additional symptoms due to a malformation, hypoplasia or aplasia of the cerebellar vermis, in the patient's midbrain-hindbrain region. This finding is detected through magnetic resonance imaging and is termed the "molar tooth sign" (Brancati et al., 2007). In addition to this classical representation of JS, patients with JSRDs present with additional disease manifestations including findings associated with LCA and SLS. Most patients

with *CEP290*-associated JS fall into the category of having a JSRD with retinal and kidney involvement (Brancati et al., 2007).

Meckel-like and Meckel Gruber Syndrome fall into the most severe end of the spectrum of *CEP290*-associated disease. These autosomal recessive diseases affect multiple organ systems including the eyes, kidneys, brain, liver, skeletal, and reproductive system (Ahdab-Barmada et al., 1990). Fetuses afflicted with MKS rarely survive past birth and those babies that do generally die within the first few months due to respiratory difficulties or kidney failure. ML patients have been reported to live slightly longer, with one patients reported to have survived until 43 months of age (Genuardi et al., 1993).

While it is accepted that the illness of *CEP290* patients who fall into this spectrum of diseases is due to the role that CEP290 plays at the primary cilium across multiple cell types, there has been much speculation attempting to explain the pleiotropic nature of *CEP290*-associated disease. As many mutations in *CEP290* are classified as nonsense mutations, it is tempting to speculate that the observed disease spectrum is associated with severity of a truncation. In this model, nonsense mutations that led to more severe truncations and shorter protein fragments would result in more severe disease. Due to nonsense-mediated decay (NMD), however, nonsense mutations rarely lead to the actual translation of truncated protein (Maquat, 2004), and even so, the nonsense mutations observed in *CEP290* patients would not fall into this model.

Another potential explanation of variable *CEP290*-associated phenotypes is the role that modifying alleles could play in determining eventual disease. In this model, there would be both a mutation in *CEP290* and a mutation in a different gene. This hypothesis was tested by Val Sheffield's laboratory at the University of Iowa. In this study, the group crossed mice homozygous for a partial deletion mutation in *Cep290* with mice that were homozygous null for a gene encoding a member of the BBSome protein complex, a complex known to interact with *Cep290* at the transition zone and centriolar satellites (Zhang et al., 2014). From this cross, the group observed that mice homozygous for both mutations had more severe disease than mice with just mutations in *Cep290*. In addition, mice homozygous for the *Cep290* mutation but heterozygous for the BBSome mutation were observed to have less severe disease than the double homozygous mutants but still more severe disease than mice with only mutations in *Cep290.* While this is a very interesting finding and modifying alleles likely play a part in the phenotypic diversity of many disease states, this model becomes very complicated when dealing with a protein such as CEP290, which is linked to multiple known, and likely more unknown, interacting partners.

The goal of my work was to determine a genotype to phenotype correlation using only mutations in *CEP290* and the associated disease states observed in patients. To this end, I took advantage of recently published findings (den Hollander et al, 2006; Littink et al., 2010) as well as a database of *CEP290* genotypes and phenotypes generated by Frauke Coppeiters, Steve Lefever, Bart Leroy, and Elfride De Baere at Ghent University Hospital (Coppieters et al.,

2010) to formulate a model in which the spectrum of observed *CEP290*-associated phenotypes may be explained by considering the effect of basal amounts of exon skipping of disease and wild-type alleles.

As mentioned previously, many of the mutations observed in *CEP290* patients are nonsense mutations, resulting in an early stop codon and likely leading to degradation of the mRNA message by nonsense-mediated decay (NMD) (Fig. 10). The most prominent mutation, c.2991+1655A>G, is a mutation in Intron 26 that leads to the insertion of a cryptic exon (den Hollander et al, 2006). Inclusion of the cryptic exon in the message also leads to a premature stop codon. This mutation became of interest to us because it is actually skipped about 50 percent of the time, leaving a wild-type message encoding full-length protein. As such, the mutation leads to the production of about half the protein compared to that produced by a wild-type allele. In addition to this well reported example of *CEP290* exon skipping, the den Hollander group at Radbound University Nijmegen recently described a *CEP290* nonsense mutation that induced exon skipping, leading to previously undescribed, near-full-length CEP290 isoforms (Littink et al., 2010).

Our current understanding of CEP290's role in the cell is that, in addition to potentially forming a diffusion barrier at the base of the cilium, CEP290

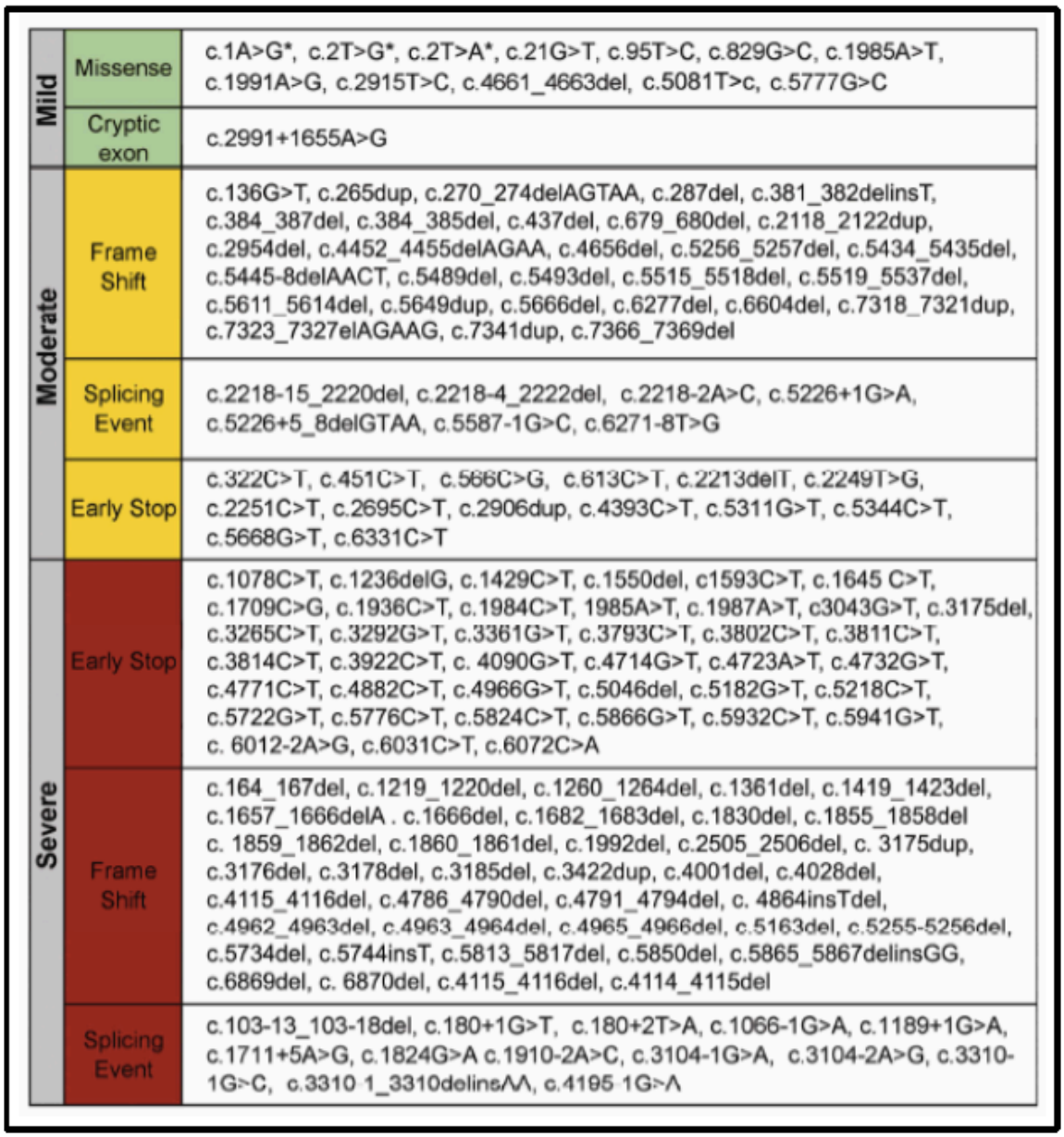

Mild	Missense	c.1A>G*, c.2T>G*, c.2T>A*, c.21G>T, c.95T>C, c.829G>C, c.1985A>T, c.1991A>G, c.2915T>C, c.4661_4663del, c.5081T>c, c.5777G>C
	Cryptic exon	c.2991+1655A>G
Moderate	Frame Shift	c.136G>T, c.265dup, c.270_274delAGTAA, c.287del, c.381_382delinsT, c.384_387del, c.384_385del, c.437del, c.679_680del, c.2118_2122dup, c.2954del, c.4452_4455delAGAA, c.4656del, c.5256_5257del, c.5434_5435del, c.5445-8delAACT, c.5489del, c.5493del, c.5515_5518del, c.5519_5537del, c.5611_5614del, c.5649dup, c.5666del, c.6277del, c.6604del, c.7318_7321dup, c.7323_7327delAGAAG, c.7341dup, c.7366_7369del
	Splicing Event	c.2218-15_2220del, c.2218-4_2222del, c.2218-2A>C, c.5226+1G>A, c.5226+5_8delGTAA, c.5587-1G>C, c.6271-8T>G
	Early Stop	c.322C>T, c.451C>T, c.566C>G, c.613C>T, c.2213delT, c.2249T>G, c.2251C>T, c.2695C>T, c.2906dup, c.4393C>T, c.5311G>T, c.5344C>T, c.5668G>T, c.6331C>T
Severe	Early Stop	c.1078C>T, c.1236delG, c.1429C>T, c.1550del, c1593C>T, c.1645 C>T, c.1709C>G, c.1936C>T, c.1984C>T, 1985A>T, c.1987A>T, c3043G>T, c.3175del, c.3265C>T, c.3292G>T, c.3361G>T, c.3793C>T, c.3802C>T, c.3811C>T, c.3814C>T, c.3922C>T, c. 4090G>T, c.4714G>T, c.4723A>T, c.4732G>T, c.4771C>T, c.4882C>T, c.4966G>T, c.5046del, c.5182G>T, c.5218C>T, c.5722G>T, c.5776C>T, c.5824C>T, c.5866G>T, c.5932C>T, c.5941G>T, c. 6012-2A>G, c.6031C>T, c.6072C>A
	Frame Shift	c.164_167del, c.1219_1220del, c.1260_1264del, c.1361del, c.1419_1423del, c.1657_1666delA . c.1666del, c.1682_1683del, c.1830del, c.1855_1858del c. 1859_1862del, c.1860_1861del, c.1992del, c.2505_2506del, c. 3175dup, c.3176del, c.3178del, c.3185del, c.3422dup, c.4001del, c.4028del, c.4115_4116del, c.4786_4790del, c.4791_4794del, c. 4864insTdel, c.4962_4963del, c.4963_4964del, c.4965_4966del, c.5163del, c.5255-5256del, c.5734del, c.5744insT, c.5813_5817del, c.5850del, c.5865_5867delinsGG, c.6869del, c. 6870del, c.4115_4116del, c.4114_4115del
	Splicing Event	c.103-13_103-18del, c.180+1G>T, c.180+2T>A, c.1066-1G>A, c.1189+1G>A, c.1711+5A>G, c.1824G>A c.1910-2A>C, c.3104-1G>A, c.3104-2A>G, c.3310-1G>C, c.3310-1_3310delinsAA, c.4195-1G>A

Figure 10: Reported *CEP290* mutations. A majority of mutations in *CEP290* are classified as frame shift or nonsense mutations. Mutations labeled with asterisks likely disrupt the start codon, potentially resulting in near normal levels of near-full-length protein after initiation of translation at the downstream AUG codon. *Figure adapted from Drivas and Wojno et al., 2015

appears to act as a stabilizing structure, helping to link the microtubule axoneme of the cilia with the surrounding membrane (Craige et al., 2010, Drivas et al., 2013) (Fig. 11). As one role of the protein appears to be connecting one structure

to another, perhaps an isoform with one less exon could still achieve this task. In addition, if stabilization, and in turn health, of the cilia determines disease, even a slight increase in the amount of cellular CEP290, full-length or near-full length, available to help stabilize the cilia may be enough to preserve its function in a given cell type. To hypothesize a mechanism by which this might be feasible, one might consider two nonsense mutations located in two different exons of *CEP290*, one exon which can be skipped while still maintaining reading frame of the protein and the other exon that can not be skipped without altering the reading frame. As it is known that the fidelity of the splicing machinery is not

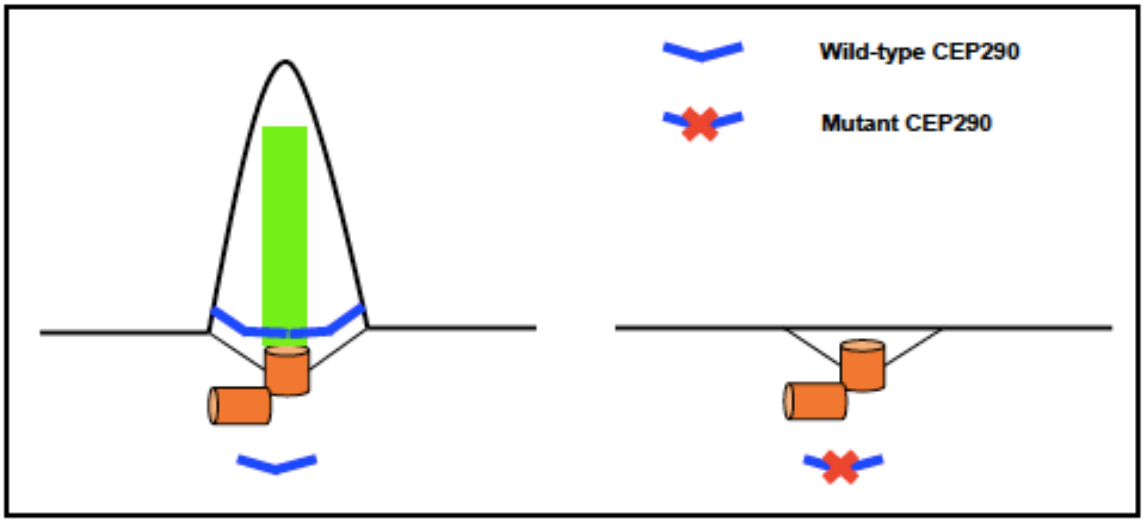

Figure 11: Illustration of one proposed role for CEP290 at the base of the cilium. In this model, Wild-type CEP290 is capable of binding the microtubule axoneme of the primary cilium to the cellular membrane. Mutant *CEP290*, however, may be unable to carry out this task due to various changes in the protein caused by mutations.

100% (Howe et al., 2003; Solis et al., 2008) and it has been suggested that 92-94% of human genes are subjected to alternative splicing (Wang et al., 2008), perhaps minimal but relevant amounts of near-full-length CEP290 will still be translated from the allele containing a nonsense mutation in an exon that can be

skipped. In contrast, no protein (full length or near-full-length) would be produced from the allele carrying a nonsense mutation that cannot be skipped (Fig. 12) without altering the reading frame of the protein.

While the amount of protein produced from randomly splicing out the exon containing the mutation on the allele would be expected to be rather minimal and not capable or rescuing the patient from disease altogether, maybe it is enough to rescue the patient from the most severe disease states. That is, in a patient with a nonsense mutation in an exon that can be skipped, successful read through of the splicing machinery would result in small amounts of near-full-length protein that ameliorates disease. In contrast, in a patient with a nonsense mutation in an exon that cannot be skipped, no protein would be produced,

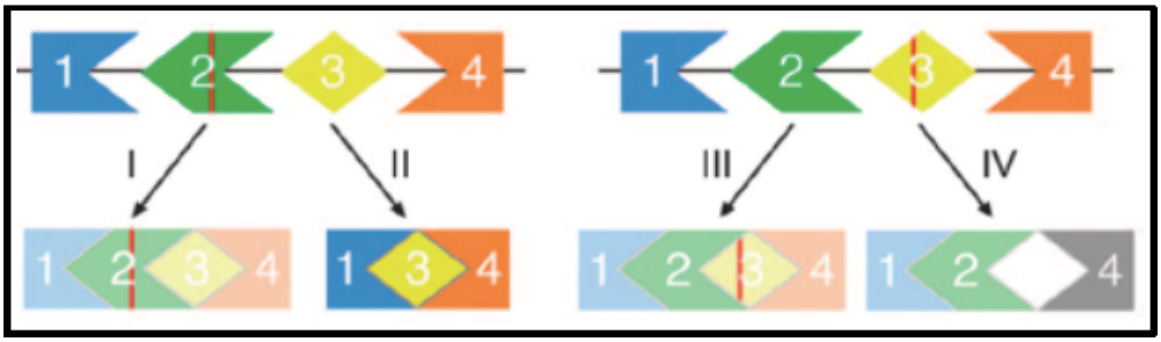

Figure 12: Proposed Model. Potential model by which low levels of near-full-length protein could be encoded by a disease allele containing a nonsense or frame shift mutation. On the left, a disease allele contains a nonsense mutation in an exon that can be skipped while still maintaining the reading frame of the protein. As a result, most mRNA message will likely be degraded through NMD (example I), however, translation of the exon-2-skipped transcript (example II) may lead to the production of a small amount of near-full-length protein. In examples III and IV, a nonsense mutation on a disease allele falls into an exon that can not be skipped without altering the reading frame of the protein. Both the original mutation-containing message and any potential exon-skipped exons are likely degraded. *Figure adapted from Drivas and Wojno et al., 2015

leading to an exacerbation of disease (Fig. 13).

The thought that variable amounts of protein could lead to differing degrees of phenotype severity is not new and, as previously discussed, was actually made during the initial IFT studies in mice. In these studies, it was observed that null mutations in the IFT88 homologue resulted in very severe developmental defects with the mice not surviving to birth. While still deadly, the phenotype of mice with hypomorphic mutations in the same gene was determined to be less severe due to small amounts of protein product being translated. This allowed the mice to survive for a few weeks before eventually succumbing to disease (Pazour et al., 2000).

With the newly developed model in mind, all classified all known *CEP290*

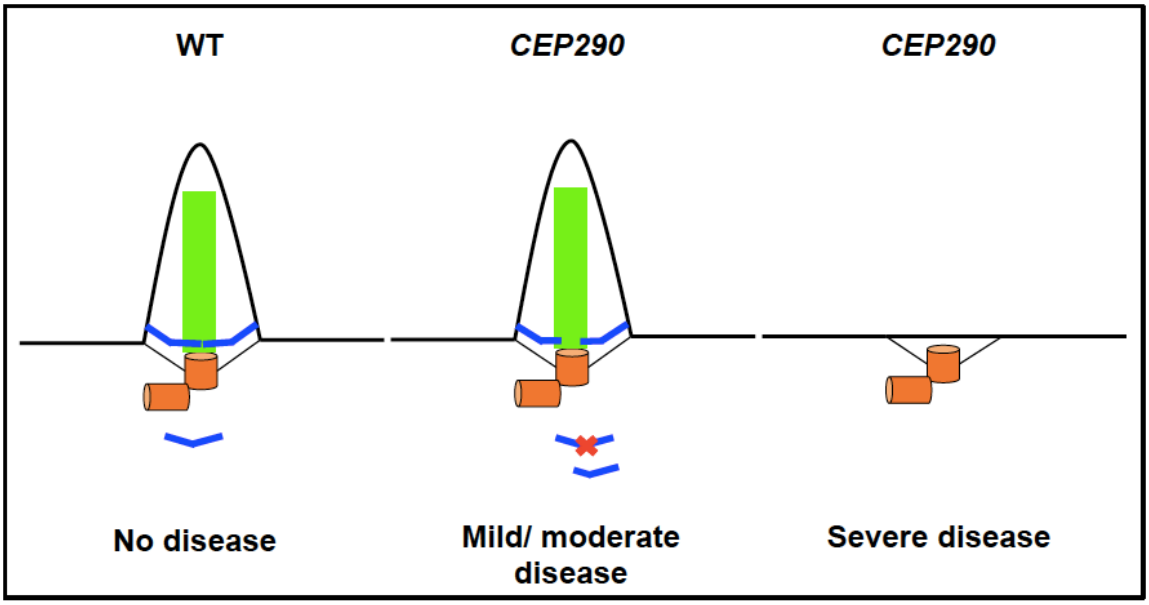

Figure 13: Model to explain the pleiotropic nature of *CEP290* mutations. The model suggests that *CEP290* mutations in exons that can be skipped may result in small amounts of near full-length protein, depicted in the middle frame. While these levels would not be enough to escape disease completely, they might contribute to a less severe disease phenotype as is depicted by no cilium formation in the right panel.

mutations were classified into categories based on the prediction of the individual

mutation's effect on the total amount of CEP290 in the cell (Fig. 10). In doing so, missense mutations were predicted to have a minimal effect on CEP290 levels. Therefore, they were classified as mild mutations. In addition, as the *CEP290* intron 26 mutation has been found to produce roughly 50% the protein of a wild-type allele (den Hollander et al., 2006), we categorized this mutation as mild, as well. Meanwhile, nonsense or frame shift mutations that fell in exons that could be skipped, potentially producing near-full-length protein (even if at low levels), were classified as moderate. Mutations falling in exons that could not be skipped without disrupting the reading frame of the protein, and which would not lead to production of any protein, were classified as severe (Fig. 10).

After classifying reported mutations based on the prediction of their effect on CEP290 protein levels, we began to correlate the genotypes and phenotypes of individual patients with *CEP290* mutations to test the hypothesis. To do so, the *CEP290* alleles of each patient were determined to be mild, moderate, or severe. Patients with a mild mutation on each allele were predicted to have relatively high amounts of CEP290 protein and therefore, the least severe disease, (i.e. LCA, with retinal findings, only). Patients with one mild and one moderate or severe mutation were predicted to have slightly less relative amounts of CEP290 protein. With the decrease in predicted protein levels, those patients were predicted to be afflicted with more severe disease, including SLS. Meanwhile, patients with two moderate mutations were predicted to generate low levels of CEP290. Thus, it was predicted that their phenotypes would fall into even more severe disease states yet, including JS and JSRD in addition to SLS. Finally, patients with alleles

classified as either moderate/severe or severe/severe were predicted to produce relatively little protein or no protein at all. These patients were predicted to be in the most severe end of the disease spectrum with phenotypes in the moderate/severe group including SLS, JS, JSRD, and ML and phenotypes in the severe/severe group including JSRD, ML, and MKS (Fig. 14).

In applying the actual phenotypes of the patients to our prediction of their relative CEP290 protein levels and hypothesizing that the predicted protein amounts produced by a given patient's *CEP290* alleles might correlate with their

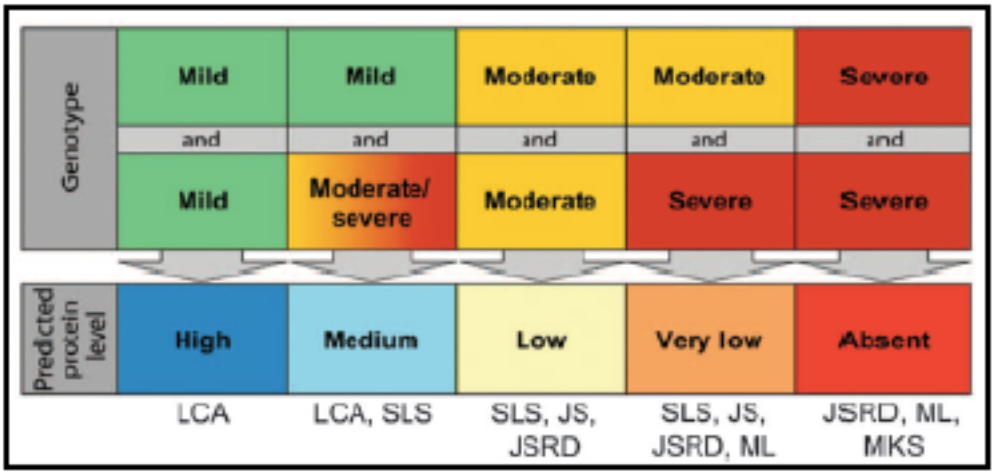

Figure 14: Classification of *CEP290* genotypes. Each allele was assigned a severity classification. The classifications were used to predict protein levels and phenotype. *Figure adapted from Drivas and Wojno et al., 2015

observed disease severity, we found the predicted protein amounts were indeed significantly associated with a given patient's phenotype ($P<0.0001$, Fisher's exact test) (Fig. 15). Of those patients with an LCA phenotype, 90 percent were predicted to have medium to high levels of CEP290. Meanwhile on the other end of the disease spectrum, all ML or MKS patients were predicted to have low to absent levels of CEP290. In between these two extremes, the level of predicted

protein varied as might be expected, with slightly higher levels weighted to the less severe phenotypes and slightly lower predicted levels falling towards the more severe end of the spectrum.

While the reported genotypes and associated phenotypes appeared to fit nicely into the model, the phenotypes of 32 of the 250 patients analyzed from the

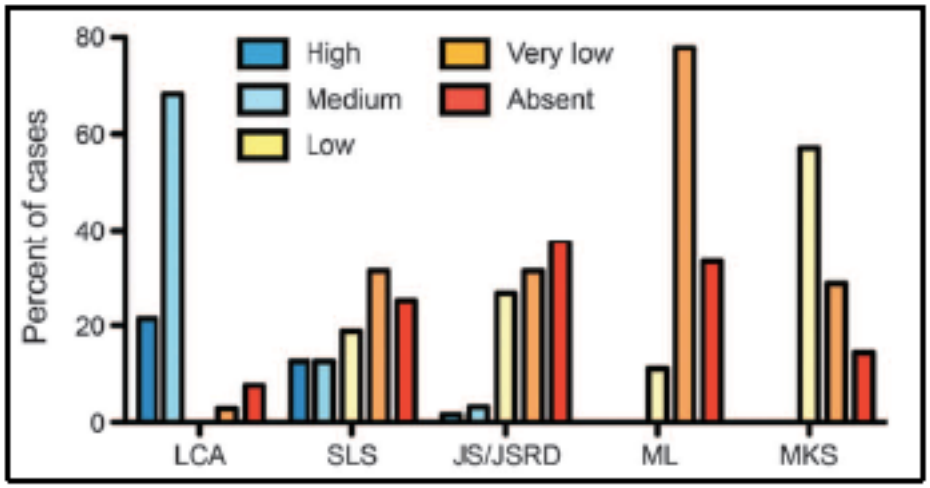

Figure 15: Predicted CEP290 protein level of patients grouped with actual phenotype. In general, patients who are predicted to have higher amounts of protein are observed to have less severe disease. *Figure adapted from Drivas and Wojno et al., 2015

literature were more severe than we would have predicted based on their genotypes. That is, while we predicted those patients to have low levels of near-full-length protein with phenotypes in the middle of the spectrum, their phenotypes actually fell into the most severe group. In looking closer at these cases, it was noted that 23 of the 32 patients had mutations that clustered in two regions of CEP290, exons 6 and 9 in the N-terminal region and exons 40 and 41 towards the C-terminal portion of the protein (Fig. 16). Mapping the location of these two regions on CEP290 shows that they fall in two domains that are likely

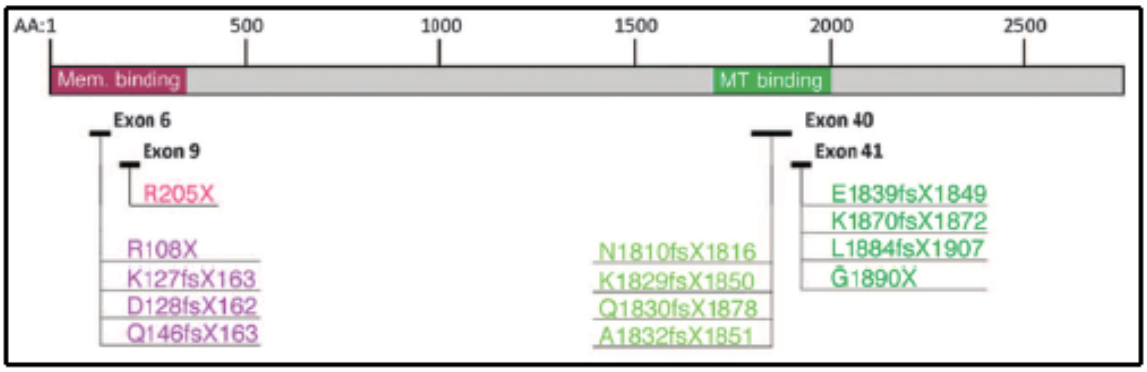

Figure 16: Illustration of the CEP290 coding region. Depicted are domains observed to be important for membrane binding and microtubule binding as well as mutations that fall in these domains. *Figure adapted from Drivas and Wojno et al., 2015

critical for the function of the protein. The first involves the N-terminal region of CEP290, which confers membrane binding. The second is closer to the C-terminal and is necessary for binding microtubules (Drivas et al., 2013). While speculative, the case might be that although we predicted these mutations to be moderate, producing low amounts of near-full-length CEP290, these particular isoforms may be totally devoid of function due to lack of a key domain. Even if these patients were expressing low amounts of near-full-length CEP290, the lack of function of the protein might push their phenotypes to the most severe end of the spectrum. In taking these assumptions into consideration, we reclassified the 23 mutations from moderate to severe. Reapplying the phenotypes of the patients to our predicted levels of their functional CEP290, the data showed that predicted protein levels were again significantly correlated with disease phenotype ($p<0.0001$, Fisher's exact test) (Fig. 17). Of note, no MKS patients were predicted to have any functional CEP290.

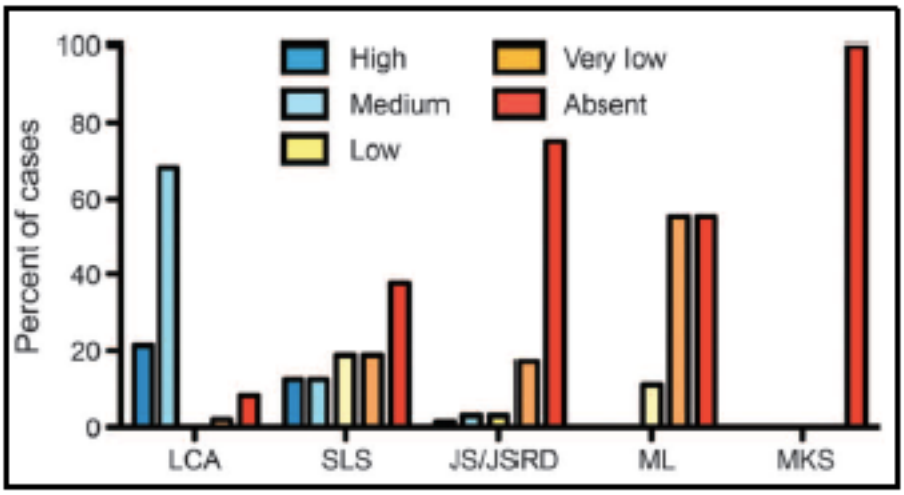

Figure 17: Predicted functional CEP290 protein levels. The predicted functional level of protein in patients grouped with actual phenotypes. Patients with higher amounts of predicted functional protein are observed to have less severe disease phenotypes. No MKS patients are predicted to have any functional CEP290. *Figure adapted from Drivas and Wojno et al., 2015

To confirm our findings, I wanted to determine if we could detect the predicted isoforms in *CEP290* patient samples. To do this, we obtained seven primary dermal fibroblast cell lines, each generated from skin biopsies taken from *CEP290* patients at the Stephen A. Wynn Institute for Vision Research of the University of Iowa. In addition to the cell lines, detailed phenotype information of each patient was also provided. This information was collected by a single clinician who was masked to the genotypes of the patients (Fig. 18).

Six of the seven patients were predicted to have high to medium levels of CEP290 protein and all of these patients had a phenotype of LCA (i.e., retinal disease only). One patient, however, was predicted to have no functional levels

Patient	Age (yrs)	Gender	Nucleotide alteration	Coding effect	Predicted protein level	Ocular symptoms	CNS symptoms	Renal symptoms	Diagnosis
54	9	F	IVS26 + 1655 A>G IVS26 + 1655 A>G	Cryptic exon Cryptic exon	High	VF	NOD	NOD	LCA
52	23	M	IVS26 + 1655 A>G Val247 739delG	Cryptic exon Exon 10 FS	Medium	VFNA	NOD	NOD	LCA
182	7	F	IVS26 + 1655 A>G Lys127 379delA 380delA	Cryptic exon Exon 6 FS	Medium	NLP	ID	NOD	LCA
294	14	M	IVS26 + 1655 A>G Thr835 2503delA 2504delC	Cryptic exon Exon 24 FS	Medium	NLP	NOD	NOD	LCA
582	19	M	Arg549Stop 1645 C>T Lys1882 5643_5644 insA	Exon 17 S Exon 41 FS	Very low	VFNA	JS	NOD	JSRD
619	5	M	IVS26 + 1655 A>G Val2093 6277delG	Cryptic exon Exon 46 FS	Medium	VFNA	NOD	NOD	LCA
620	4	M	IVS26 + 1655 A>G Val2093 6277delG	Cryptic exon Exon 46 FS	Medium	VFNA	NOD	NOD	LCA

Figure 18: Genotypes, phenotypes, and clinical information of seven *CEP290* patients. Color-coding as in Figure 14. Orange with red stripe overlay signifies mutations expected to produce low levels of CEP290 lacking exon 6 or 41. FS, frameshift; S, premature stop codon; VF, measurable visual fields; VFNA, visual fields not able to be measured, light perception only; NLP, no light perception; ID, Intellectual disability; NOD, no overt disease. *Figure adapted from Drivas and Wojno et al., 2015

of CEP290 due to two nonsense mutations, one in exon 17 and one in exon 41. This patient had been diagnosed with Joubert syndrome and retinal dystrophy, the most severe phenotype of the group. (Fig. 18)

The first goal with these cell lines was to determine if the relationship between our predictions regarding the relative amount of protein in the cells and actual, measured amounts in samples held true. To do so, we analyzed the amount of CEP290 in each of the cell lines and compared these amounts to three wild-type controls. Confirming our predictions, the highest amount of CEP290, at roughly 50% of wild-type levels, was observed in the cells generated from patient 54, who we predicted would have the highest amount of CEP290 protein due to having two mild *CEP290* mutations (Fig. 19). In addition, CEP290 amounts isolated from the cells of patients that we predicted to have medium levels of

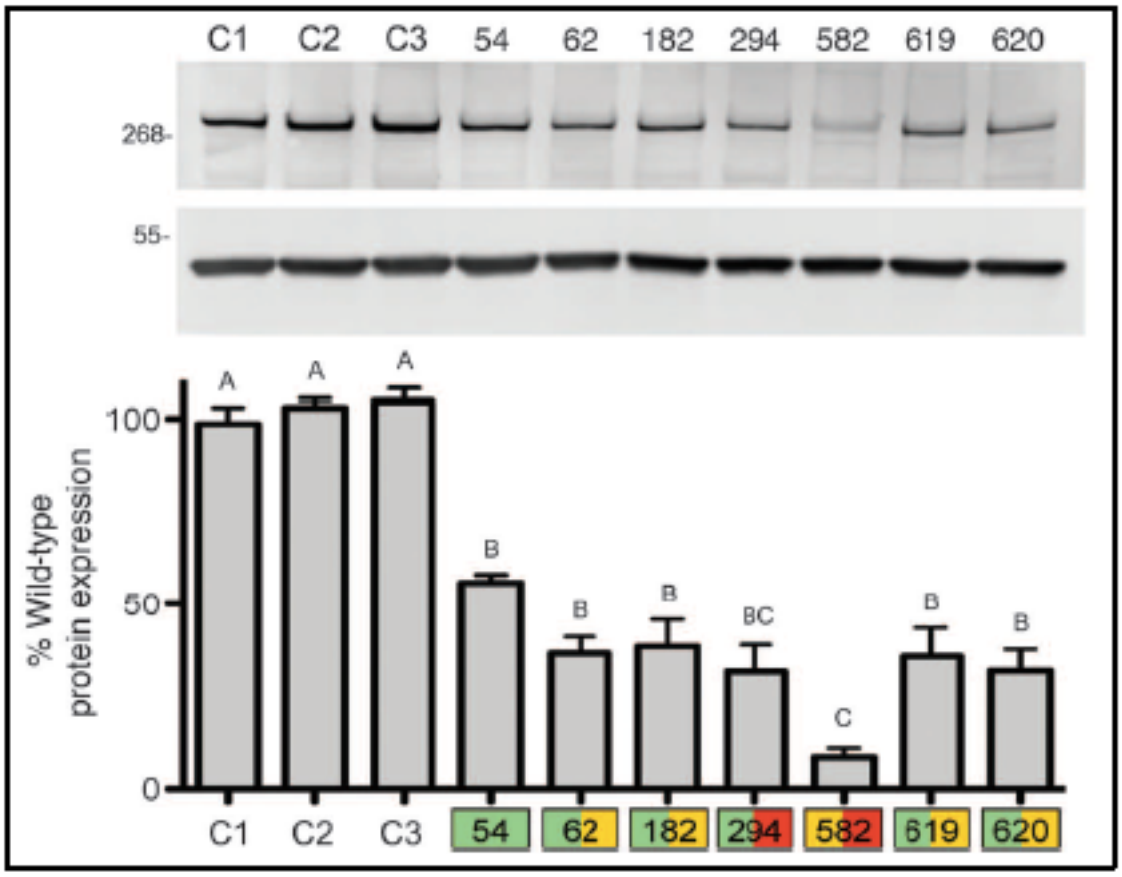

Figure 19: Observed CEP290 levels. Predicted CEP290 protein levels of the patients and three controls correlates with observed protein expression by western blot. Top panel- Primary dermal fibroblasts associated with each patient and three controls were lysed and protein run by SDS-PAGE. Bands associated with CEP290 were observed around 290 kDa. Loading control alpha-tubulin was also probed in each lysate. Bottom panel- Densitometric analysis of blot in top panel. *Figure adapted from Drivas and Wojno et al., 2015

protein were all observed to be lower than those observed in patient 54 but still around 33% of wild-type levels. Of particular interest, however, was the amount of CEP290 observed in the cells isolated from patient 582. Despite two nonsense mutations (one skippable but likely resulting in non-functional protein), a small amount of CEP290 (8.5% of wild-type levels) was observed in these cells. This finding is contrary to traditional models of nonsense mutations that would dictate no full-length or near-full-length levels of protein in these cells due to either

truncation of the protein or degradation of the message by nonsense mediated decay.

We next sought to determine if the isoforms that our model predicted could be detected in the patient isolated cell lines. To correlate this, we generated custom polymerase chain reaction (PCR) assays for each isoform of interest. These included isoforms lacking exon 6, exon 10, exon 41, and exon 46, exons that could be skipped without altering the reading frame. Complementary DNA (cDNA) generated from the RNA isolated from the patient specific cell lines was used as the template of the PCR reactions. We attempted to isolate the exon 6 skipped isoform using cDNA from patient 182, the exon 10 skipped isoform using cDNA from patient 62, the exon 41 skipped isoform using cDNA from patient 582, and the exon 46 skipped isoform using cDNA from patients 619 and 620. In addition, cDNA isolated from wild-type control fibroblasts was also

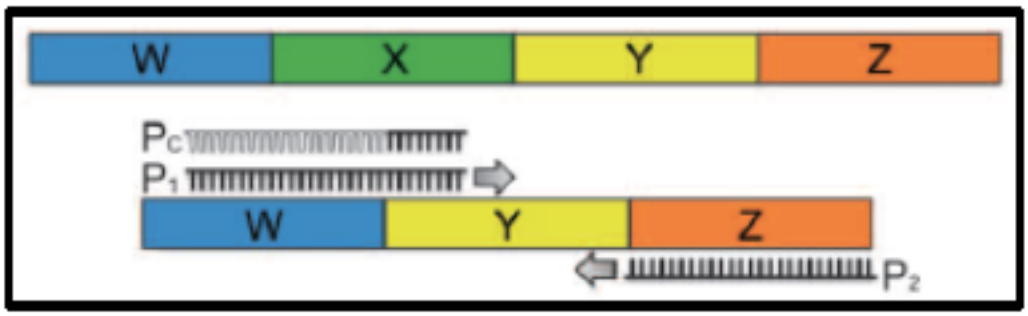

Figure 20: Isoform detection using a three-primer PCR approach. Exon X signifies the exon to be skipped. *Figure adapted from Drivas and Wojno et al., 2015

used as a template for each assay. The assays were designed to amplify the isoform using a three primer approach, as depicted with W-X-Y-Z signifying a wild-type message and with exon X as the skipped exon (Fig.20). As illustrated, two forward primers were designed. The first primer (P_1) was designed to sit at

the hypothetical W-Y junction, which should only be present in isoforms lacking exon X. A second forward primer (P_C) was designed with a 3' portion complementary to the 5' portion of exon Y and a scrambled sequence making up the 5' portion of the primer. This primer serves as the control of the reaction. Finally, a reverse primer was designed to a downstream exon to create an amplicon of roughly 200 bp. Using this approach and the cDNA from the patient derived fibroblasts as well as control cDNA, we were able to isolate the predicted isoform in each assay using both the patient-specific and control cDNA (Fig. 21). Of note, observing the isoforms in the control cDNA led us to conclude that the

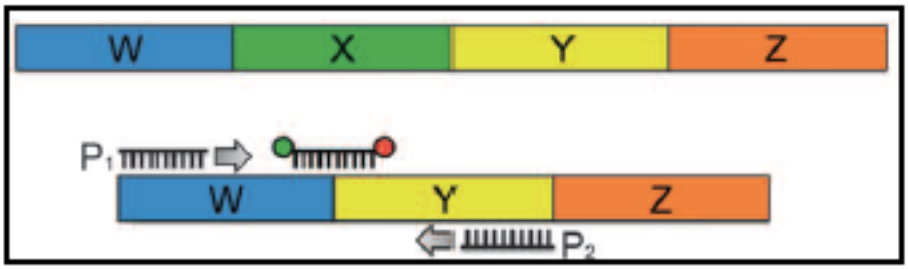

Figure 22: Quantification of isoform levels. TaqMan qPCR was used to quantitatively measure isoform levels in patient and control samples. Probe designed to sit on hypothetical border created by skipped exons. *Figure adapted from Drivas and Wojno et al., 2015

exon skipping we were observing was not influenced by an effect of each mutation, as is the case with nonsense-induced alternative splicing (Cartegni et al., 2002). Rather, the skipped isoform seemed to be another member of the cDNA population, potentially due to infidelity of the splicing machinery. As such, we termed the process by which these isoforms are produced as Basal Exon Skipping.

After observing the isoforms through traditional PCR, TaqMan qPRC assays were designed for each exon-skipped isoform in an effort to quantitatively analyze their presence in the cDNA population. The probe of the TaqMan assay was designed to sit at the hypothetical W-Y border with upstream and downstream primers specific to the exons of each particular isoform as illustrated (Fig. 22). As our standard PCR approach suggested the isoforms were not mutation-specific but likely part of the normal cDNA population, we attempted to measure the level of each isoform in the lysates of all patients-specific cells and controls. As expected, isoforms lacking exons 6, 10, 41, and 46 were detected in all cell lysates and levels are depicted as a percentage of those observed in the control sample after all values were normalized to GAPDH (Fig. 23). In most cases, the amount of all skipped isoforms in each sample seemed to

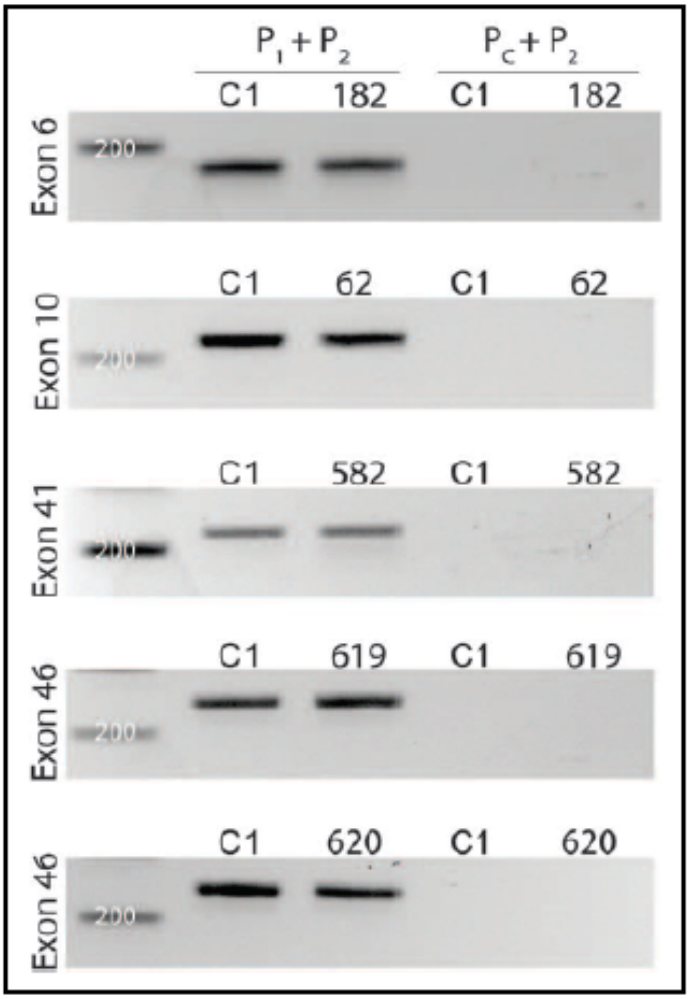

Figure 21: Isoform detection in patient and control cDNA samples. Isoforms were detected in exon 6, 10, 41, and 46-skipped transcripts in both patients and controls. *Figure adapted from Drivas and Wojno et al., 2015

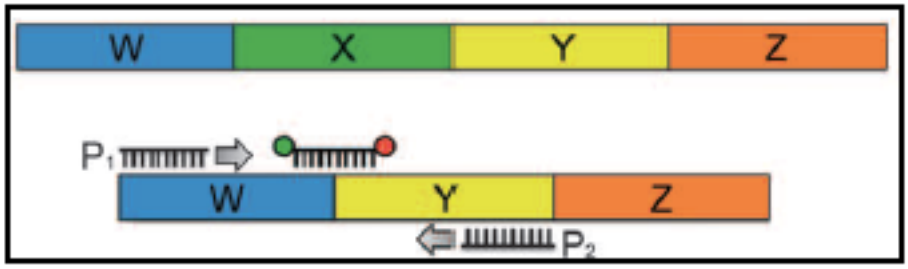

Figure 22: Quantification of isoform levels. TaqMan qPCR was used to quantitatively measure isoform levels in patient and control samples. Probe designed to sit on hypothetical border created by skipped exons. *Figure adapted from Drivas and Wojno et al., 2015

be correlated with total *CEP290* transcripts, supporting our model that a population of isoforms is likely produced through randomness of the splicing machinery. When analyzing the amount of skipped isoform specific to a given patient (such as exon 10-skipped isoforms for patient 62), however, we would have expected to see enrichment of that isoform compared to total *CEP290* levels. For example, in regards to exon 10-skipped isoforms, transcripts containing the nonsense mutation in exon 10 would likely be degraded by NMD while those isoforms skipping the mutation should survive and make up a larger percentage of total *CEP290* transcripts in the cell. To analyze this further, we normalized the level of each exon-skipped *CEP290* transcript to total *CEP290* transcript level in each patient (Fig. 24). This analysis showed an almost 6-fold increase of exon 41-skipped transcript relative to total *CEP290* transcript levels in patient 582, whose genotype includes a nonsense mutation in exon 41. While similar increases in skipped isoforms associated with the genotypes of the other patients were not observed, it should be noted that the genotypes of the other patients all included the mild intron 26 mutation, potentially concealing the

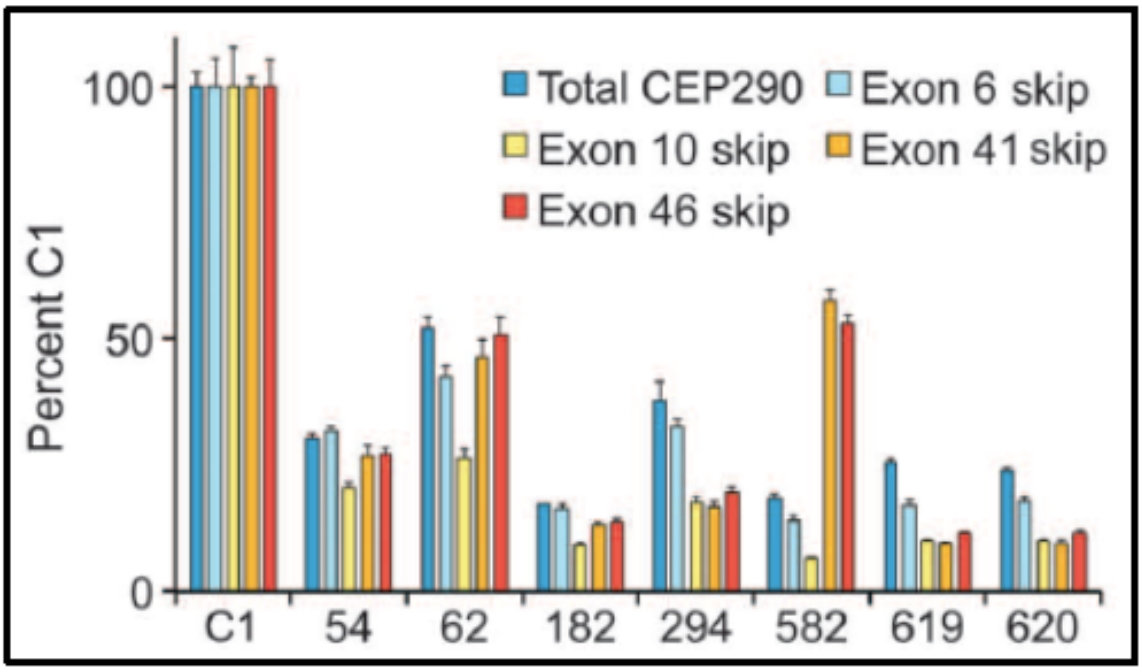

Figure 23: Comparison of isoform levels. Expression of full length *CEP290* and exon-skipped isoforms was determined for each patient and control. Relative expression for each transcript was determined using the $\Delta\Delta C_t$ method normalizing to *GAPDH* and adjusting transcript to percent of that observed in the control (C1). *Figure adapted from Drivas and Wojno et al., 2015

relative increase in skipped isoform through elevated levels of total *CEP290* transcript.

Taking into account the results presented here, we concluded the model may be one way to explain the pleiotropic nature of *CEP290*-associated phenotypes. However, to confirm the generality of the result, we sought confirmation that a similar process could affect the genotype/phenotype relationship with another protein. To investigate this, we selected another ciliary gene/protein to study: coiled-coil and C2 domain containing 2A (*CC2D2A*). CC2D2A was recently described as necessary for the successful assembly of sub-distal appendages which in turn aid in vesicle docking and anchoring of

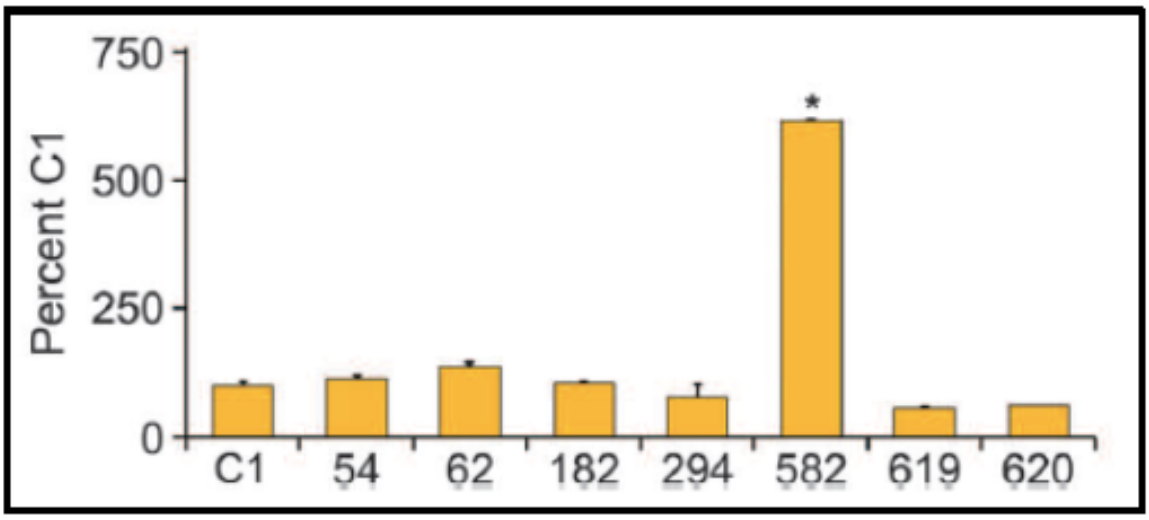

Figure 24: Exon 41-skipped isoforms. Exon 41-skipped isoforms in cDNA of patient and control fibroblasts determined by TaqMan PCR. Data normalized to total *CEP290* transcript level and adjusted to percent of normal control (C1) using the $\Delta\Delta C_t$ method. Data presented as means +/- SD (n=3). Asterisk marks significantly different mean from other, P<0.0001. *Figure adapted from Drivas and Wojno et al., 2015

microtubules to the mother centrioles (Veleri et al., 2014). Like *CEP290,* mutations in *CC2D2A* lead to a spectrum of disease states, including JS, JSRD, and MKS. In addition, many of these mutations are nonsense mutations. Unlike CEP290-associated disease, a relatively large number of *CC2D2A* mutant patients have JS without further symptoms associated with JSRDs. As such, we were able to separate the disease states into three phenotypic groups. In applying the gathered patient genotypes and phenotypes, our model again fit the patient population, with predicted CC2D2A protein expression correlating with severity of disease (P<0.0001, Fisher's exact test) (Fig. 25). Further refinement of this relationship in CC2D2A, as was undertaken for CEP290, however, is made difficult by a few factors. First, our understanding of structural and

functional domains in CC2D2A is relatively limited outside of an observed C2 domain near the C-terminal end of the protein (Tallila et al., 2008). In addition, the number of patients and described mutations is much smaller than that of *CEP290*, currently making outliers difficult to spot. Finally, *CC2D2A*-associated disease appears to be much more severe than that witnessed in *CEP290* patients, narrowing the spectrum of phenotypes observed to more detrimental disease. It will be interesting to monitor this disease group, however, as the number of described genotypes and phenotypes increases to determine if important domains of the protein might be implicated by their failure to follow the proposed model.

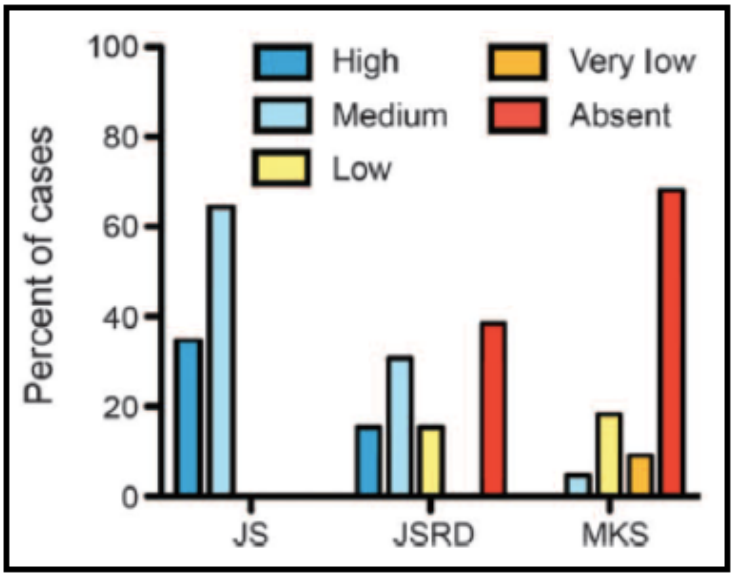

Figure 25: Application of the model to *CC2D2A* patients. Predicted protein levels in *CC2D2A* patients correlate with disease severity. *Figure adapted from Drivas and Wojno et al., 2015

Recently, in an effort to determine if these spliced isoforms could be detected in other cell types, cDNA isolated from wild-type human retinal tissue was analyzed for exon 10-skipped isoforms. Reactions using either cDNA from dermal fibroblasts, as before, or retina were run side-by-side, resulting in the isolation of exon 10-skipped isoform from both samples (Fig. 26).

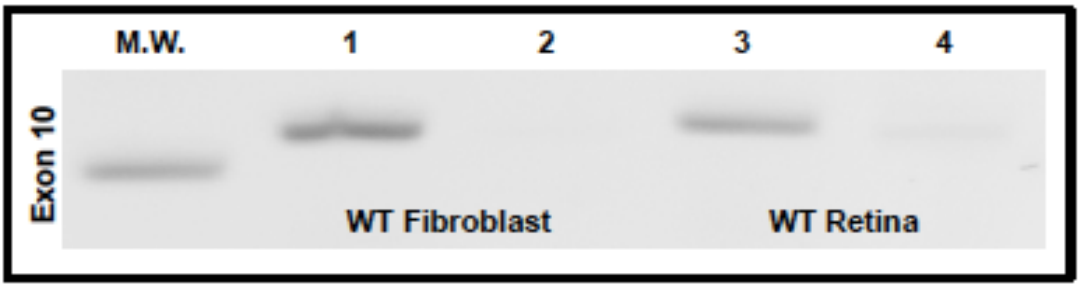

Figure 26: Detection of exon-skipped isoform in WT retina. cDNA isolated from either WT dermal fibroblast (lane 1,2) or WT retina (3,4) was used to probe for the presence of exon 10-skipped isoform. Reactions ran in lanes 1 and 3 used the experimental primer set for exon 10-skipped isoforms, and reactions run in lanes 2 and 4 used the control primer set for exon 10-skipped isoforms described in Fig. 20.

Discussion

The results of this portion of my studies provide an explanation for the observed pleiotropy caused by two ciliary disease genes, *CEP290* and *CC2D2A.* While the model offers an explanation for observations that have proven quite puzzling over the years, the suggested mechanism by which this model works may be just as interesting. Basal amounts of exon skipping, dictates that heterogeneous populations of mRNA isoforms in the body may lead to small populations of near-full-length proteins, which in many cases may retain some of the function provided by the wild-type form. It is important to note that we are predicting the levels of these isoforms to be very small, compared to the wild-type message. In fact, initial studies utilizing an RNAseq approach did not detect the isoforms that we present here, potentially due to an inability to detect minimal levels of alternatively spliced isoforms from an already low number of reads through individual *CEP290* splice junctions. However, while small and without the ability to totally eliminate disease, this heterogeneous population of protein may

be sufficient to rescue patients from the most severe form of disease when composed of the correct isoforms. Further investigation will be needed to determine if there are other diseases in which this mechanism provides global rescue. While alternatively spliced isoforms have been implicated in disease through the production of dominant-negative proteins (Solis et al., 2008), investigations into the positive benefits of alternatively spliced isoforms have been relatively overlooked- likely due to a lack of studies analyzing the mRNA populations of healthy individuals related to disease.

While we believe this model provides a potential explanation to the pleiotropic nature of *CEP290* and *CC2D2A*- associated disease, our studies were limited in a few aspects. First, we have applied this model to all tissues and cell types associated with CEP290 disease while only attempting to detect CEP290 isoforms in the cDNA of the primary dermal fibroblasts and whole retina that were available. While, exon skipping and alternative splicing has previously been reported in several tissue types (Wang et al., 2003), including human retina (Littink et al., 2010), detection of CEP290-specific isoforms in all tissues associated with *CEP290* disease would indeed strengthen our claims. In addition, an increase in the number of reported *CC2D2A* patients and an increase in the diversity of described mutations for this gene would definitely strengthen its association with this model and allow for further investigations of the protein, potentially using the model as a guide. Finally, determining if this model holds true to other pleiotropic disease genes, both ciliary and not, would be of great benefit.

Materials and Methods

Study Design

Review of CEP290 and CC2D2A genotype/phenotype relationships was carried out using published data (see below). Additional genotype/phenotype data were collected from patients seen at the retinal degeneration clinics at the Center for Advanced Retinal and Ocular Therapeutics and from the Stephen A. Wynn Institute for Vision Research. Genotyping was carried out at the John and Marcia Varver Nonprofit Genetic Testing Laboratory, University of Iowa. Tissue samples were also collected from patients seen at both centers using protocols approved by the respective Institutional Review Boards (IRBs). Molecular Genetic testing of the samples was carried out to determine transcript and protein expression as described below. Results of molecular genetic testing were correlated with the predictions based on review of genotype/ phenotype data.

Mutation analysis

Human mutations in *CEP290* were compiled from published articles and from the *CEP290* mutation database developed by F. Coppieters, S. Lefever, B. P. LeRoy, and E. De Baere at Ghent University and Ghent University Hospital, Ghent, Belgium (19). The coding effect of each mutation was noted, particularly with respect to whether an exon was predicted to be disrupted by a premature stop codon (because of either nonsense or frameshift mutations) or skipped because of a mutation affecting exon splicing. Mutations were then sorted into three groups. Mild mutations were those that were predicted to have little effect

on total CEP290 protein levels (in-frame deletions, missense mutations, truncating mutations occurring within the last exon, and splicing mutations in which there is evidence for high levels of normal transcript production). Moderate

mutations were those that were predicted to significantly reduce CEP290 protein levels (i.e., those that resulted in a premature stop codon within, or splicing mutation likely to result in the skipping of, an in frame exon). Severe mutations were those that were predicted to act as null alleles (those that resulted in a premature stop codon within, or splicing mutation likely to result in the skipping of, an out-of-frame exon). The sorted mutations are listed in fig. S1. Mutations in the gene CC2D2A were sorted in an identical fashion. For our modified CEP290 model, mutations affecting exon 6, 9, 40, or 41 were considered severe.

Patient assessment

Patients were seen at the retinal degeneration clinics of the University of Iowa, Children's Hospital of Philadelphia, or Center for Advanced Retinal and Ocular Therapeutics (University of Pennsylvania Perelman School of Medicine) where a family history was ascertained and the individuals received standard clinical examinations including assessments of visual acuity, visual fields, and retinal structure. The diagnosis of LCA was made by electroretinogram, and the diagnosis of JS was made by brain magnetic resonance imaging. Screening was carried out for renal disease and imaging studies were carried out, as warranted, for CNS (and renal) evaluations. Molecular genetic testing was carried out after obtaining IRB-approved consent/assent (plus parental permission).

Cells and cell culture

Primary dermal fibroblasts were isolated from patient skin punches after obtaining informed consent/assent, and these were grown in Dulbecco's modified Eagle's medium supplemented with 10% fetal bovine serum and 1% penicillin-streptomycin at 37°C in a humidified 5% CO2 atmosphere. Fibroblasts were passaged fewer than 10 times before analysis.

CEP290 protein

Patient fibroblasts were washed with phosphate-buffered saline, and $5X10^6$ cells were lysed by incubation in 50 ml of radioimmunoprecipitation assay buffer (50 mM tris, 150 mM NaCl, 0.1% SDS, 0.5% sodium deoxycholate, 1% Triton X-100) supplemented with a protease inhibitor cocktail for 30 min at 4°C. Cell lysates were centrifuged at 20,000g for 15 min to remove insoluble material, and the resulting supernatants were analyzed by SDS–polyacrylamide gel electrophoresis and immunoblotting using standard techniques. Blots were probed with antibodies against CEP290 (Abcam, ab85728) and a-tubulin (Abcam, ab7291) and imaged with a Typhoon 9400 instrument (GE).

cDNA isolation

cDNA was isolated from patient fibroblasts using Qiagen's RNeasy kit and Invitrogen's SuperScript III First-Stand Synthesis kit following the manufacturer's protocols.

Exon junction detection

Two primers plus a control forward primer were designed to amplify across the hypothetical exon junction of CEP290 transcripts lacking each exon examined, as in Fig. 4A, and used for PCR amplification of patient and control cDNAs. The resulting PCR products were resolved by agarose gel electrophoresis, imaged, gel-excised, and submitted for confirmatory Sanger sequencing. Primer sets for hypothetical exon junctions were as follows:

Exons 6

P_1: GAAAATGAACTGGAGTTGGCTCTTC

P_2: CACTGTCTTCCCCTCTTCTTG

P_C: CTCTCTCTCTCTCTTGGCTCTTC

Exons 10

P_1: CTTGATGAAATTCAGGTGCAGGAGC

P_2: CTGCTGTAGAGCCATAACATTAC

P_C: CTCTCTCTCTCGTGCAGGAGC

Exons 41

P_1: CCAGTGGATTACAGAATGCTAAAG

P_2: CCTGATCAACAGTCATGCCAG

P_C: CTCTCTCTCTCTCTAATGCTAAAG

Exons 46

P_1: GATTTGCCAAGATTAAAGTCTGGTAG

P_2: GATTCATAGTGCATGCTCAACTG

P_C: CTCTCTCTCTCTCTTCTGGTAG

TaqMan assay design and analysis

Custom TaqMan PCR assays were designed to specifically quantify levels of CEP290 transcript lacking particular exons as described in Fig. 4C. Additional TaqMan assays were carried out using commercially available kits for GAPDH and full-length CEP290 (Invitrogen). TaqMan assays were run using TaqMan Fast Universal Master Mix (Invitrogen), and all reactions were carried out on an Applied Biosystems 7500 Fast Real-Time PCR instrument. Relative quantification was accomplished with the DDCt method using Invitrogen's CloudSuite software. Custom primer and probe sets were as follows:

Exon 6

Primer 1:GAAGAACAAGCAAAATTTGAAAATC

Primer 2: CGTTTGTTCTCTCTTCTTAATTTGC

Probe: CGAAGAGCCAACTCCAGTTCATTTTCCA

Exon 10

Primer 1: ACAGTGACTACCGATCACAGTTGT,

Primer 2: CAAAATTAGCTTCCATTCTTCTACTTTT

Probe: AATATCTTGATGAAATTCAGGTGCAGGAGCTTAC

Exon 41

Primer 1: GATCAAGAGAATGATGAACTGAAAAG

Primer 2: CTTGTTTCGAATTCCTTCTATTTTG

Probe: AAGACTAACCAGTGGATTACAGAATGCTAAAGAAGAATT

Exon 46

Primer 1: GAAGGAAAACTTGAAGTTGTCATCTG

Primer 2: TCAACTACTTTTTTCATTAAACCAATGG

Probe: TGTCTTTCCACTTCTACCAGACTTTAATCTTGGCA

Statistical Analysis

The statistical significance of the difference between three or more means was determined using a two-way ANOVA and Tukey's HSD (honest significant difference) test. The statistical significance of the difference in predicted protein amounts across different phenotypes was determined using Fisher's exact test. Statistical analysis was performed using GraphPad Prism software 5.0b. P values <0.05 were considered significant.

CHAPTER 3- CEP290 and the initiation of ciliogenesis

While findings related to the functional processes of the primary cilium and clarification of its role in human disease have tremendously increased our understanding of the organelle over the past twenty years, we are still in the dark concerning many aspects of ciliary biology. In particular, one detail that we know very little about is the signal that begins the process of ciliogenesis. We know that with few exceptions most cells do not have a primary cilium during the cell cycle but form one shortly after entrance into G_0 (Seeley and Nachury, 2010). While a pro-ciliary signal has yet to be defined, work in recent years, has begun to identify several inhibitors of ciliogenesis. Among these proteins, the centrosomal protein of 110 kDa (CP110) appears to be the main, negative regulator of ciliogenesis (Spektor et al., 2007). CP110 appears to act by forming a complex at the distal ends of the centrioles, preventing the elongation of microtubules from the centriolar end. In addition to other negative regulators, some pro-ciliary proteins, such as CEP290, are found in this complex (Tsang et al., 2008; Jiang et al., 2012) as well. It is thought that these proteins may be kept in an inactive state by the CP110 complex, preventing them from functioning in ciliogenesis (Tsang et al., 2008).

While it is known that the CP110 complex must be removed for the elongation of the ciliary axoneme to begin, the mechanism by which this occurs is only beginning to be elucidated. A common speculation (Cao et al., 2009) is that phosphorylation of targeted ciliary proteins may be the signal that begins the

process of ciliogenesis. Specifically, recent results have demonstrated that the arrival of two kinases, tau tubulin kinase 2 (TTBK2) and microtubule-associated protein/ microtubule affinity regulating kinase 4 (MARK4), to the distal and sub-distal appendages of the mother centriole, respectively, in cells shortly after serum starvation corresponds to the dissolution of the CP110 complex (Goetz et al., 2012; Kuhns et al., 2013). With the arrival of these kinases and the exit of CP110 from the basal bodies, ciliogenesis is observed to occur. Understanding the protein population at the basal bodies shortly before ciliogenesis and identifying the final targets of these kinases, and other kinases recently described, is crucial to understanding their role, if any, in the development of primary cilia. In this chapter, the specific role of CEP290 in this process will begin to be evaluated, and a commentary on the process as a whole will be provided as an appendix.

CEP290 as a potential kinase target

Given our interest in CEP290 through its association with LCA, we wanted to take a closer look at its role in the initiation of ciliogenesis and whether it was a substrate for one of the previously discussed kinases. CEP290's position at the distal end of the mother centriole, where it is believed to be in a complex with and inhibited by CP110, make it an attractive option when considering a target for a pro-ciliary kinase. We chose to first investigate TTBK2 as an interacting kinase for a number of reasons. Included in these is the likely association of TTBK2 with the distal appendages, placing the kinase in very close proximity to the CP110

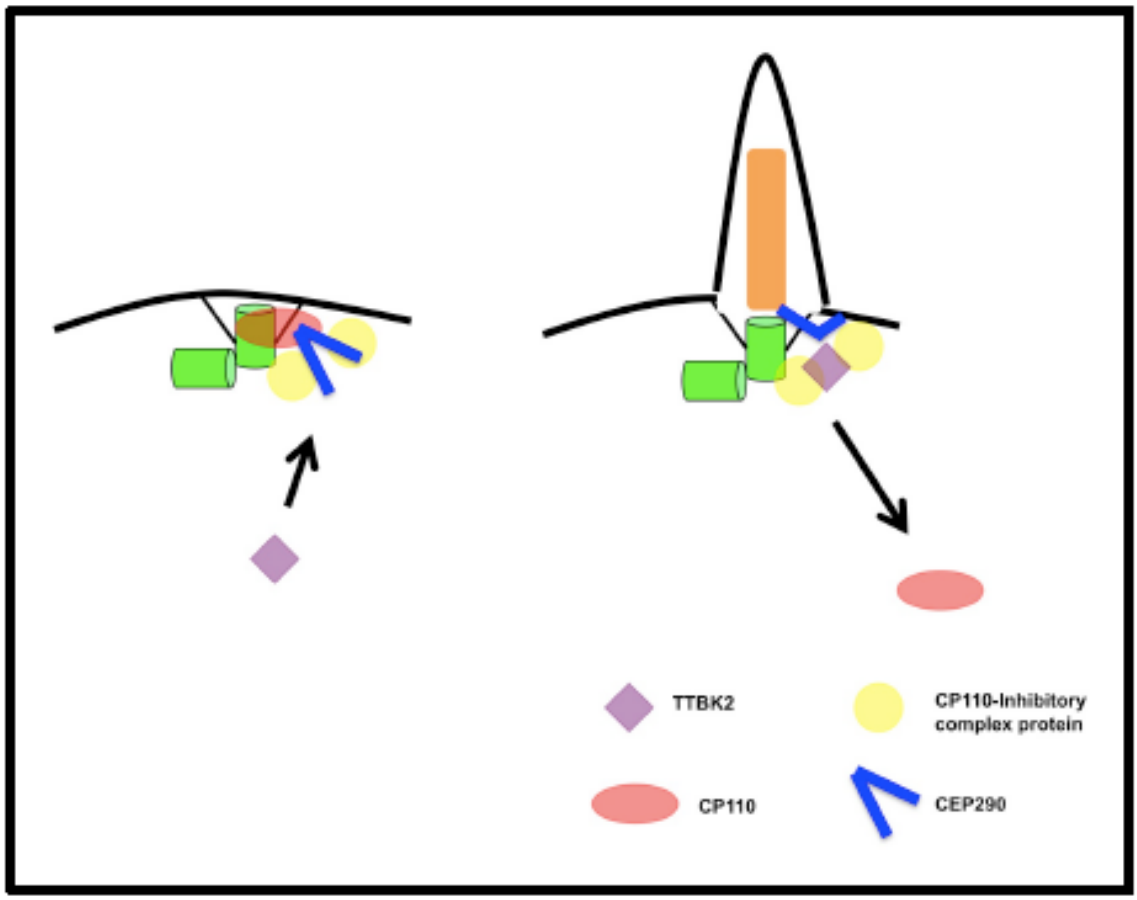

Figure 27: CEP290 and TTBK2. Upon an unknown signal, I hypothesize that TTBK2 traffics to the primary cilium where it phosphorylates CEP290 during the initiation of ciliogenesis.

complex (Oda et al., 2014; Cajanek et al., 2014). In addition, CEP290 falls into the category of a microtubule-associated protein, a protein type that TTBK2 has been shown to phosphorylate (Goetz et al., 2012). Further, TTBK2's reported amino acid binding motif is found in CEP290's sequence. As such, I hypothesize that TTBK2 interacts with CEP290 at the base of the primary cilium and this interaction is crucial for the initiation of ciliogenesis (Fig. 27).

TTBK2 specificity

TTBK2 has been described as having specificity for serine/threonine residues with a phosphotyrosine at a +2 position (Bouskila et al., 2011). In analyzing the amino acid sequence of CEP290, two such potential locations can be found. The first involves serine 202 and tyrosine 204 in Exon 9, and the second involves serine 1380 and tyrosine 1382 in exon 32. In further analyzing these two locations for potential phosphorylation using the NetPhos 2.0 server (Blom et al., 1999), the probablity of phosphorylation of serine 202 and tyrosine 204 was determined to be likely (Fig. 28). Of note, the location of CEP290 serine 202 is very close to the region of the protein (amino acid residues 237- 526) previously identified through a yeast two-hybrid screen to be capable of interacting with CP110 (Tsang et al., 2008).

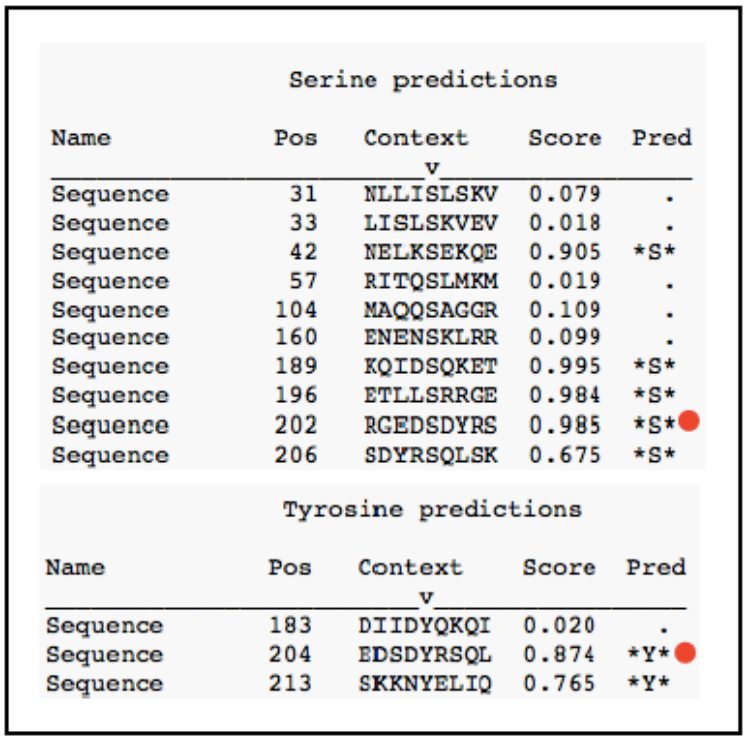

Serine predictions

Name	Pos	Context	Score	Pred
		v		
Sequence	31	NLLISLSKV	0.079	.
Sequence	33	LISLSKVEV	0.018	.
Sequence	42	NELKSEKQE	0.905	*S*
Sequence	57	RITQSLMKM	0.019	.
Sequence	104	MAQQSAGGR	0.109	.
Sequence	160	ENENSKLRR	0.099	.
Sequence	189	KQIDSQKET	0.995	*S*
Sequence	196	ETLLSRRGE	0.984	*S*
Sequence	202	RGEDSDYRS	0.985	*S*
Sequence	206	SDYRSQLSK	0.675	*S*

Tyrosine predictions

Name	Pos	Context	Score	Pred
		v		
Sequence	183	DIIDYQKQI	0.020	.
Sequence	204	EDSDYRSQL	0.874	*Y*
Sequence	213	SKKNYELIQ	0.765	*Y*

Figure 28: Predicted phosphorylation of CEP290. Both Serine 202 and Tyrosine 204 are predicted to be phosphorylated using the NetPhos 2.0 server.

TTBK2 and CEP290

To investigate a potential interaction between the two proteins, a co-immunoprecipitation (co-IP) approach was utilized. Previous reports identifying interacting partners of TTBK2 did so through co-IP using the lysates of cells, typically human embryonic kidney (HEK) 293 cells, which had been transfected with plasmids expressing tagged versions of both proteins of interest (Cajanek and Nigg, 2014; Oda et al., 2014). In an effort to observe potential interactions of CEP290 with endogenous TTBK2, I attempted to use a co-IP approach using cell lysates that had only been transfected with GFP-tagged CEP290, either tagged full-length protein or GFP tagged to specific portions of the protein. First, I tested our anti-TTBK2 antibody on cell lysates from HEK293 cells and human telomerase reverse transcriptase immortalized retinal pigment epithelial 1 (hTERT-RPE1) cells. Initial western blot analysis of the lysates showed two bands in both lysates, with one corresponding to the expected molecular weight of TTBK2 (~137 kDa) and one slightly lower (Fig. 29). While at least three alternatively spliced isoforms of human TTBK2 are predicted according to the

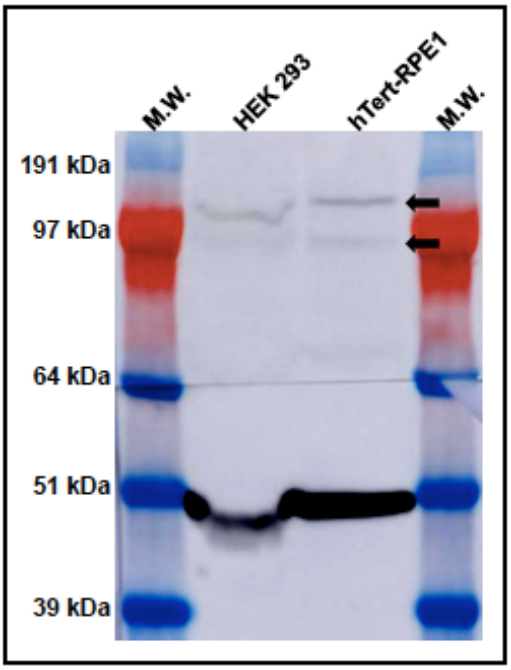

Figure 29: Western blot analysis of HEK293 and hTert-RPE1 cell lysates. Two prominent bands appear in each lysate, labeled with black arrows. The calculated molecular weight of TTBK2 is 137.5 kDa. A band corresponding to the loading control alpha tubulin is also visible in each lane at the expected molecular weight of 50 kDa.

Universal Protein Resource (http://www.uniprot.org/uniprot/Q6IQ55) only the 1244 amino acid isoform with a predicted molecular weight of 137 kDa has been characterized. The other two isoforms are predicted to result in proteins of approximately 129 kDa and 54 kDa. In further western blot analysis of HEK293 cells, a third band can be observed at the approximate level of the 54 kDa isoform (Fig. 30). Taken together, these results indicate that the antibody appears capable of detecting endogenous TTBK2 in the cell lysates. In addition, it is possible that I am detecting shorter isoforms of the protein that have yet to be characterized, however, given the relative weakness in staining of even the expected long isoform of the protein, further work is warranted to confirm these are indeed the shorter TTBK2 isoforms.

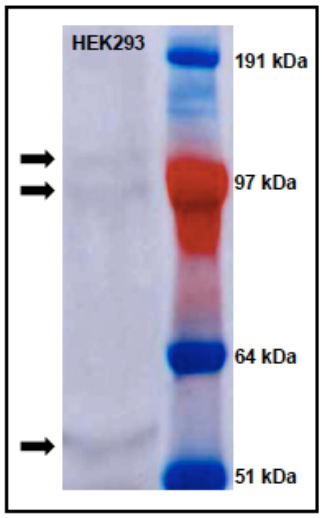

Figure 30: Further western blot analysis of HEK293 cells. Three faint bands, labeled with black arrows, are visible in cell lysates stained with anti-TTBK2 antibodies.

In an effort to detect an interaction between CEP290 and TTBK2, hTert-RPE1 cells were transfected with full-length GFP-tagged CEP290, GFP-tagged CEP290 portions, or GFP alone. The location of these constructs on CEP290 can be found in figure 31. Approximately 24 hours post transfection, the cells were serum starved in an effort to induce formation of primary cilia. As enriched levels of CEP290 and TTBK2 are both found at the base of the cilium during the initiation of ciliogenesis, I hypothesized this

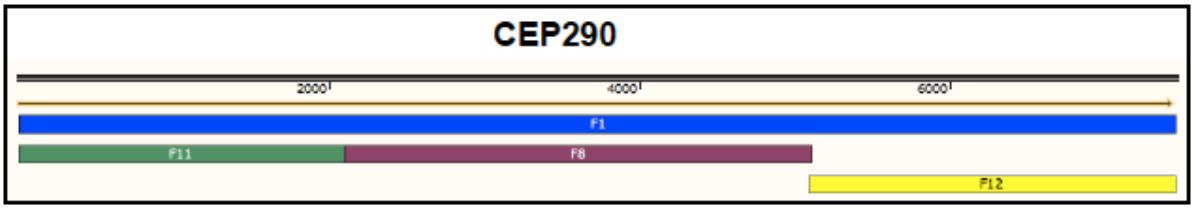

Figure 31: CEP290 constructs used to transfect cells. Constructs encoding either full length (F1- blue), N-terminal (F11- green), middle (F8- purple), or C-terminal (F12- yellow) were used. All constructs were GFP-tagged and human codon optimized.

environment might aid in the detection of any potential TTBK2 and CEP290 interaction in the cell. Following 24 hours of serum starvation, the cells were lysed and complexes in the lysates associated with CEP290 or portions of CEP290 were co-immunoprecipitated using anti-GFP antibodies. As depicted (Fig. 32), western blot analysis of these complexes shows a band was

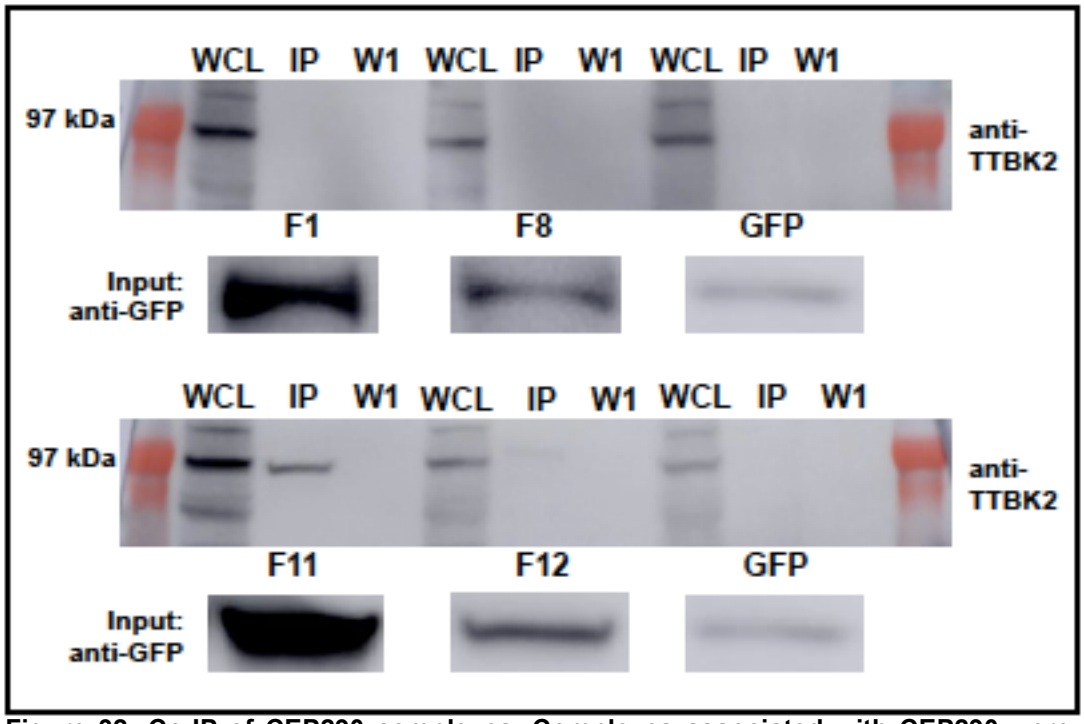

Figure 32: Co-IP of CEP290 complexes. Complexes associated with CEP290 were stained with anti-TTBK2 antibodies. As depicted, a potential interaction is observed between TTBK2 and the N-terminal (F11) portion of CEP290.

consistently observed in the IP lane (the lane in which the complex was run) of

lysates taken from cells that had been transfected with an N-terminal portion of CEP290. Interestingly, the band appeared to migrate with the lower of the potential doublet TTBK2 bands previously described (Fig. 29). Also of note, no TTBK2 was ever observed in the IP lane of lysates corresponding to cells transfected with full length CEP290. Taken together, these results suggest a potential interaction between TTBK2 and the N-terminal portion of CEP290.

To further investigate this potential interaction, a smaller N-terminal CEP290 portion was utilized in an attempt to narrow down the observed TTBK2 interacting region of CEP290 (Fig. 33). Again, interaction between TTBK2 and both CEP290 N-terminal portions was analyzed by co-IP and western blot after the hTert-PRE1 cells were transfected, serum starved, and lysed as above. Surprisingly, no potential interaction between TTBK2 and the smaller CEP290 N-terminal portion was observed (Fig. 34). The longer of the two constructs, F11, includes an addition 116 amino acids of CEP290 compared to the shorter N-terminal construct F10. This finding suggests that if TTBK2 and CEP290 are indeed interacting at the N-terminal portion of CEP290, these 116 amino acids

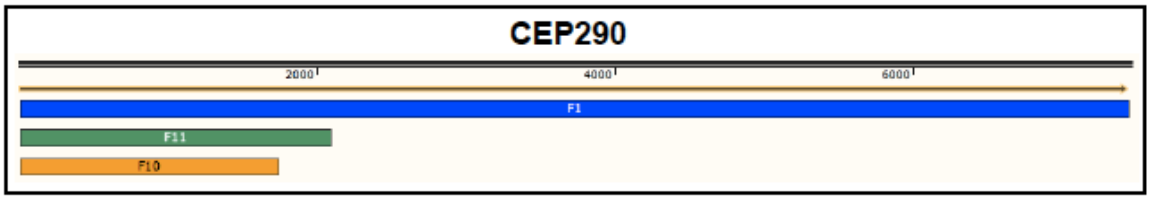

Figure 33: F10 construct. A slightly smaller N-terminal CEP290 portion (F10- orange) was used to define the area of CEP290 observed to interact with TTBK2.

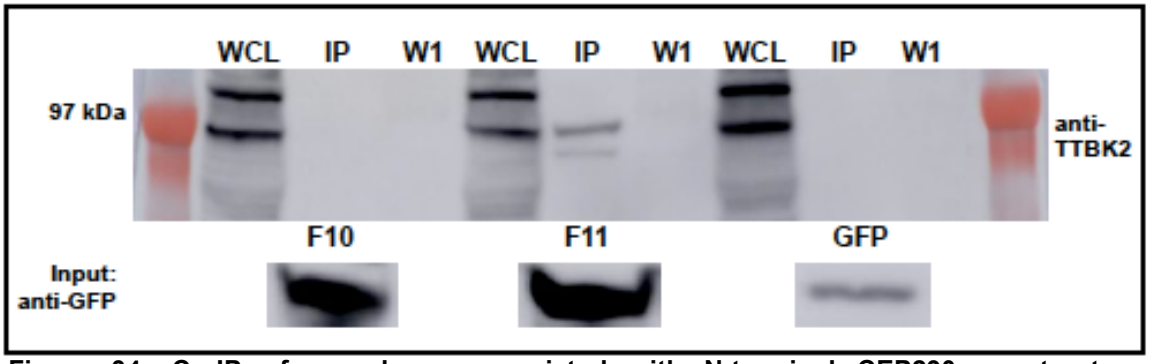

Figure 34: Co-IP of complexes associated with N-terminal CEP290 constructs. Complexes were stained with anti-TTBK2 antibodies and analyzed by western blot. As depicted, an interaction is again observed in the IP lane of the F11 construct. A second, faint band in the lane is also observed, potentially due to background staining caused by the transfected construct.

are crucial for that interaction.

Discussion

Fully interpreting these observations will require further investigations. Understanding the TTBK2 staining of the cell lysates will be necessary to determining the nature of the observed interaction. This is currently made difficult by relatively limited knowledge of endogenous TTBK2 staining. As mentioned, previous studies involving TTBK2 biology or investigation of TTBK2 interacting proteins have taken advantage of tagged constructs. If the band which consistently appears in the IP lane of lysates taken from cells transfected with N-terminal CEP290 is associated with an isoform of TTBK2, the finding would be novel, both in terms of the interaction between the two proteins and in terms of a smaller isoform of TTBK2 being identified as the interacting protein.

Not observing an interaction between full-length CEP290 and TTBK2 after potentially observing a relationship between TTBK2 and a portion of CEP290's

N-terminus was unexpected. Findings made by Gerd Walz's group at the University Hospital Freiburg and Anand Swaroop's group at the National Eye Institute regarding an interaction between CEP290 and another ciliary protein, NPHP5 however, may help explain this observation (Schafer et al., 2008; Chang et al., 2006). In an initial study, the Swaroop group failed to record an interaction between full-length CEP290 and full-length NPHP5. Upon further analysis in a separate study, however, the Walz group observed a CEP290 fragment composed of amino acids 665-1288 and NPHP5 were capable of interacting. In addition, the Walz group also demonstrated the N-terminus and C-terminus of CEP290 were capable of forming heterodimers with each other and homodimers with themselves. In light of these observations, the group hypothesized CEP290 may be capable of folding on itself, potentially in an auto-inhibitory manner, and this folding may in some cases limit access of interacting proteins to their binding location on CEP290. A similar mechanism of auto-inhibition has been proposed for the kinesin-2 motor protein OSM-3 in C. elegans (Imanishi et al., 2006). Taking this into consideration, it may be that the TTBK2 binding domain on full length CEP290 is only available under certain circumstances, which are not mimicked by overexpression of the full-length protein.

A potential interaction between TTBK2 and CEP290 was investigated first for reasons previously described, however, with our current knowledge of the CP110 complex and associated proteins, speculations can be made regarding the potential interactions of other ciliary proteins that might lead to the dissolution of CP110 at the end of the mother centriole. A commentary on this topic is

covered in detail in the appendix below. As mentioned, the definitive role of CEP290 and TTBK2 in this process requires further investigation with many questions remaining. Taking into consideration the preliminary findings here, however, I believe those investigations would be warranted.

Materials and Methods

Cell Culture

HEK293 and hTert-RPE1 cells were utilized for these studies. HEK293 cells were grown in DMEM supplemented with 10% FBS. hTert-RPE1 cells were grown in DMEM:F12 in a 1:1 mixture supplemented with 10% FBS. Both cell types were grown at 37 degrees Celsius in 5% CO_2. Replacing media with low nutrient Opti-MEM immediately after washing cells 1X with warm PBS induced serum starvation.

Transfections, co-IP, and western blot

Cells were transfected with GFP-tagged CEP290 constructs using FuGENE6 transfection reagent (Promega). Media on cells was replaced 8 hours post-transfection. Cell lysates were harvested 48-60 hours post transfection. Lysates from serum-starved cells were harvested no earlier than 24 hours post-serum starvation and 48 hours post-transfection. Cells were lysed using Triton-X cell lysis buffer supplemented with protease inhibitor tablets (Roche, Complete, Mini, EDTA-free). A 50ul aliquot was taken of each lysate to use for western

analysis of GFP-expression. Remaining lysates were either used immediately for co-IP or snap-frozen to be used at a later date. Co-IP was carried out using anti-GFP antibodies coupled to magnetic Dynabeads (Life Technologies Dynabeads antibody coupling kit, Cat. 14311D) as recommended by manufacturer. Beads were coupled using 6ug ab/ 1ug beads. Antibody-coupled beads and cell lysates were allowed to incubate 3-5 hours at 4 degrees Celsius on a spinning wheel. Samples were run on NuPAGE 4-12% Bis-Tris gels (Life Technologies) before being transferred to nitrocellulose membranes. After incubation with appropriate antibodies and developed using ECL2 reagent (Pierce), images of the membranes were taken using an Amersham Imager 600. Images were analyzed using ImageJ64 software.

CEP290 plasmids

CEP290 plasmids encoding full-length or portions of CEP290, N-terminally tagged with GFP were obtained from the Bennett laboratory plasmid repository. Plasmids were originally generated using human codon optimized *CEP290* as a template and cloned into Gateway vectors (pcDNA-DEST53) (Invitrogen).

Antibodies

For western blot analysis, Rabbit anti-GFP antibodies from Life Technologies (A11122); Rabbit anti-TTBK2 antibodies from Sigma (HPA018113-100UL); mouse anti- Alpha tubulin antibodies from Abcam (ab7291). For IP, Mouse anti-GPF antibodies from Roche (11814460001). HRP-conjugated anti-mouse and anti-rabbit secondary antibodies (GE- Amersham Biosciences) were

used.

APPENDIX

Roles of the CP110 complex and associated proteins in the initiation of ciliogenesis

Since the identification of CP110's inhibitory role in ciliogenesis, multiple interacting partners of the protein have been identified in a complex with it at the distal end of both centrioles before the induction of cilia formation. Included in this complex are both promoters of ciliogenesis and proteins described to be inhibitory in this process. In addition, several proteins associated with the distal and sub-distal appendages of the mother centriole/basal body (putting them in close proximity to members of the CP110 complex) have been described to be involved in ciliary development and maintenance. Our current understanding of many of these proteins as well as a set of kinases recently described to traffic to the base of the cilium shortly before axoneme extension will be discussed below. In addition, speculations regarding potential interactions yet to be observed between some of these proteins will also be covered.

CP110 and associated proteins

Inhibitory proteins of mention

CP110

As mentioned above, CP110 plays a prominent role in the inhibition of ciliogenesis. The protein was first characterized in a screen for substrates of

cyclin-dependent kinases (CDKs) carried out by Brian Dynlacht's laboratory of New York University's School of Medicine (Chen et al., 2002). In addition to successfully identifying the protein as a CDK substrate, the group also observed it as a component of the centrosome. In investigating cellular levels of CP110, they found levels of the protein to peak in the entrance of cells to S phase from G1 phase. Meanwhile, minimal levels of CP110 were observed in lysates of quiescent cells (Chen et al., 2002). In addition, RNAi knockdown of the protein led to multiple examples of genomic instability, resulting in the group concluding CP110 was likely playing a role in the cell cycle through its interaction with the centrosomes. This conclusion was later confirmed when Erich Nigg's group of the Max-Planch Institute observed CP110 to aid in early centriole biogenesis (Kleylein-Sohn et al., 2007).

Around the same time that the cell cycle role for CP110 was being described by Nigg's group, the Dynlacht laboratory published findings characterizing a ciliary role for the protein. In this paper, the group observed that CP110 acts to suppress ciliogenesis from the basal body, potentially by forming a cap at the distal end of the centrioles to prevent axoneme extension. It was found that this cap must be removed from the mother centriole for ciliogenesis to occur. Supporting this, it was observed that knockdown of CP110 leads to inappropriate formation of cilia-like structures from at least one but sometimes both centrioles (Spektor et al., 2007). These structures were observed to positively stain for acetylated tubulin and polycystin-2, markers of ciliogenesis (Spektor et al., 2007; Cai et al., 1999). In contrast, when cells are transfected with plasmids expressing

CP110, the percentage of cells that form primary cilia is greatly reduced despite pro-ciliary environments (Spektor et al., 2007) again supporting an inhibitory role for CP110 at the basal bodies (Fig 35). Taken together, CP110 appears to have at least two distinct roles, one functioning early in the production of centrioles at the centrosome and another in inhibiting the process of ciliogenesis at the basal body.

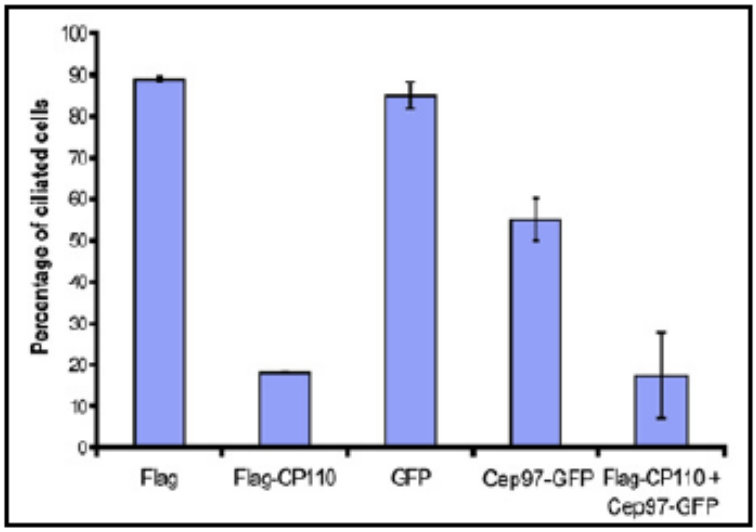

Figure 35: CP110, Cep97 and cilia formation. Overexpression of CP110, Cep97, or both reduces primary cilia formation in NIH 3T3 cells. *Figure adapted from Spektor et al., 2007

Cep97

In order to further discuss the role of CP110 at the primary cilium, centrosomal protein 97 kDa (Cep97) should be introduced. Leading up to the observation of its ciliary role, the Dynlacht group also purified complexes associated with CP110, identifying Cep97. Initial experiments undertaken to define the relationship of these two proteins demonstrated that Cep97 is required for localization of CP110 to the centrosomes and the depletion of Cep97 leads to CP110 instability as well as a significant reduction of CP110 cellular amounts. Interestingly, while CP110 depletion also led to a loss of Cep97 at the centrosomes, no effect was observed on cellular Cep97 amounts. This suggests that both proteins play a role in the other's recruitment to the centrosomes but

only Cep97 functions in the stabilization of CP110 (Spektor et al., 2007). Similar to CP110 depletion, siRNA knockdown of Cep97 also leads to the appearance of cilia-like structures. Overexpression of Cep97 did not lead to as severe a reduction of cells forming primary cilia compared to that of CP110, however, suggesting the definitive role of ciliary inhibition may be due to CP110.

Cep76

Another inhibitory member of the CP110 complex is centrosomal protein 76 kDa (Cep76) (Tsang et al., 2009). In addition to interacting with CP110, Cep76 also appears to be associated with Cep97 at the centrosome. Relatively little is known about this protein other than it seems to function in inhibiting reduplication of the centrioles during S phase, perhaps by inhibiting pro-centriolar proteins such as CP110. While CP110 appears to have both a cell cycle and ciliary role, a function of Cep76 at the primary cilium has yet to be described.

Kif24

A rather unique member of the ciliary CP110 complex and one of the more recently described is Kinesin family member 24 (Kif24) (Kobayashi et al., 2011). As its name implies, Kif24 is a member of the kinesin family (specifically kinesis-13) of M-kinesin molecular motor proteins (Ems-McClung and Walczak, 2010). While N-kinesins and C-kinesins are involved in moving cargo along microtubules in the cell, M-kinesins are involved in depolymerizing microtubules (Shipley et al., 2004). Kif24 has been shown to not only interact with both CP110 and Cep97 at the distal end of the mother centriole but also phenocopy both of

these proteins in that knockdown of Kif24 leads to the formation of primary cilia in cycling cells (Kobayashi et al., 2011). Hinting at its precise role in the inhibition of ciliogenesis, Kif24 was found to specifically depolymerize centriolar microtubules but not cytoplasmic microtubules. This suggests a model by which Kif24 interacts with CP110/Cep97 at the distal end of the mother centriole and functions to counteract any attempt of axoneme extension by depolymerizing microtubule extension from the basal body until the complex is removed.

Pro-ciliary proteins of mention

CEP290

The association of CEP290, a promoter of ciliogenesis, with the ciliary CP110 complex was an important finding and one that introduced a new mechanism by which CP110 may be inhibiting ciliogenesis. Again, the Dynlacht group was behind the observation, demonstrating that CEP290 and CP110 are capable of interacting and that the interaction could be mapped to the N-terminus of CEP290. As mentioned previously, CEP290 is found at the distal ends of the mother and daughter centrioles, both during the cell cycle and G_0 while CP110 is observed to leave the end of the mother centriole during G_0 but maintain its association and co-localization with CEP290 at the end of the daughter centriole (Spektor et al., 2007; Tsang et al., 2008). In addition, knockdown of *CEP290* mRNA by siRNA leads to a suppression of ciliogenesis, a phenotype that is in direct contrast to the pro-ciliary effect of knocking down CP110 levels. Of note,

however, knockdown of *CEP290* mRNA had no effect on the cell cycle, suggesting only a ciliary role for the protein. Furthermore, depletion of CEP290 has been shown to result in altered organization of PCM-1, a pericentriolar matrix protein known to be required for ciliogenesis (Kim et al., 2008), and the loss of Rab8a, a regulator of vesicle trafficking (Zerial and McBride, 2001) that functions in generation of the ciliary membrane, in the primary cilium (Kim et al., 2008).

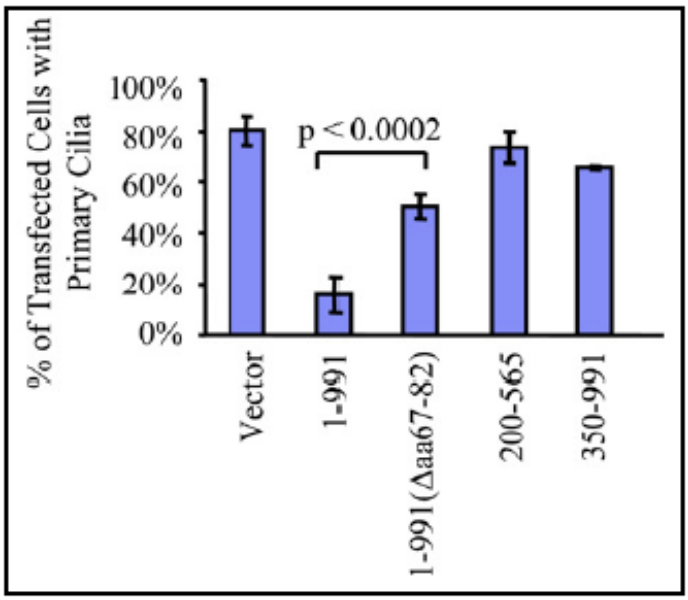

Figure 36: Ectopic expression of CP110 plasmids in NIH 3T3 cells. As depicted above, expression of CP110 plasmids result in a decrease in primary cilia. This phenotype is suppressed when the transfected CP110 plasmid is missing a region described as crucial for its interaction with CEP290. *Figure adapted from Tsang et al., 2008

As ciliogenesis is not observed to occur until after CP110 leaves the end of the mother centriole, the Dynlacht group hypothesized that CP110 may be interacting in an inhibitory way on CEP290, suppressing its ability to function in ciliogenesis. To test this, the group repeated their initial experiment in which they had demonstrated that overexpression of CP110 in cells led to almost complete suppression of primary cilia. Instead of overexpressing wild-type CP110, however, the group transfected the cells with a version of CP110 incapable of binding CEP290. In doing so, the suppression of primary cilia was almost

completely reversed, suggesting the inhibitory nature of CP110 before ciliogenesis is dependent on its ability to interact with CEP290 (Fig. 36)(Tsang et al., 2008).

Talpid3

Talpid3 was first recognized as being essential for the formation of primary cilia by Cheryll Tickle's group at the University of Bath (Yin et al., 2009). Another promoter of ciliogenesis and a member of the ciliary CP110 complex, the protein appears to localize with the centrosome during the cell cycle and the basal body of the primary cilium in quiescence (Kobayashi et al., 2014). Specifically, Talpid3 is observed at the distal ends of both the mother and daughter centrioles close to the distal appendages during ciliogenesis. Knockdown of Talpid3 phenocopies that of CEP290 in that depletion leads to suppression of primary cilia formation, altered organization of PCM1 granules, and depletion of Rab8a in the primary cilium- all while having no effect on the cell cycle. In regards to Talpid3 function, intricate transition electron microscopy (TEM) analysis of retinal pigment epithelial (RPE) cells at the initiation of ciliogenesis in Talpid3-depleted and control cells seems to indicate that Talpid3 acts to help capture primary ciliary vesicles on the distal appendage of the mother centriole shortly after the cell receives the signal to begin ciliogenesis (Kobayahi et al., 2014). These vesicles go on to mature into ciliary vesicles at the top of the mother centiole and eventually form the ciliary membrane, Sorokin, 1962). Together, these results suggest Talpid3 function is critical for early ciliary vesicle capture and ciliary

membrane maturation.

Cep104

Another pro-cliliary member of the CP110 complex is Cep104. In addition to its previously described presence at the centrioles (Jakobsen et al., 2011), the Akhmanova laboratory at Utrecht University first characterized the ciliary involvement of the protein after it was identified in a screen for microtubule plus end trafficking proteins (+TIPs) (Jiang et al., 2012). +TIPS are typically found at the growing ends of microtubules where they are observed to play various roles, including recruiting other factors to the microtubule ends and aiding in their connection to other cellular structures. The group showed Cep104 immunoprecipitates with both CP110 and Cep97 and that Cep104 and CP110 co-localize to the distal ends of the centrioles during interphase. Interestingly, the two also co-localize after the initiation with ciliogenesis, with both found at the tip of the daughter centriole but neither at the distal end of new basal body. As CP110 and Cep97 are known in inhibitors of ciliogenesis, these findings would seem to indicate a similar role for Cep104. However, depletion of Cep104 actually leads to a reduction in the ability of cells for form primary cilia with no other defects observed in cell cycle or centriole length (Jiang et al., 2012). Taken together, a role of Cep104 could be hypothesized where it helps to stabilize the CP110 complex during the cell cycle, but its presence is necessary for the process of ciliogenesis to occur.

Distal Appendage Proteins

Cep164

Cep164 was first associated with the centrosome in 2003, having been identified in a mass-spectrometry-based analysis of human centrosomes (Andersen et al., 2003). Shortly after, the protein's localization was narrowed down to the distal appendages of the mother centriole. In addition, Cep164 was determined to be required for ciliogenesis with cilia formation suppressed in Cep164 depleted cells. (Graser et al., 2007). Of note, the location of Cep164 at the distal appendages puts it in close proximity with the CP110 complex members at the end of the mother centriole including Talpid3 and CEP290 (Spektor et al., 2007; Kobayashi et al., 2014)(See model below).

A very recent finding by two independent laboratories describes Cep164 as a recruiter of Tau Tubulin Kinase 2 (TTBK2) to the basal bodies before the initiation of ciliogenesis. As will be discussed later in further detail, TTBK2 has been described to be crucial for the initiation of ciliogenesis, and its arrival at the basal body coincides with the removal of CP110 (Goetz et al., 2012). In addition, the recruitment of TTBK2 by Cep164 was shown to depend on a N-terminal WW domain on Cep164.

In light of the observation of Cep164 at the distal appendages and its interaction with TTBK2, Erich Nigg's group at the University of Basel set up a clever experiment to determine if one function of Cep164 was to recruit TTBK2 to the basal body, specifically the distal appendages of the mother centriole. In this

experiment, the group fused the C-terminal portion of Cep164, the portion known for targeting Cep164 to the distal appendages, to TTBK2. They then transfected this construct into Cep164-depleted cells and observed a rescue of ciliogenesis, suggesting Cep164 aids in the recruitment of TTBK2 to the distal appendages and this recruitment plays a role in the formation of the primary cilium (Cajanek and Nigg, 2014).

Cep123

Cep123, also referred to as Cep89 is another distal appendage protein. Like Cep164, Cep123 is required for ciliogenesis and the C-terminal portion of the protein appears to target it to the distal appendages (Sillibourne et al., 2013). Interestingly, siRNA-mediated depletion of Cep123 after the induction of ciliogenesis had little effect on primary cilia, suggesting the protein is only involved in initiation of ciliogenesis and not maintenance.

The role of Cep123 in the initiation of ciliogenesis was investigated by the Bomens laboratory at the Institut Curie. In doing so, the group observed that while distal appendages still formed in Cep123-depleted cells, the docking of ciliary vesicles to the distal end of the mother centriole was perturbed, suggesting a very early role for the protein in ciliary initiation (Sillibourne et al., 2013).

Interestingly, Cep123 was also found to co-immunoprecipitate with PCM-1 and CEP290, likely at the centriolar satellites where CEP290 can be found in addition to its transition zone localization (Kim et al., 2008; Sillibourne et al., 2013).

Cep83

Another member of the DAPs is Cep83. Only recently characterized by the Tsou group at Memorial Sloan-Kettering, Cep83 appears to be required for recruitment of both Cep123 as well as Cep164 to the DAPs as depletion of Cep83 leads to their loss at the appendages. Depletion of the other DAP proteins has no effect on Cep83's DAP localization, however, suggesting Cep83 forms the connection required for the other proteins' association (Tanos et al., 2013). In regards to this role, it is no surprise that Cep83 is also required for the initiation of ciliogenesis, and as DAPs are involved in docking the mother centriole to the cellular membrane, mother centrioles in Cep83 depleted cells fail to dock to the cellular membrane (Tanos et al., 2013)

Kinases

TTBK2

Several groups have recently placed Tau Tubulin Kinase 2 (TTBK2), a serine/threonine kinase capable of phosphorylating microtubule associated proteins, at the base of the cilium during the initiation of ciliogenesis (Goetz et al., 2012; Cajanek and Nigg, 2014; Oda et al., 2014). TTBK2, in addition to TTBK1, is a member of the TTBK family of the casein kinase 1 (CK1) group (Ikezu and Ikezu, 2014). While the kinase domains of these two proteins are very similar, their sequences outside of these domains differ substantially. TTBK1 appears to be exclusively expressed in the CNS (Sato et al., 2006) where it is found to be upregulated in the brains of human Alzheimer disease (AD) patients (Sato et al.,

2008). TTBK2 appears to be ubiquitously expressed throughout the body with mutations in the protein associated with Spinocerebellar ataxia type 11 (SCA11) (Houlden et al., 2007). In light of its expression throughout the body and its recent implication in ciliary health, however, it is likely that mutations in this protein will soon be linked to several other conditions.

The largest TTBK2 isoform is composed of 1244 amino acids. Most of the protein (~960 amino acids) is dedicated to a portion C-terminal to the kinase domain, which appears to be involved in localization (Goetz et al., 2012)(Fig.37). While this region is known to contain a SxIP motif, which, as mentioned previously, can be found on microtubule plus-end trafficking proteins, (Jiang et al., 2012) the rest of the C-terminal region remains mostly uncharacterized. The kinase domain of TTBK2, which appears to be necessary for the induction of

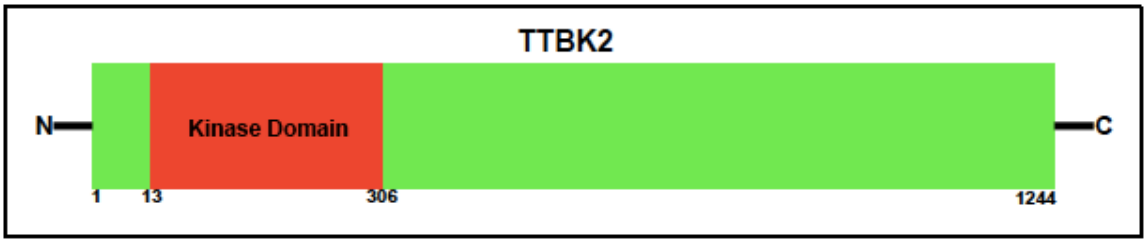

Figure 37: Illustration of TTBK2. The C-terminal tail of TTBK2 makes up most of the protein. The kinase domain, however, has been shown to be crucial for the function of the protein in ciliogenesis.

ciliogenesis (Goetz et al., 2012), has been shown to be capable of phosphorylating serines 208 and 210 of the tau protein and is described to have specificity for substrates with a phosphotyrosine at a +2 position of the phosphorylation site.

As mentioned previously, TTBK2 was recently found to localize to the base of the primary cilium during the initiation of ciliogenesis. This observation was first made by Kathryn Anderson's laboratory at the Sloan-Kettering Institute using a screen to identify mutations leading to defects in neural patterning of mouse embryos (Goetz et al., 2012). Embryos with null Ttbk2 mutations were identified after arresting in mid-gestation, a hallmark phenotype of Shh defects (Huangfu et al., 2003). Altered Shh signaling in the embryos was confirmed by the absence of ventral neural cell types, specifically Shh-expressing floor plate cells (Fig. 38). As the Anderson group was the first to link Shh signaling to Ift-88 and ciliary health, the group examined the primary cilia of the neural tubes in the mutant embryos, finding a complete absence of cilia on the null Ttbk2 cells (Fig. 39). Interestingly, however, mature basal bodies with formed distal appendages could be detected in the cells near the membrane, suggesting the cell was primed to form a cilium but was restricted from doing so and that Ttbk2 may be involved in this process. Moreover, staining for CP110 showed the protein to remain in place at the distal end of the mother centriole in serum starved, *Ttbk2* null mice, narrowing in on a potential function for Ttbk2 at the primary cilium. Further experiments with GFP-tagged Ttbk2 constructs

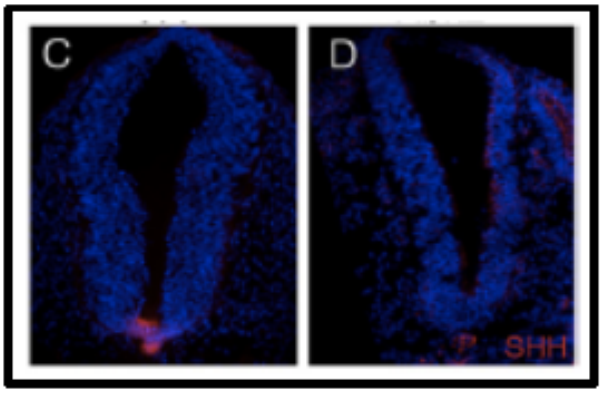

Figure 38: Absence of Shh expression in *Ttbk2* null mice. Shh is depicted as purple staining in the floor plate cells of wild-type animals (C). No Shh is visible in the floor plates of *Ttbk2* null mice. *Figure adapted from Goetz et al., 2012.

showed that the protein traffics to the basal bodies upon serum starvation, the C-terminal portion of the protein is required for this trafficking, and a functional kinase domain is necessary to rescue CP110 removal and initiation of ciliogenesis in *Ttbk2* null cells (Goetz et al., 2012).

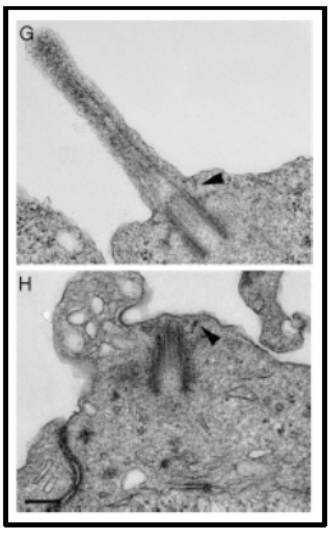

Figure 39: Cells of the neural tube lack cilia in *Ttbk2* null mice. Cila extend normally in cells of wild-type mice (G) but do not in cells of *Ttbk2* null mice (H). Arrows point to distal appendages.*Figure adapted from Goetz et al., 2012.

While the Anderson laboratory did not described a target for TTBK2 at the basal body, subsequent work has shown that the protein is likely recruited to the basal body through interactions with Cep164, which it has been shown to bind to and be capable of phosphorylating (Cajanek and Nigg et al., 2014; Oda et al., 2014). Interestingly, an *in vitro* kinase assay involving TTBK2 and Cep97 showed that TTBK2 was also capable of phosphorylating Cep97 as well, but the relevance of this potential interaction was not described *in vivo* (Oda et al, 2014). Regarding TTBK2 and Cep164, their interaction was determined to be crucial for ciliogenesis to occur (Oda et al., 2014). Interestingly, further work by the Nigg laboratory showed that overexpression of TTBK2 led to recruitment of Cep164, Cep83, and Cep123 to the daughter centrioles. This observation, that TTBK2 may be capable of recruiting DAPs to the centrioles which then in turn recruit more TTBK2, suggests a potential positive feedback loop for the protein, involving TTBK2 both in the maturation of the basal body and the final step if CP110 removal (Cajanek and Nigg, 2014).

MARK4

Another kinase observed to locate to the basal body before the initiation of ciliogenesis is Microtubule-associated Proteins/Microtubule Affinity-regulating Kinase 4 (MARK4) (Kuhns et al., 2013). First identified by the Furukawa laboratory at the University of Tokyo due to its elevated expression in hepatocellular carcinogenesis (Kato et al., 2001), the centrosomal association of MARK4 was characterized shortly thereafter (Trinczek et al., 2004).

The sub-distal appendage protein (SAP), ODF2, was recently identified as an interacting partner of MARK4 at the basal body (Kuhns et al., 2013). As the name implies, sub-distal appendages are found directly below the distal appendages on the basal body. Here, the SAPs appear to be involved in the anchoring of microtubules and aiding in vesicle docking (CC2D2A, saps). While Cep164 is described as the major component of the DAPs, SAPs appear to be largely composed of ODF2 (Tateishi et al., 2013). The Pereira Laboratory of the German Cancer Research Center was the first to report the interaction of MARK4 and ODF2. In very similar findings to the relationship of TTBK2, Cep164, and the DAPs, the Pereira group reported that MARK4 and ODF2 interact *in vivo*, MARK4 is capable of phosphorylating ODF2 *in vitro*, and that a functional MARK4 kinase domain is important for ciliogenesis. In addition, MARK4 appears to be at least partially responsible for ODF2 localization to the centrosome as mislocalization of ODF2 was observed in MARK4 depleted cells and overexpression of MARK4 resulted in enhanced centrosomal association of

ODF2. Interestingly, depletion of either MARK4 or ODF2 resulted in inhibition of axoneme extension but not early vesicle docking to the end of the mother centriole. In addition, overexpression of ODF2 in MARK4 depleted cells rescued the reduction of cilia observed after the loss of MARK4 (Kuhns et al., 2013). Taken together, the findings by the Pereira group also seem to highlight a positive feedback role of the MARK4/ODF2 interaction where ODF2 is present at the SAPs before axoneme extension but not necessarily aiding in early vesicle recruitment. Upon an unknown signal, however, and after docking of the ciliary vesicle to the end of the mother centriole, MARK4 might be targeted to basal body where it interacts with ODF2, and likely other targets, stabilizing the SAPs and leading to the recruitment of more ODF2. This increased concentration of ODF2 at the SAPs may allow the nascent cilium to deal with the larger amount of incoming vesicles throughout the process of ciliogenesis, leading to maturation of the structure (Kuhns et al., 2013).

Nek kinases

The Nek kinases are a group of relatively uncharacterized mammalian kinases with closely related catalytic domain sequence homology (Holland et al., 2002). Currently, eleven Nek family members (Nek 1-11) have been described, ranging in proposed function from cell cycle control and DNA damage response to cytoskeletal organization (Fry et al., 2012). Of note, ciliary roles have been proposed for Nek1, Nek8, and most recently, Nek4. Nek1 and Nek 8 were first linked to the primary cilium through their association with the polycystic kidney

disease phenotype of the *kat* mouse and *jck* mouse, respectively (Upadhya et al., 2000; Liu et al., 2002).

While the mechanisms behind the phenotypes observed in both mouse models requires further investigation, recent work involving Nek1 describes a reduction of cilia observed in cultures of embryonic fibroblasts isolated from a *kat* mouse strain when compared to wild-type cultures (Ohad et al., 2008). In addition, a yeast two-hybrid screen of human fetal brain cDNA using the C-terminal regulatory domain of human NEK1 as bait identified Kif3a, a subunit of kinesin-II, as a likely interacting partner (Surpili et al., 2003). As described previously, anterograde intraflagellar transport is dependent on Kinesin-II (Cole et al., 1998), and knock-outs of *Kif3a* result in loss of cilia (Zhao et al., 2012). The observation that NEK1 and Kif3A could be interacting partners is important given the crucial role of Kif3A in the initiation and maintenance of ciliogenesis. If Kif3A is indeed a substrate of NEK1, determining the timing of this interaction, as well as potentially others involving NEK1, with the onset of ciliogenesis, will be necessary to determine its role at the primary cilium.

Ronald Roepman's group at the Radboud University Nijmegen Medical Center is responsible for the recent observation of NEK4 at the primary cilium. In looking for potential binding partners of retinitis pigmentosa GTPase regulator-interacting protein 1 (RPGRIP1) and RPGRIP1-like protein (RPGRIP1L), two proteins in which mutations lead to a spectrum of phenotypes from LCA to MKS, the group identified NEK4 as a member of complexes formed by both proteins

(Coene et al., 2011). Both RPGRIP1 and RPGRIP1L can be observed at the basal bodies of cilia with RPGRIP1 also observed in the connecting cilium of mouse photoreceptors (Zhao et al., 2003). NEK4 staining showed similar localization of the protein, appearing at basal bodies in human retinal pigment epithelial (hTert-RPE) cells and closely related to the connecting cilium of rat photoreceptors (Coene et al., 2011). Specifically, the group showed that NEK4 appears to locate to the ciliary rootlet, extensions of the basal body that project into the cell and are thought to be associated with ciliary stability (Coene et al., 2011, Yang et al., 2005), in several ciliated tissues. Functionally, depletion of *NEK4* through siRNA, led to a decrease in ciliated cells without any observed effects on the cell cycle. The group did not, however, find any evidence that RPGRIP1 or RPGRIP1L are targets of NEK4 phosphorylation, suggesting the proteins may be acting as a scaffold to bring NEK4 and potentially its substrate or substrates to the base of the cilium.

CP110 complex and associated proteins, interactions and predictions

The nature of the environment around the CP110 complex at the end of the mother centriole appears both dynamic and fragile, with multiple kinases trafficking to it before cilium formation begins and the integrity of the entire complex itself dependent on the individual integrity of most of its members. An interesting finding related to this environment is the suggested positive feedback relationships between TTBK2 and MARK4 and the DAPs and SAPs, respectively. These interactions, discussed further by Tsang and Dynlacht,

provide a logical mechanism by which levels of both kinases and structural proteins are effectively recruited to and maintained at the cilium to ensure formation and maintenance (Tsang and Dynlacht, 2013). However, like the observation of NEK4 at the ciliary rootlets, they do not necessarily implicate a target substrate which, when phosphorylated, clearly leads to the dissolution of the CP110 complex and the initiation of ciliogenesis. In fact, outside of TTBK2's ability to phosphorylate Cep97 *in vitro* and NEK1's potential interaction with Kif3a, the roles of the kinases described above so far appear to be mostly structural in nature. That being said, however, it could be that interactions between the kinases and members of the CP110 complex (interactions that might lead to demise of the complex) are simply more difficult to observe in contrast to the interaction of the kinases with DAPs and SAPs, which lead to stabilization of the structures and amplification of the readout through further recruitment of each protein. If this is the case (which I believe it to be), investigations into further interacting partners of the kinases and specifically interactions with members of the CP110 complex should be made. While the CP110 complex and associated proteins are just a subset of the ciliary proteome, the observations described above of each protein's individual role in the initiation of ciliogenesis reinforce the importance of their presence. Using the information obtained from these data provides a map of known protein interactions and allows the possibility to speculate the potential of some interactions yet to be observed (See model below).

Outside of CEP290, a protein whose close relationship with CP110 is well

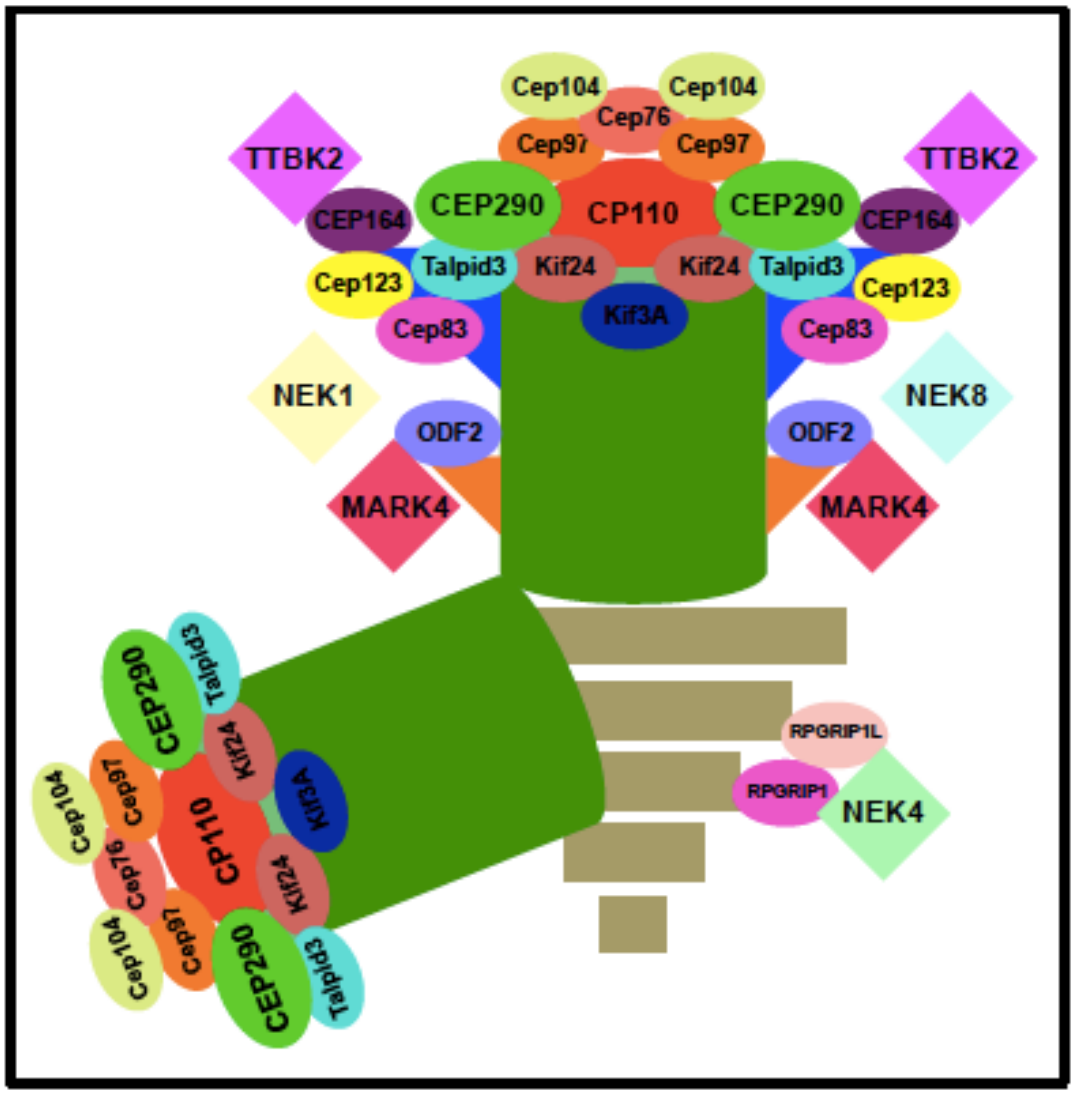

Model of CP110 complex and associated proteins: CP110 complex composed of CP110, Cep97, Cep104, Cep76, CEP290, Kif24, and Talpid3 is observed on the distal end of each centriole (dark green cylinders). In addition, Kif3A, a Kinesin-II subunit, may be found in close proximity. Distal appendages of the mother centiole (blue triangles near distal end of top centriole) appear to be composed of several proteins, including CEP164, Cep123, and Cep83, with Cep83. ODF2 can be found at the sub-distal appendages (orange triangles directly below the distal appendages of the mother centriole). RPGRIP1 and RPGRIP1L are associated with the ciliary rootlets (depicted as brown bars below the mother centriole). Kinases (represented as diamond shapes) are located in the model near their described interacting partners with the exception of NEK1 and NEK8. NEK1 potentially interacts with Kif3A. No interacting partner of NEK8 at the cilium has been described.

documented, and the potential interactions of TTBK/Cep97 and NEK1/Kif3a just mentioned, Cep104 may be the best substrate candidate for further investigation into a kinase driven model for the initiation of ciliogenesis. As previously described, Cep104 appears to be a prociliary factor as its deletion leads to a loss of cilia formation. Interestingly, however, the protein is found to co-localize with CP110 both before ciliogenesis and after, when it is observed to leave the centriolar end along with CP110. As the protein is required for formation but leaves shortly after and is a known interacting protein of both CP110 and Cep97, perhaps Cep104 serves to recruit one of the kinases to its final destination at the end of the centriole where either Cep104 or another member of the complex is then phosphorylated, leading to the dissolution of the CP110 complex.

How the CP110 complex and associated proteins described here, as well as those yet to be identified, interact will continue to be clarified as more focus is placed on ciliary biology. Determining the definitive signal that leads to the formation of the cilium, whether it is kinase driven or not, will be a seminal finding in the field. Given the close relationship of cilia formation and the cell cycle, identification of such a signal would likely be welcomed by basic and applied scientist, alike.

CHAPTER 4- Remaining questions and future directions

The field of ciliary biology is currently in an interesting and exciting period. In one sense, the description of cilia and flagella as the first organelles to be observed makes the field the oldest of cellular and molecular biology. On the other hand, recognition of the cilia's cellular role has only recently expanded from an organelle solely involved in locomotion to one of exceptional complexity and variability. How the work presented here plays a part in the field as a whole will continue to be evaluated as investigations into the biology of the cilium, from formation and maintenance to its role in disease, continue to expand our knowledge of the organelle.

Regarding the model of *CEP290*-associated disease pathogenesis presented, several questions remain. One of these is the likelihood of this model applying to other genes associated with a spectrum of diseases. While we lack complete understanding of CEP290 and CC2D2A's cellular function, both proteins appear to be structural in nature. The model assigns degrees of severity to the different types of mutations based on the hypothesized effect of each mutation on levels of functional protein of interest, with missense mutations in the least severe category. As missense mutations have the potential to severely affect enzymes, it is likely that proteins such as these may not readily fit into the model as currently described. As such, it is probable that potential future disease genes of which this model applies will also encode structural proteins. Identifying these genes requires, at the very least, a defined patient population with readily

accessible genotype and phenotype information. This is currently a limiting factor in finding new candidate genes, specifically ciliary genes, as most diseases associated with ciliary health are very severe due to the role of cilia in development. As developmental defects are often embryonic lethal, large, defined populations of patients with mutations in ciliary genes are quite rare.

Another question regarding observed pathogenesis in *CEP290* cases is why some tissues appear to be rescued from disease and others, such as the eye, appear to always be affected. One hypothesis regarding this is that the levels of alternative splicing may be different for each tissue type. This hypothesis would suggest higher amounts of alternative splicing in the cells of tissue that appear more resistant to disease, such as those of the neural floor plate. In theory, the increased alternative splicing would provide these cells with more near full-length protein with which to function. In comparison, it would suggest cell types in tissue more susceptible to disease, such as the retina, have relatively less alternative splicing, resulting in smaller amounts of exon-skipped isoforms and, as a result, more observable disease. Further investigations using qPCR of cDNA isolated from each tissue of interest would shed light on this hypothesis. In addition, the use of induced pluripotent stem cells (iPSCs), which could be differentiated into different cell type precursors, might be a useful way to investigate this possibility. A difference in splicing between the tissue types playing a role in presentation of disease is particularly attractive in terms of potential therapeutic approaches. Isolating a specific splicing factor that could be used to increase splicing in cells or isolating a drug capable of increasing the

amount of alternative splicing might prove to alleviate symptoms specific to those cell types. While the affect of increasing alternative splicing on the health of those tissues is unknown, the approach would be rather straightforward if you were able to treat the tissue early enough.

Another hypothesis is that the necessity of absolute ciliary health may be different for each tissue. That is, the normal role of the cilia in each tissue may dictate how well that tissue deals with mutations that affect the integrity of the organelle. As described earlier Ptch and Smo, two players in Shh signaling, are observed to locate to the cilium, and their function and location is necessary for successful hedgehog signaling. In this sense, the cilium appears to be involved in providing a location of enriched Ptch and Smo for the initial stages of hedgehog signaling which is crucial for normal development. In a photoreceptor, however, the cilium serves as a structural component of the cell, physically linking the inner segment to the outer segment, and, in doing so, anchoring the outer segment while providing a connection through which it receives newly synthesized proteins and removes waste. As the role of the cilium can vary in each tissue type, perhaps tissues that depend less on the structural integrity of the cilium are more resistant to disease. As an example, we can return to the oak ridge polycystic kidney *orpk* mouse in which two different mutations have been described. One mutation leads to a complete knockout of the *Ift88* allele, which encodes an IFT protein known to be necessary for cilia formation. The resulting phenotype is a failure of the embryo to develop past mid-gestation and a complete lack of cilia on ventral node cells. The other mutation, however, is

hypomorphic, resulting in the production of minimal amounts of Ift88 and a rescue from the embryonic lethal phenotype of the null mice. The hypomorphic mice do experience severe kidney disease, however, eventually leading to death within a few weeks. Closer analysis of the kidney tubule cells in these mice show they are capable of forming primary cilia, however, the cilia are much shorter than those observed in wild-type mice. Of note, retinal degeneration is also observed in these mice. While further investigations regarding functional Shh pathways in both forms of this model are needed (specifically whether the ventral node cells of the hypomorphic mice also exhibit shortened primary cilia), it is enticing to hypothesize the hypomorphic embryos are rescued from the embryonic lethal phenotype due to minimal but present activity of the Shh pathway. That is, while the primary cilia of hypomorphic mice are much smaller and this leads to defects in kidney and retinal function, two aspects of ciliary function highly dependent on structural integrity of the cilium, they may still be capable of providing the enriched Smo and Ptch levels necessary for Shh activity and embryonic development.

Finally, another question to be explored regarding this model is its clinical significance related to *CEP290* disease. While there is currently no cure for *CEP290*-assoicated disease, palliative treatment is available. As the symptoms associated with *CEP290* disease progress in severity as the patient ages, understanding the likely severity of an individual's eventual disease before symptoms worsen, or in some cases appear, would be valuable knowledge for clinicians and patients, alike, allowing the monitoring of a patient's disease to be

adjusted accordingly overtime.

In general, we are still a long way from understanding the relationship of the CP110 complex and associated proteins in the initiation and maintenance of ciliogenesis explored in the second part of my work. Understanding the roles of CEP290 and TTBK2 in these processes will require further investigations. However, in addition to increasing our basic understanding of ciliary biology, continuing to map the interactions of all ciliary proteins could lead to the identification of new disease genes and potential therapeutic approaches for patients suffering from ciliopathies. Currently, gene augmentation strategies involving many of the known ciliary genes are prohibited by the limited cargo capacity of AAV vectors. In this regard, understanding the roles of ciliary proteins, especially those believed to be involved in the recruitment of others, is especially important. In analyzing the relationship of CEP164 and TTBK2 (as discussed earlier), the Nigg group used an interesting approach to rescue ciliogenesis in CEP164 depleted cells by transfecting in constructs composed of TTBK2 fused to the distal appendage-targeting portion of CEP164. While the group used this approach to demonstrate CEP164 was involved in TTBK2 recruitment to the base of the cilium, a similar therapeutic approach could theoretically be used to treat disease associated with mutations in proteins responsible for kinase recruitment. The coding sequence of a theoretical fusion protein composed of, at minimum, the catalytic domain of a kinase or another small ciliary protein and a targeting sequence should fit into an AAV vector. Such a construct may be capable of rescuing disease in a patient with specific

mutations in a large recruiting protein.

As cilium formation appears to be a highly regulated step in the cell cycle, identification of a protein that functions as the definitive step in the initiation of ciliogenesis could theoretically have anti-cancer implications. In such a scenario, targeting cancerous cells with a strong, pro-ciliary factor might lead to sequestration of the centrosome and its conversion to the basal body and an inhibition of cellular replication.

Discussing any novel treatment approach, however, always comes with additional concerns. In terms of the use of a theoretical fusion protein, application of such methods would likely be confined to the retinal phenotypes associated with cilia disease due to immunologic concerns. While the retina is only one of the many tissues affected by ciliary disease, it may be the only practical tissue to target when taking into consideration the point at which cells would have to be treated in order to prevent irreversible disease. It is very unlikely, even without taking the political and legal implications of *in utero* gene therapy into account, ciliary disease in the embryo will ever be targeted for correction as the point by which the embryo would have to be genotyped and treated would be very early in development. In less severe disease, the kidney might be a treatment target if likely immune responses to the vector and/or transgene could ever be circumvented.

The likelihood of any theoretical cilopathy treatment will depend on the success of continued investigations and sustained efforts aimed at understanding

the complex protein environment of these structures. More than likely, observations made from these studies will also aid our understanding of the disease pathogenesis associated with mutations in ciliary genes. As more diseases are classified into the category of ciliopathies, this once disregarded structure will continue to receive the attention of a diverse group of scientists, from developmental and structural biologists to clinicians, alike. There is no longer denying the role of the primary cilium in cellular health and function. With continued investigation, it will be exciting to observe just how right Karl Zimmerman and an undeterred group of scientists were regarding the importance of a once vestigial organelle.

BIBLIOGRAPHY

Ahdab-Barmada, M., Claassen, D. “A distinctive triad of malformation of the central nervous system in the Meckel-Gruber syndrome.” *Journal of Neuropathology and Experimental Neurology* 49(6) (1990): 610-620.

Andersen, J.S., Wilkinson, C.J., Mayo, T., Mortensen, P., Nigg, E.A., Mann, M. “Proteomic characterization of the human centrosome by protein correlation profiling.” *Nature* 426 (2003): 570-574.

Avasthi P., Marshall, W.F. “Stags of ciliogenesis and regulation of ciliary length.” *Differentiation* 83(2) (2012): 1-29.

Barnes, B.G. “Ciliated secretory cells in the pars distalis of the mouse hypophysis.” *Journal of Ultrastructure Research* 5 (1961): 453-467.

Basten, S.G., Giles, R.H. “Functional aspects of primary cilia in signaling, cell cycle and tumorigenesis.” *Cilia* 2(6) (2013): 1-23.

Blom, N., Gammeltoft, S., Brunak, S. “Sequence- and structure-based predition of eukaryotic protein phosphorylation sites.” *Journal of Molecular Biology* 294(5) (1999): 1351-1362.

Bloodgood, R.A. “From central to rudimentary to primary: the history of an underappreciated organelle whose time has come. The primary cilium.” *Methods in Cell Biology* 94 (2009): 1-51.

Bouskila, M., Esoof, N., Gay, L., Gang, E.H., Deak, M., Begley, M.J., Cantley, L.C., Prescott, A., Storey, K.G., Alessi, D.R. “TTBK2 kinase substrate specificity and the impact of spinocerebellar-ataxia-causing mutations on expression, activity, localization and development.” *Biochemical Journal* 437 (2011): 157-167.

Brancati, F., Barrano, G., Silhavy, L., March, S.E., Travaglini, L., Bielas, S.L., Amorini, M., et al. "*CEP290* mutations are frequently identified in the oculo-renal form of Joubert Syndrome-related disorders." *The American Journal of Human Genetics* 81 (2007): 104-113.

Cai, Y., Maeda, Y., Cedzich, A., Torres, V.E., Wu, G., Hayashi, T., Mochizuki, T., Park, J.H., Witzgall, R., Somlo, S. Identification and characterization of polycystin-2, the *PKD2* gene product." *The Journal of Biological Chemistry* 274(40) (1999): 28557-28565.

Cajanek, L., Nigg, E.A. "Cep164 triggers ciliogenesis by recruiting Tau tubulin kinase 2 to the mother centriole." *Proceeding of the National Academy of Sciences* 111(28) (2014): 1-10.

Cao, M., Li, G., Pan, J. "Regulation of cilia assembly, disassembly, and length by protein phosphorylation." *Methods in Cell Biology* 94 (2009): 333- 346.

Cartegni, L., Chew, S.L., Krainer, A.R. "Listening to silence and understanding nonsense: exonic mutations that affect splicing." *Nature Reviews Genetics* 3 (2002): 285-298.

Chang, B., Khanna, H., Hawes, N., Jimeno, D., He, S., Lillo, C., Parapuram, S.K., Cheng, H., Scott, A., et al. "In-frame deletion in a novel centrosomal/ciliary protein CEP290/NPHP6 perturbs its interaction with RPGR and results in early-onset retinal degeneration in the *rd16* mouse." *Human Molecular Genetic* 15(11) (2006): 1847-1857.

Chen, Z., Indejeian, V.B., McManus, M., Wang, L., Dynlacht, B.D. "CP110, a cell cycle-dependent CDK substrate regulates centrosome duplication in human cells." *Developmental Cell* 3 (2002): 339-350.

Chiang, S.Y., Litingtung, Y., Lee, E., Young, K.E., Corden, J.L., Westphal, H., Beachy, P.A. "Cyclopia and defective axial patterning in mice lacking sonic hedgehog gene function." *Nature* 838 (1996): 407-413.

Cideciyan A.V., Aleman T.S., Jacobson, S.G., Khanna, H., Sumaroka, A., Aguirre, G.K., Schwartz, S.B., Windsor, E.A., He, S., Chang, B., Stone, E.M., Swaroop, A. “Centrosomal-ciliary gene CEP290/BPHP6 mutations result in blindness with unexpected sparing of photoreceptors and visual brain: implications for therapy of Leber congenital amaurosis.” *Human Molecular Genetics* 28 (2007): 1074-1083.

Coene, K.L.M., Mans, D.A., Boldt, K., Gloeckner, C.J., van Reeuwijk, J., Bolat, E., Roosing, S., Letteboer, S.J.F., Peters, T.A., Cremers, F.P.M., Ueffing, M., Roepman, R. “The ciliopathy-associated protein homologs RPGRIP1 and RPGRIP1L are linked to cilium integrity through interaction with Ned4 serine/threonine kinase.” *Human Molecular Genetics* 20(18) (2011): 3592-3605.

Cole, D.G., Diener, D.R., Himelblau, A.L., Beech, P.L., Fuster, J.C., Rosenbaum, J.L. “*Chlamydomonas* Kinesin-II-dependent Intraflagellare Transport (IFT): IFT particles contain proteins required for ciliary assembly in *Caenorhabditis elegans* sensory neurons.” *The Journal of Cell Biology* 141(4) (1998): 993-1008.

Coppieters, F., Lefever, S., Leroy, B.P., De Baere, E. “*CEP290*, a gene with many faces: mutation overview and presentation of CEP290base.” *Human Mutation* 31(10) (2010): 1097-1108.

Corbit, K.C., Aanstad, P., Singla, V., Norman, A.R., Stainier, D.Y.R., Reiter, J.F. “Vertebrate smoothened functions at the primary cilium.” *Nature* 437 (2005): 1018-1021.

Craige B., Tsao, C.C., Diener, D.R., Hou, Y., Lechtreck, K.F., Rosenbaum, J.L., Witman, G.B. “CEP290 tethers flagellar transition zone microtubules to the membrane and regulates flagellar protein content.” *The Journal of Cell Biology* 190(5) (2010): 927-940.

Dawe, H.R., Farr, H., Gull, K. “Centriole/ basal body morphogenesis and migration during ciliogenesis in animal cells.” *Journal of Cell Science* 120 (2007): 7-15.

De Brabander, M., Geuens, G., Nuydens, R., Willebrords, R., De Mey, J. “Microtubule stability and assembly in living cells: the influence of metabolic inhibitors, taxol, and pH. *Cold Spring Harbor Symposia on Quantitative Biology* 46 (1982): 227-240.

de Robertis, E. “Electron microscope observations on the submicroscopic organization of the retinal rods.” *The Journal of Biophysical and Biochemical Cytology* 2(3) (1956): 319- 337.

Kozminski, K.G., Johnson, K.A., Forscher, P., Rosenbaum, J.L. “A motility in the eukaryotic flagellum unrelated to flagellar beating.” *Proceedings of the National Academies of Scientists* 90 (1993): 5519-5523.

den Hollander, A.I., Koenekoop, R.K., Yzer, S., Lopez, I., Arends, M.L., Voesenek, K.E.J., Zonneveld, M.N., et al. “Mutations in the *CEP290* (*NPHP6*) gene are a frequent cause of leber congenital amaurosis.” *The American Journal of Human Genetics* 79 (2006); 556-561.

Dobell F.R.S., C. Antony van Leeuwenhoek and his “little animals.” (1932)

Drivas, T.G., Holzbaur, E.L.F., Bennett, J. “Disruption of CEP290 microtubule/membrane-binding domains causes retinal degeneration.” *The Journal of Clinical Investigation* 123(10) (2013): 4525-4539.

Echelard, Y., Epstein, D.J., St. Jacques, B., Shen, L., Mohler, J., McMahon, J.A., McMahon, A.P. “Sonic hedgehog, a member of a family of putative signaling molecules, is implicated in the regulation of CNS polarity.” *Cell* 75 (1993): 1417-1430.

Ems-McClung, S.C., Walczak, C.E. “Kinesin-13s in mitosis: Key players in the spatial and temporal organization of spindle microtubules.” *Seminars in Cell & Developmental Biology* 21 (2010): 276-282.

Fry, A.M., O'Regan, L., Sabir, S.R., Bayliss, R. "Cell cycle regulation by the NEK family of protein kinases." *Journal of Cell Science* 125(Pt 19) (2012): 4423-4433.

Howe, K.J., Kane, C.M., Ares Jr., M. "Perturbation of transcription elongation influences the fidelity of internal exon inclusion in *Saccharomyces cerevisiae*." *RNA* 9 (2003): 993-1006.

Genuardi, M., Dionisi-Vici, C., Sabetta, G., Mignozzi, M, Rissoni, G., Cotugno, G., Neri, M.E.M. "Cerebro-Reno-Digital (Meckel-like) syndrome with Dandy-Walker malformation, cystic kidneys, hepatic fibrosis, and polydactyly." *American Journal of Medical Genetics* 47 (1993): 50-53.

Gest, H. "The discovery of microorganisms by Robert Hooke and Antoni van Leeuwenhoek, fellow of the Royal Society." *Notes Rec. R. Soc. Lond.* 58 (2004): 187- 201.

Goetz, S.C., Liem Jr., K.F., Anderson, K.V. "The spinocerebellar ataxia-associated gene *Tau Tubulin Kinase 2* controls the initiation of ciliogenesis." *Cell* 151 (2012): 847-858.

Gorden, N.T., Arts, H.H., Parisi, M.A., Coene, K.L.M. Letteboer, S.J.F., van Beersum, S.E.C., Mans, D.A., et al. "*CC2D2A* is mutated in Joubert Syndrome and interacts with the ciliopathy-associated basal body protein CEP290." *The American Journal of Human Genetics* 83 (2008): 559-571.

Guo, J., Jin, G., Meng, L., Ma, H., Nie, D., Wu, J., Yuan, L., Shou, C. "Subcellular localization of tumor-associated antigen 3H11Ag." *Biochemical and Biophysical Research Communications* 324 (2004): 922-930.

Graser, S., Stierhof, Y.D., Lavoie, S.B., Gassner, O.S., Lamla, S., Le Clech, M., Nigg, E.A. "Cep164, a novel centriole appendage protein required for primary cilium formation." *The Journal of Cell Biology* 179(2) (2007):321-330.

Holland, P.M., Milne, A., Garka, K., Johnson, R.S., Willis, C., Sims, J.E., Rauch, C.T., Bird, T.A., Duke Virca, G. “Purification, cloning, and characterization of Nek8, a novel NIMA-related kinase, and its candidate substrate Bicd2.” *The Journal of Biological Chemistry* 277(18) (2002): 16229-16240.

Hooper, J.E., Scott, M.P. “Communicating with hedgehogs.” *Nature Reviews Molecular Cell Biology* 6 (2005): 306-317.

Houlden, H., Johnson, J., Gardner-Thorpe, C., Lashley, T., Hernandez, D., Worth, P., Singleton, A.B., Hilton, D.A., Holton, J., Revesz, T., Davis, M.B., Giunti, P., Wood, N.W. “Mutations in *TTBK2*, encoding a kinase implicated in tau phosphorylation, segregate with spinocerebellar ataxia type 11.” *Nature Genetics* 39(12) (2007): 1434-1436.

Ikezu, S., Ikezu, T. “Tau-tubulin kinase.” *Frontiers in Molecular Neuroscience* 7 (2014): 1-10.

Imanishi, M., Endres, N.F., Gennerich, A., Vale, R.D. “Autoinhibition regulates the motility of the C. elegans intraflagellar transport motor OSM-3.” *The Journal of Cell Biology* 174(7) (2006): 931-937.

Jakobsen, L., Vanselow, K., Skogs, M., Toyoda, Y., Lundberg, E., Poser, I., Falkenby, L.G., Bennetzen, M., Westendorf, J., Nigg, E.A., Uhlen, M., Hyman, A.A., Andersen, J.S. “Novel asymmetrically localizing components of human centrosomes identified by complementary proteomics methods.” *The EMBO Journal* 30 (2011): 1520-1535.

Johnson, K.A., Rosenbaum, J.L. “Flagellar regeneration in *Chlamydomonas:* a model system for studying organelle assembly.” *Trends in Cell Biology* 3 (1993): 156-161

Jiang, K., Toedt, G., Montenegro Gouveia, S., Davey, N.E., Hua, S., van der Vaart, B., Grigoriev, I., Larsen, J., Pedersen, L.B., Bezstarosti, K., Lince-Faria, M., Demmers, J., Steinmetz, M.O., Gibson, T.J., Akhmanova, A. “A proteome-

wide screen for mammalian SxIP motif-containing microtubule plus-end tracking proteins." *Current Biology* 22 (2012): 1800-1807.

Kato, T., Satoh, S., Okabe, H., Kitahara, O., Ono, K., Kihara, C., Tanaka, T., Tsunoda, T., Yamaoka, Y., Nakamura, Y., Furukawa, Y. "Isolation of a novel human gene, *MARKL1*, homologous to MARK3 and its involvement in hepatocellular carcinogenesis." 3(1) (2001): 4-9

Kim, J., Krishnaswami, S.R., Gleeson, J.G. "CEP290 interacts with the centriolar satellite component PCM-1 and is required for Rab8 localization to the primary cilium." *Human Molecular Genetics* 17(23) (2008): 3796-3805.

Kleylein-Sohn, J., Westendorf, J., Le Clech, M., Habedanch, R., Stierhof, Y.D., Nigg, E.A. "Pik4-induced centriole biogenesis in human cells. *Developmental Cell* 13 (2007): 190-202.

Kobayashi, T., Dynlacht, B.D. "Regulating the transition from centriole to basal body." *The Journal of Cell Biology* 193(3) (2011): 435-444.

Kobayashi, T., Kim, S., Lin., Y.C., Inoue, T., Dynlacht, B.D. "The CP110-interacting proteins Talpid3 and Cep290 play overlapping and distinct roles in cilia assembly." *The Journal of Cell Biology* 204(2) (2014): 215-229.

Koenekoop, R.K., Wang, H., Majewski, J., Wang, X., Lopez, I., Ren, H., Chen, Y., Li, Y., Fishman, G.A., et al. "Mutations in *NMNAT1* cause Leber congenital amaurosis and identify a new disease pathway for retinal degeneration." *Nature Genetics* 44(9) (2012): 1035-1040.

Kozminski, K.G., Johnson, K.A., Forscher, P., Rosenbaum, J.L. "A motility in the eukaryotic flagellum unrelated to flagellar beating." *Proceedings of the National Academies of Scientists* 90 (1993): 5519-5523.

Kuhns, S., Schmidt, K.N., Reymann, J., Gilbert, D.F., Neuner, A., Hub, B., Carvalho, R., Wiedemann, P., Zentgraf, H., Erfle, H., Klingmuller, U., Boutros, M.,

Pereira, G. “The microtubule affinity regulating kinase MARK4 promotes axoneme extension during early ciliogenesis.” *The Journal of Cell Biology* 200(4) (2013): 505-522.

Lancaster, M.A., Schroth, J., Gleeson, J.G. “Subcellular spatial regulation of canonical Wnt signaling at the primary cilium.” *Nature Cell Biology* 13(6) (2011): 700-708.

Littink, K.W., Pott, J.R., Collin, R.W., Kroes, H.Y., Verheij, J.B.G.M., Blokland, E.A.W., et al. “A novel nonsense mutation in *CEP290* induces exon skipping and leads to a relatively mild retinal phenotype.” *Investigative Ophthalmology & Visual Science* 51(7) (2010): 3646-3652.

Liu, S., Lu, W., Obara, T., Kulda, S., Lehoczky, J., Dewar, K., Drummond, I.A., Beler, D.R. “A defect in a novel Nek-family kinase causes cystic kidney disease in the mouse and in zebrafish.” *Development and Disease* 129 (2002): 5839-5846.

Maquat, L.E. “Nonsense-mediated mRNA decay: splicing, translation and mRNP dynamic.” *Nature Reviews Molecular Cell Biology* 5 (2004): 89-98.

McMahon, A.P., Ingham, P.W., Tabin, C.J. “Developmental roles and clinical significance of hedgehog signaling.” *Current Topics in Developmental Biology* 53 (2003): 1-114.

Moyer, J.H., Lee-Tischler, M.J., Kwon, H.Y., Schrick, J.J., Avner, E.D., Sweeney, W.E., Godfrey, V.L., Cacheiro, N.L.A., Wilkerson, J.E., Woychik, R.P. “Candidate gene associated with a mutation causing recessive polycystic kidney disease in mice.” *Science* 264 (1994): 1329-1333.

Munger, B.L. “A light and electron microscopic study of cellular differentiation in the pancreatic islets of the mouse.” *American Journal of Anatomy* 103 (1958): 275-311.

Murcia, N.S., Richards, W.G., Yoder, B.K., Mucenski, M.L., Dunlap, J.R., Woychik, R.P. “The *Oak Ridge Polycystic Kidney (orpk)* disease gene is required for left-right axis determination.” *Development* 127 (2000): 2347-2355.

Nagase, T., Ishikawa, K., Nakajima, D. Ohira, M., Seki, N., Miyajima, N., Tanaka, A., Kotani, H., Nomura, N., Ohara, O. “Prediction of the coding sequence of unidentified human genes. The complete sequences of 100 new cDNA clones from brain which can code for large proteins *in vitro*.” *DNA Research* 4 (1997): 141-150.

Oda, T., Chiba, S., Nagai, T., Mizuno, K. “Binding to Cep164, but not EB1, is essential for centriolar localization of TTBK2 and its function in ciliogenesis.” *Genes to Cells* 19(12) (2014): 927-940.

Pazour, G.J., Dickert, B.L., Vucica, Y., Seeley, E.S., Rosenbaum, J.L., Witman, G.B., Cole, D.G. “*Chlamydomonas IFT88* and its mouse homologue, polycystic kidney disease gene *Tg737,* are required for assembly of cilia and flagella.” *The Journal of Cell Biology* 151(3) (2000): 709-718.

Pazour, G.J., Rosenbaum, J.L. “Intraflagellar transport and cilia-dependent diseases.” *Trends in Cell Biology* 12(12) (2002): 551-555.

Pazour, G.J., Wilkerson, C.G., Witman, G.B. “A dynein light chain is essential for the retrograde particle movement of intraflagellar transport (IFT).” *The Journal of Cell Biology* 141(4) (1998): 979-992.

Perrault, I., Delphin, N., Hanein, S., Gerber, S., Dufier, J., Roche, O., Defoort-Dhellemmes, S., et al. “Spectrum of NPHP6/CEP290 mutation in Leber Congenital Amaurosis and delineation of the associated phenotype.” *Human Mutation* 956 (2007): 1-10.

Piel, M., Myeter, P., Khodjakov, A., Rieder, C.L., Bornens, M. “The respective contributions of the mother and daughter centrioles to centrosome activity and behavior in vertebrate cells.” *The Journal of Cell Biology* 149 (2000): 317-330.

Praetorius, H.A., Spring, K.R. “Bending the MDCK cell primary cilium increases intracellular calcium.” *The Journal of Membrane Biology* 184 (2001): 71-79.

Ohad, S., Shalva, N., Altschuler, Y., Motro, B. “The mammalian Nek1 kinase is involved in primary cilium formation.” *FEBS Letters* 582 (2008): 1465-1470.

Huangfu, D., Liu, A., Rakeman, A.S., Murcia, N.S., Niswander, L., Anderson, K.V. “Hedgehog signaling in the mouse requires intraflagellar transport proteins.” *Nature* 426 (2003): 83-87.

Prosser, S.L., Morrison, C.G. “Centrin 2 regulates CP110 removal in primary cilium formation.” *The Journal of Cell Biology* 208(6) (2015): 693-701.

Romero, C.C., Solano, J.L.G., De Cabo De La Vega, C. “Ciliopathies: Primary cilia and signaling pathways in mammalian development.” *Neuroimaging for Clinicians- Combining Research and Practice* (2011): 1-21.

Sayer, J.A., Otto, E.A., O’Toole, J.F., Nurnberg, G., Kennedy, M.A., Becker, C., Hennies, H.C., Helou, J. et al. “The centrosomal protein nephrocystin-6 is mutated in Jourbert syndrome and activates transcription factor ATF4.” *Nature Genetics* 38(6) (2006): 674- 681.

Schneider L., Clement, C.A., Teilmann, S.C., Pazour, G.J., Hoffmann, E.K., Satir, P., Christensen, S.T. “PDGFRαα signaling is regulated through the primary cilum in fibroblasts.” *Current Biology* 15 (2005):1861-1866.

Seeley, E.S., Nachury, M.V. “The perennial organelle: assembly and disassembly of the primary cilium.” *Journal of Cell Science* 123 (2010): 511-518.

"Senior-Loken Syndrome." *Genetics Home Reference*. U.S. National Library of Medicine, 19 July 2015. Web. 24 July 2015.

Shipley, K., Hekmat-Nejad, M., Turner, J., Moores, C., Anderson, R., Milligan, R., Sakowicz, R., Fletterick, R. “Structure of a kinesin microtubule depolymerization maching.” *The EMBO Journal* 23 (2004): 1422-1432.

Sillibourne, J.E., Hurbain, I., Grand-Perret, T., Goud, B., Tran, P., Bomens, M. “Primary ciliogenesis requires the distal appendage component Cep123.” *Biology Open* 2 (2013): 535-545.

Singla, V., Reiter, J. F. “The primary cilium as the cell’s antenna: signaling at a sensory organelle.” *Science* 313 (2006): 629-633.

Sjostrand, F.S. “The ultrastructure of the inner segments of the retinal rods of the guinea pig eye as revealed by electron microscopy.” *Journal of Cellular and Comparative Physiology* 42(1) (1953): 45-70.

Solis, A.S., Peng, R., Crawford, J.B., Phillips III, J.A., Patton, J.G. “Growth hormone deficiency and splicing fidelity.” *The Journal of Biological Chemistry* 283(35) (2008): 23619-23626.

Sorokin, S. “Centrioles and the formation of rudimentary cilia by fibroblasts and smooth muscle cells.” *The Journal of Cell Biology* 14 (1962): 363-377.

Spektor, A., Tsang, W.Y., Khoo, D., Dynlacht, B.D. “Cep97 and CP110 suppress a cilia assembly program.” *Cell* 130 (2007): 678-690.

Sato, S., Cerny, R.L., Buescher, J.L., Ikezu, T. “Tau-tubulin kinase 1 (TTBK1), a neuron-specific tau kinase candidate, is involved in tau phosphorylation and aggregation.” *Journal of Neurochemistry* 98 (2006): 1573-1584.

Sato, S., Xu, J., Okuyama, S., Martinez, L.B., Walsh, S.M., Jocobsen, M.T., Swan, R.J., Schlautman, J.D., Ciborowski, P., Ikezu, T. “Spatial learning impairment, enhanced CDK5/p35 activitiy and downregulation of NMDA receptor expression in transgenic mice expressing tau-tubulin kinase I.” *Neurobiology of Disease* 28(53) (2008): 14511-14521.

Schafer, T., Putz, M., Lienkamp, S., Ganner, A., Bergbreiter, A., Ramachandran, H., Gieloff, V., Gerner, M., Mattonet, C., Czarnecki, P.G., Sayer, J.A., Otto, E.A., Hildebrandt, F., Kramer-Zucker, A., Walz, G. “Genetic and physical interaction between the NPHP5 and NPHP6 gene products.” *Human Molecular Genetics* 17(23) (2008): 3655-3662.

Surpili, M.J., Delben, T.M., Kobarg, J. “Identification of proteins that interact with the central coiled-coil region of the human protein kinase NEK1.” *Biochemistry* 42 (2003): 15369-15376.

Tachi, S., Tachi, C., Lindner, H.R. “Influence of ovarian hormones on formation of solitary cilia and behavior of the centrioles in uterine epithelial cells of the rat.” *Biology of Reproduction* 10 (1974): 391-403.

Tallila, J., Jakkula, E., Peltonen, L., Salonen, R., Kestila, M. “Identification of *CC2D2A* as a Meckel Syndrome gene adds an important piece to the ciliopathy puzzle.” *The American Society of Human Genetics* 82 (2008): 1361-1367.

Tanos, B.E., Yang, H.J., Soni, R., Wang, W.J., Macaluso, F.P., Asara, J.M., Tsou, M.F.B. “Centriolar distal appendages promote membrane docking, leading to cilia initaiton.” *Genes and Development* 27 (2013): 163-168.

Tateishi, K., Yamazaki, Y., Nishida, T., Watanabe, S., Kunimoto, K., Ishikawa, H., Tsukita, S. “Two appendages homologous between basal bodies and centrioles are formed using distinct *Odf2* domains.” *The Journal of Cell Biology* 203(3) (2013): 417-425.

Trinczek, B., Brajenovic, M., Ebneth, A., Drewes, G. “MARK4 is a novel microtubule-associated proteins/microtubule affinity-regulating kinase that binds to the cellular microtubule network and to centrosomes.” *The Journal of Biological Chemistry* 279(7) (2004): 5915-5923.

Tsang, W.Y., Bossard, C., Khanna, H., Peranen, J., Swaroop, A., Malhotra, V., Dynlacht, B.D. “CP110 suppresses primary cilia formation through its interaction

with CEP290, a protein deficient in Human Ciliary Disease." *Developmental Cell* 15 (2008): 187-197.

Tsang, W.Y., Spektor, A., Vijayakumar, S., Bista, B.R., Li, J., Sanchez, I., Duensing, S., Dynlacht, B.D. "Cep76, a centrosomal protein that specifically restrains centriole reduplication." *Developmental Cell* 16 (2009): 649-660.

Kobayashi, T., Tsang, W.Y., Li, J., Lane, W., Dynlacht, B.D. "Centriolar kinesin Kif24 interacts with CP110 to remodel microtubules and regulate ciliogenesis." *Cell* 145 (2011): 914-925.

Upadhya, P., Birkenmeier, E.H., Birkenmeier, C.S., Barker, J.E. "Mutations in a NIMA-related kinase gene, *Nek1*, cause pleiotropic effects including a progressive polycystic kidney disease in mice." *Proceedings of the National Academy of Sciences* 97(1) (2000): 217-221.

Valente, E.M., Silhavy, J.L., Brancati, F., Barrano, G., Krishnaswami, S.R., Castori, M., Lancaster, M.A., Boltshauser, E., Boccone, L., Al-Gazali, L., Fazzi, E., Signorini, S., Louie, C.M. et al. "Mutations in *CEP290*, which encodes a centrosomal protein, cause pleiotropic forms of Joubert syndrome." *Nature Genetics* 38(6) (2006): 623-625.

Veleri, S., Manjunath, S.H., Fariss, R.N., May-Simera, H., Brooks, M., Foskett, T.A., Gao, C., Longo, T.A., Liu, P., Nagashima, K., Rachel, R.A., Li, T., Dong, L., Swaroop, A. "Ciliopathy-associated gene *Cc2d2a* promotes assembly of subdistal appendages on the mother centriole during cilia biogenesis." *Nature Communications* 5 (2014): 1-12.

Wang, E.T., Sandberg, R., Luo, S., Khrebtukova, I., Zhang, L., Mayr, C., Kingsmore, S.F., Schroth, G.P., Burge, C.B. "Alternative isoform regulation in human tissue transcriptomes." *Nature* 456 (2008); 470- 476.

Waggoner, B. "Antony van Leeuwenhoek (1632-1723)" (1996) http://www.ucmp.berkeley.edu/history/leeuwenhoek.html

Wheatley, D.N., Wang, A.M., Strugnell, G.E. “Expression of primary cilia in mammalian cells.” *Cell Biology International* 20(1) (1996):73-81.

Wong, S.Y., Reiter, J.F. “The primary cilium: at the crossroads of mammalian hedgehog signaling.” *Current Topics in Developmental Biology* 85 (2008): 225-260.

Yang, J., Gao, J., Adamian, M., Wen, X.H., Pawlyk, B., Zhang, L., Sanderson, M.J., Zuo, J., Makino, C.L., Li, T. “The ciliary rootlet maintains long-term stability of sensory cilia.” *Molecular and Cellular Biology* 25(10) (2005): 4129-4137.

Tsang, W.Y., Dynlacht, B.D. “CP110 and its network of partners coordinately regulate cilia assembly.” *Cilia* 2(9) (2013): 1-8.

Ye, X., Zeng, H., Ning, G., Reiter, J.F., Liu, A. “C2cd3 is critical for centriolar distal appendage assembly and ciliary vesicle docking in mammals.” *Proceeding of the National Academy of Sciences* 111(6) (2014): 2164-2169.

Yin, Y., Bangs, F., Paton, I.R., Prescott, A., James, J., Davey, M.G., Whitley, P., Genikhovich, G., Technau, U., Burt, D.W., Tickle, C. “The *Talpid3* gene (*KIAA0586*) encodes a centrosomal protein that is essential for primary cilia formation.” *Development* 136 (2009): 655-664.

Yoder, B.K., Richards, C., Sommardahl, W.E., Sweeney, W.E., Michaud, E.J., Wilkinson, J.E., Avner, E.D., Woychik, R.P. “Differential rescue of the renal and hepatic disease in an autosomal recessive polycystic kidney disease mouse mutant.” 150 (1997): 2231-2241.

Yoder, B.K., Richards, C., Sommardahl, W.E., Sweeney, W.E., Michaud, E.J., Wilkinson, J.E., Avner, E.D., Woychik, R.P. “Functional correction of renal defects in a mouse model for ARPKD through expression of the cloned wild-type *Tg737* cDNA.” 50 (1996): 1240-1248.

Zerial, M., McBride, H. “Rab proteins as membrane organizers.” *Nature Reviews Molecular Cell Biology* 2 (2001): 107-119.

Zhang, Y., Seo, S., Bhattarai, S., Bugge, K., Searby, C.C., Zhang, Q., Drack, A.V., Stone, E.M., Sheffield, V.C. “BBS mutations modify phenotypic expression of *CEP290*-related ciliopatheis.” *Human Molecular Genetics* 23(1) (2014): 40-51.

Zhao, Y., Hong, D.H., Pawlyk, B., Yue, G., Adamian, M., Grynberg, M., Godzik, A., Li, T. “The retinitis pigmentosa GTPase regulator (RPGR)-interacting protein: subserving RPGR function and participating in disk morphogenesis.” *Proceedings of the National Academy of Sciences* 100(7) (2003): 3965-3970.

Zhao, C., Omori, Y., Brodowska, K., Kovach, P., Malicki, J. “Kinesin-2 family in vertebrate ciliogenesis.” *Proceedings of the National Academy of Sciences* 109(7) (2012): 2388-2393.